PRECAMBRIAN PALEOSOLS AS INDICATORS OF PALEOENVIRONMENTS ON THE EARLY EARTH

by

Sherry Lynn Stafford

B.S., University of Pittsburgh at Johnstown, 1995

M.S., University of Pittsburgh, 1999

Submitted to the Graduate Faculty of

Arts and Sciences in partial fulfillment

of the requirements for the degree of

Doctor of Philosophy

University of Pittsburgh

2007

UNIVERSITY OF PITTSBURGH

FACULTY OF ARTS AND SCIENCES

This dissertation was presented

by

Sherry Lynn Stafford

It was defended on

July 12, 2005

and approved by

Hiroshi Ohmoto, Ph.D., Pennsylvania State University

Charles E. Jones, Ph.D., University of Pittsburgh

Edward G. Lidiak, Ph.D., University of Pittsburgh

Brian W. Stewart, Ph.D., University of Pittsburgh

Dissertation Advisor: Rosemary C. Capo, Ph.D., University of Pittsburgh

PRECAMBRIAN PALEOSOLS AS INDICATORS OF PALEOENVIRONMENTS ON THE EARLY EARTH

Sherry Lynn Stafford, Ph.D.

University of Pittsburgh, 2007

Paleosols, or fossil soils, document past atmospheric composition, climate, and terrestrial landscapes and are key to understanding the composition and evolution of the Earth's atmosphere and the environments in which life developed and evolved. Micromorphological, geochemical and isotopic studies of two Precambrian weathering profiles (Steep Rock, Canada and Hokkalampi, Finland) place constraints on the age of soil formation, document pedogenic processes and post-pedogenic alteration and metamorphism, and yield information about the terrestrial environment at a critical time in Earth history. The textures and geochemistry of the Early Proterozoic Hokkalampi paleosol and the Archean Steep Rock paleosol are consistent with *in situ*, subaerial weathering under varying soil redox conditions. The upper portion of both profiles have lost >40% of their iron relative to the parent material, similar to Phanerozoic vertisols, while retaining Fe^{3+}/Fe^{2+} ratios >1. Redistribution of phosphorus in the Steep Rock profile and thorium in some Hokkalampi profiles suggests that organic ligands could have enhanced the mobility of redox-sensitive elements. In addition, copper mobility in the Steep Rock profile could indicate the presence of oxygen in the soil. Loss of base cations in both paleosols is similar to modern ultisols or oxisols, which form in warm, moist environments. Whole rock Rb-Sr isochrons indicate that post-pedogenic potassium metasomatism affected both weathering profiles, and the apparent ages are consistent with the timing of regional greenschist metamorphic events. Whole rock Sm-Nd isotope data demonstrate that rare earth element (REE)

systematics were largely unaffected by metamorphism, and that the observed mobility and fractionation of REE could represent a record of Precambrian weathering processes. In the Hokkalampi profiles, Sm-Nd isotope data suggest that pedogenesis took place 2.35±0.19 Ga; this also places a minimum age for Huronian glaciation in the area. The Sm-Nd age of 3.02±0.09 Ga for the Steep Rock paleosol suggests that pedogenesis occurred very soon (<60 Ma) after emplacement and erosional uplift of the parent granitoid. This study demonstrates that Rb-Sr and Sm-Nd analysis combined with geochemical, field, and microscopic examination of Precambrian paleosols can help constrain the nature and timing of ancient Earth-surface processes.

TABLE OF CONTENTS

LIST OF TABLES

LIST OF FIGURES

PREFACE

I would like to thank the many people that have contributed to this work. My advisor, Rosemary Capo and my advisor by association, Brian Stewart, have been true mentors to me. I have always appreciated the fact that I got a "two-for-one" deal. They have stuck by me even when things were tough. Each with their own talents, they have helped me to realize my strengths and weaknesses, have encouraged me to follow my heart, and have stretched my mind. I am a better person because of the time, effort, and financial support that they have both invested in me.

Other members of my dissertation committee, past and present including Harold Rollins, Charles Jones, Edward Lidiak, and Hiroshi Ohmoto, have also contributed greatly to the quality of my dissertation and to my educational experience.

Jukka Marmo, Hiroshi Ohmoto, and Yumiko Watanabe have all played significant roles in the field observations and data interpretation. They made fieldwork enjoyable with their jokes and challenging with their scientific discussions. The red wine was good too. Gwen Macpherson also made highly valuable scientific contributions and feedback to this work.

Many thanks go to a number of people in the Department of Geology and Planetary Science for their help. Brian Games has helped preserve my sanity by assisting me with laboratory methods and analysis. The administrative staff, past and present, including Dolly Chavez, Candy Weller, T.J. Lipple, Deanna Hitchcock, Todd Bowers and Mat Romick, kept me organized.

Financial support was provided in part by the NASA Astrobiology Institute (NAI), NSF-EAR-0214212 to Rosemary Capo and Brian Stewart, the Penn State Astrobiology Research Center (PSARC), the Pennsylvania Space Grant Consortium, and the University of Pittsburgh.

Friends who helped me to laugh and encouraged me through this process include (in no particular order) Mary Lynn and Ray, the Mest family, Diane, Candace and Lee, Veronica and Chris, Jen and James, Jeff and Janette, the McElfresh family, Amanda, Sally, Deemer, and Adam. Thanks for all of the good times and for not catching too many embarrassing moments on film.

Last but not least, I would like to thank my parents for instilling in me a burning desire to acquire knowledge and to use my mind. They helped me to keep my priorities straight and supported me even when my vision of life was cloudy. My entire family has always supported me through the good times and the occasional catastrophe. Thank you all for your financial and emotional support. I could not have achieved this level without each and every one of you.

1.0 INTRODUCTION

Soils represent the interface between the atmosphere and the lithosphere. Paleosols, preserved ancient soils, preserve a record of past life, climate, and landscapes on planetary surfaces. Paleosols (fossil soil profiles) can provide an important record of atmosphere-lithosphere interactions, which is necessary for accurate reconstructions of the environment in which life developed and evolved on Earth. Pre-Devonian paleosols, however, are devoid of root traces or other overt signs of life and often affected by major post-pedogenic events that can obscure or obliterate the original features indicative of the terrestrial environment. Within early Paleozoic and Precambrian stratigraphic sections, subaerial weathering profiles can be difficult to distinguish from sedimentary deposits, fault breccia, and hydrothermal alteration zones.

Many challenges inhibit the identification and interpretation of the Precambrian soil record, including difficulties constraining ages, chemical overprinting, and post-depositional deformation and obliteration of soil textures and structures (Rye and Holland, 1998). Due to successive post-pedogenic alteration events, such as burial decomposition of organic matter, burial gleization, burial recrystallization of iron compounds, cementation of primary porosity, lithostatic compaction, illitiztion of smectite, and metamorphism, Precambrian paleosols often lack features diagnostic of more modern soils. Physical characteristics common in Paleozoic paleosols and modern soils are typically missing from Precambrian profiles; these include traces

of terrestrial life, distinct soil horizons, and soil structures. Thus, geochemical trends down profile from a sharp erosional contact are often used to recognize Precambrian fossil soils (Retallack, 1997).

To better interpret the soil record of Earth and other ancient planetary surfaces, an integrated approach involving field observations, micromorphological study, geochemical analysis, and isotopic analysis is necessary. An integrated approach to paleosol study should allow us to (1) identify elemental fractionation patterns due to pedogenic processes, (2) better constrain the age of paleosols, (3) examine hydrothermal overprinting, and (4) constrain redox conditions in the weathering profiles. This research focused on two Precambrian sections (in Hokkalampi, Finland and Steep Rock, Canada), previously identified as possible paleosols. Chapter 1 provides an overview of my approach to these research goals.

Chapter 2 examines the Hokkalampi paleosol in north Karelia, Finland. The Hokkalampi paleosol is of particular interest because it formed between 2.44 and 2.2 Ga (Marmo and Kohonen, 1992; Vuollo *et al.*, 1992; Sturt *et al.*, 1994), possibly during the proposed rise of atmospheric oxygen at ca. 2.3 Ga ($>10^{-5}$ present atmospheric level, PAL) (Bekker *et al.*, 2004). To better understand the diagenetic and metamorphic processes that have obscured the ancient soil record, I used an integrated approach involving field observations, micromorphological (soil texture) study, geochemical analysis, and isotopic analysis. One of my goals was to identify pedogenic textures and geochemical signatures, including redox signatures that have survived post-weathering overprinting events. Speciation and mobility of redox-sensitive elements such as iron (Fe) and cerium (Ce) in paleosols have been used to constrain the atmospheric oxygen (pO_2) levels of the early part of Earth's history (Zbinden *et al.*, 1988; Feakes *et al.*, 1989; Holland *et al.*, 1989; Holland and Beukes, 1990; Kirkham and Roscoe, 1993; Holland, 1994;

Macfarlane *et al.*, 1994; Ohmoto, 1996). I also address the key question of whether pedogenic processes during the Precambrian were capable of mobilizing and fractionating rare earth elements (REE). Pedogenic fractionation of REE leads to the possibility of achieving a significant spread in Sm/Nd ratios during soil formation, and thus some constraints of the timing of pedogenesis (Stafford *et al.*, 2000). Additionally, application of the Sm-Nd system in conjunction with the Rb-Sr isotopic system should also provide a better evaluation of element mobility during pedogenesis and subsequent metamorphic events.

Chapter 3 presents a geochemical and textural study of the Steep Rock paleosol at the South Roberts Pit (SRP) exposure in northwestern Ontario, Canada. Rye and Holland (1998) evaluated and ranked Precambrian paleosols based on textural, mineralogical, and chemical evidence as well as soft-sediment deformation. In their review, the Steep Rock profile was categorized as a possible paleosol. This would make it one of the oldest preserved weathering profiles on Earth. The purpose of the present study is to evaluate whether or not the Steep Rock profile can be considered a paleosol, and to determine the extent to which it can serve as a dependable recorder of the Archean paleoenvironment. This involves the acquisition and evaluation of new geochemical evidence of pedogenic processes in the SRP profile; (2) identification of sedimentary features at the unconformity indicative of subaerial weathering in the SRP profile; (3) characterization of the diagenetic and hydrothermal events that altered the SRP profile after pedogenesis, as alteration events lead to the addition and loss of elements and affect paleoenvironmental interpretations; and (4) better constraints on the age of the SRP profile, which has implications for understanding granitoid-greenstone relationships and the origin of the original continental crust in the Superior Province.

Chapter 4 focuses on the paleoenvironmental interpretation of the Steep Rock paleosols and a comparison with that of the Hokkalampi weathering profiles. Because Precambrian paleosols lack significant effects from land plants, researchers (e.g., Holland and Zbinden, 1988; Pinto and Holland, 1988; Kirkham and Roscoe, 1993; Macfarlane *et al.*, 1994; Ohmoto, 1996) have applied a variety of geochemical methods to interpret atmosphere-mineral interaction in Precambrian paleosol profiles formed under different atmospheric conditions. This research builds on earlier work, including the interpretation of iron and cerium concentration variations within the profiles, but includes additional redox sensitive elements such as uranium (U), vanadium (V) and copper (Cu) to further constrain Eh-pH conditions. This will help develop a more accurate interpretation of the redox conditions in the fossil soil record and thus the paleoenvironmental record from the Archean.

2.0 GEOCHEMICAL EVOLUTION OF THE PROTEROZOIC HOKKALAMPI PALEOSOL, EASTERN FINLAND

2.1 INTRODUCTION TO THE HOKKALAMPI PALEOSOL INVESTIGATION

Paleosols, or fossil soils, are a document of past life, atmospheric composition, climate, and terrestrial landscapes. The products of atmosphere-mineral interaction preserved in Precambrian weathering profiles are key to understanding the early composition and evolution of the Earth's atmosphere and the environments in which life developed and evolved. The identification and interpretation of this cryptic paleo-record usually hinges on the analysis of stratigraphic relationships and geochemical signatures. This can be challenging owing to: (1) the lack of overt signs of terrestrial life found in modern soils; (2) difficulty constraining the age of subaerial weathering, which typically can only be bracketed by radiometric dating of underlying, overlying, and/or cross-cutting igneous rocks; (3) chemical overprinting by post-pedogenic events including diagenesis, hydrothermal/metamorphic alteration, and modern weathering processes that frequently lead to addition or loss of elements to the weathering profile; and (4) post-depositional deformation and obliteration of soil textures and structures (e.g., Holland and Zbinden, 1988; Retallack, 1992; Rye and Holland, 1998).

Aurola (1959) recognized that certain Proterozoic aluminosilicate rocks in Karelia, eastern Finland, could represent clay that was recrystallized during a metamorphic event. Marmo (1992) established textural and geochemical evidence for a widespread paleosol in the

Hokkalampi area of the Koli-Kaltimo region in northern Karelia. Here we present the results of an in-depth study of two Hokkalampi weathering profiles from Nuutilanvaara and Paukkajanvaara, Finland, interpreted to have formed under oxidizing and reducing groundwater conditions, respectively (Marmo, 1992).

One goal of this study was to identify pedogenic textures and geochemical signatures, including redox signatures that have survived post-weathering overprinting events. Speciation and mobility of redox-sensitive elements such as iron and cerium in paleosols have been used to constrain the atmospheric oxygen levels of the early part of Earth's history (Zbinden *et al.*, 1988; Feakes *et al.*, 1989; Holland *et al.*, 1989; Holland and Beukes, 1990; Holland, 1994; Macfarlane *et al.*, 1994; Ohmoto, 1996; Watanabe *et al.*, 2000; Beukes *et al.*, 2002; Nedachi *et al.*, 2005). The Hokkalampi paleosol is of particular interest because it formed between 2.44 and 2.2 Ga (Marmo, 1992; Vuollo *et al.*, 1992; Sturt *et al.*, 1994), during the proposed rise of atmospheric oxygen (e.g., Bekker *et al.*, 2004). However, based on recent analyses of multiple sulfur isotope ratios of Archean sedimentary rocks, Ohmoto *et al.* (2006) suggest that the atmospheric pO_2 history may have been more complicated than recognized by previous investigators, and that the atmospheric oxidation may have occurred much earlier than ~2.7 Ga ago. Paleo-redox interpretations of the Hokkalampi paleosol have been difficult due to limited trace element data, particularly from the most heavily weathered sections. In addition, the redox implications of iron data from previous studies of Hokkalampi samples are somewhat ambiguous (Marmo, 1992; Ohmoto, 1996; Rye, 1998). This study integrates petrology, micromorphology, geochemistry, and radiogenic isotope analysis, and includes new samples from a paleosol zone in the Paukkajanvaara section, which is more heavily weathered than zones typically preserved in Precambrian profiles.

A major goal of this study was to evaluate the use of radiogenic isotope systems for identifying and quantifying element mobility during pedogenesis, and for developing a chronology of pedogenesis and post-pedogenic processes. Pedogenic fractionation of rare earth elements (REE) leads to the possibility of achieving a significant spread in Sm/Nd ratios during soil formation, and thus some constraints on the timing of pedogenesis through application of the Sm-Nd isotope system (Stafford *et al.*, 2000). Pedogenesis is unlikely to rigorously satisfy all requirements for the use of the Sm-Nd system as a geochronologic tool, particularly the requirement of uniform initial $^{143}Nd/^{144}Nd$. However, in cases where weathering leads to significant fractionation of Sm from Nd in different parts of a weathering profile, Sm-Nd isotope data might be able to constrain the timing of soil formation better than stratigraphy alone. In addition, application of the more easily reset Rb-Sr isotope system can potentially provide information about the timing of post-pedogenic processes such as metamorphism.

2.2 GEOLOGIC SETTING OF THE HOKKALAMPI PALEOSOL

The Hokkalampi paleosol is one of several Paleoproterozoic weathering profiles developed on the western part of the Archean Karelian Craton. During the Svecokarelian orogeny (1.9-1.8 Ga), the Karelian Craton became part of the Fennoscandian Shield, and today it is the broadest section of preserved and exposed continental core on the European continent. The Archean Presvecokarelidic basement rocks include wide areas of granitoids that intruded mafic metavolcanics and small areas of ultramafics and banded iron formations that formed between 2.5 and 3.1 Ga (Kouvo and Tilton, 1966; Meriläinen, 1980; Simonen, 1980).

A generalized map and stratigraphic section of the study area are shown in **Figure 2.1**. Overlying the Archean basement (in the south only) are glaciogenic sedimentary deposits of the Sariola Group. These sedimentary units and the Archean basement were extensively weathered during an erosional event that caused much denudation and leveling of the paleolandscape. During this event, enormous volumes of continentally derived, supermature, first-cycle quartz sands were deposited across the Karelian Craton (Ojakangas, 1965; Marmo *et al.*, 1988; Kohonen and Marmo, 1992; Marmo, 1992; Marmo and Ojakangas, 1998; Ojakangas *et al.*, 2001). Overlying this unconformity is a sequence of sedimentary rocks (Jatuli Group) with a maximum thickness of 2600 m. The laterally extensive Hokkalampi paleosol consists of 15-80 m of aluminosilicate-rich rocks formed by intense weathering of sedimentary and basement rocks of the Sariola Group (Aurola, 1959; Marmo, 1992). The paleosol grades upward from partially altered parent material consisting of carbonate-bearing, quartz-feldspar sericite (zone 3 of Marmo, 1992), to a weathered zone consisting of quartz-sericite schist (zone 2 of Marmo, 1992), to a highly weathered zone consisting of quartz kyanite andalusite schist (zone 1 of Marmo, 1992) truncated by an erosional boundary. The Hokkalampi paleosol localities sampled for this study developed on granitoid basement, but to the south of the study area are weathering profiles formed on Sariola Group (Urkkavaara Formation) glaciogenic sedimentary rock (Marmo and Ojakangas, 1984; Marmo *et al.*, 1988).

The widespread weathering event that produced the Hokkalampi paleosol also produced weathering profiles in the youngest plutonic rock in the regional area, a 2.44 Ga gabbro in northeast Norway (Sturt *et al.*, 1994; Rye and Holland, 1998). Therefore, the oldest possible age for the Hokkalampi paleosol is 2.44 Ga; the youngest possible age is ~2.2 Ga, the age of the oldest dikes cutting across the paleosol and the overlying sedimentary rocks (Vuollo, 1991). The

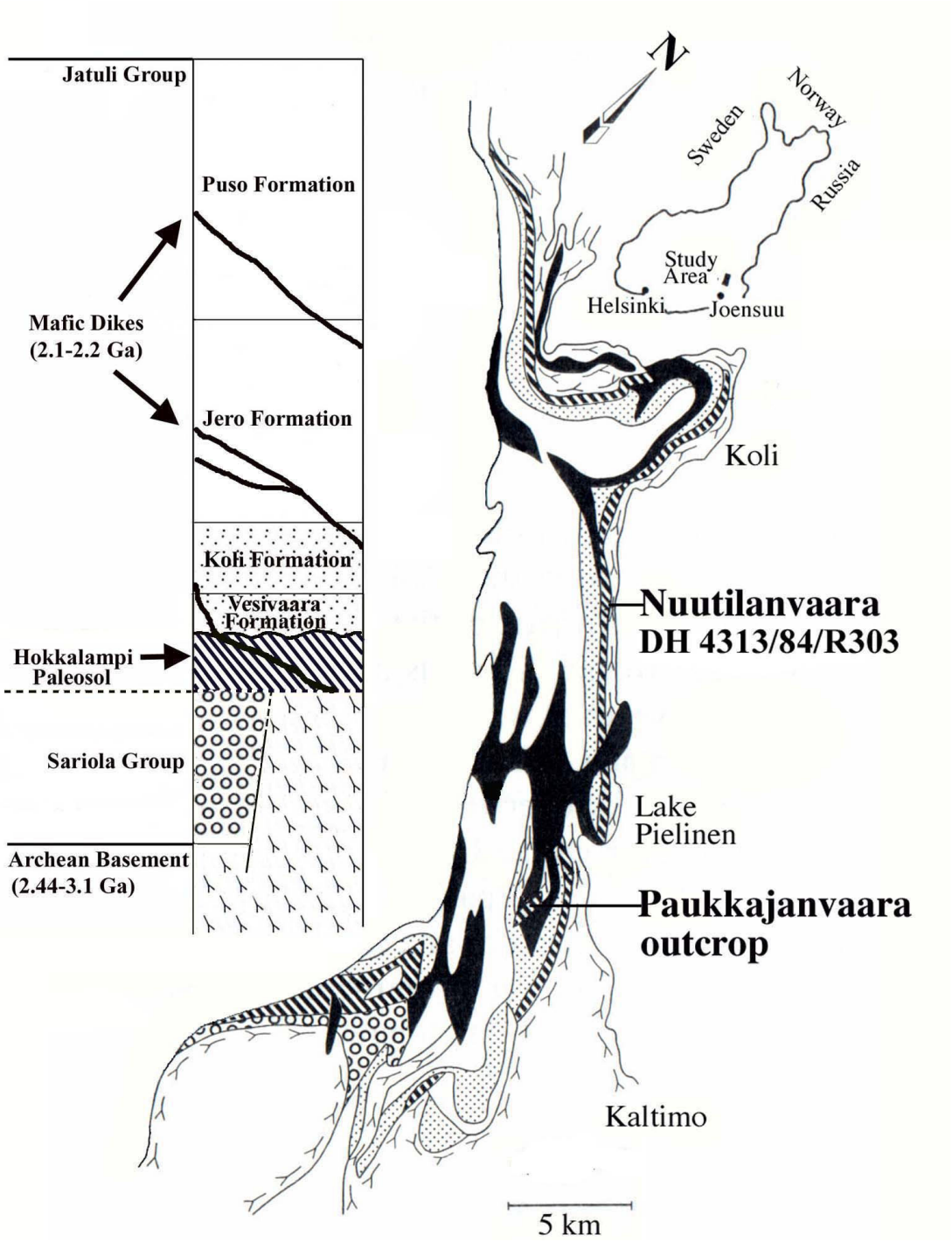

Figure 2.1: Generalized geology and stratigraphy of the Hokkalampi area, eastern Finland. Sample localities (Paukkajanvaara and Nuutilanvaara) are noted. Modified from Marmo (1992).

region underwent greenschist metamorphism during the Svecofennian orogeny, which peaked at 1.9 Ga (Marmo, 1992). Paleomagnetic data place Karelia in low to intermediate latitudes between 2.45 and 2.15 Ga (Neuvonen *et al.*, 1997), making lateritic-type conditions plausible in the Hokkalampi region. However, it is unclear whether climatic zoning of the Paleoproterozoic Earth resembled that of the present day Earth.

Based on the inferred position of the paleo-water table as well as the distribution of overlying pedolith-bearing sedimentary deposits, Marmo (1992) suggested the paleotopographic model for the Hokkalampi soils illustrated in **Figure 2.2**. The weathering profiles exhibit total iron (Fe_T) loss at the top, and down-profile enrichment of Fe_T. Marmo (1992) suggested that the Fe mobilization occurred under reducing conditions (either anoxic atmosphere or waterlogged), with precipitation at or near the paleo-water table. The study also cited the presence of abundant Fe^{2+} in the topographically lower parts of the paleosol (chlorite zones) as further evidence for reducing conditions, but noted that an increase in Fe^{3+} in the lower sections of some profiles could reflect some oxidation. Oxidized zones with excess Fe^{3+} and almost complete absence of Fe^{2+} at the top of the topographically higher, eroded profiles were interpreted as evidence of an increase in atmospheric oxygen just before erosion and burial of the Hokkalampi soils by the alluvial sediments of the Vesivaara Formation. Sedimentary deposits immediately overlying the paleosol contain detrital hematite (Marmo, 1992), likely derived from the paleosol, and serve as additional evidence of soil formation under an oxic atmosphere.

Marmo (1992) analyzed several cores from different parts of the Hokkalampi paleosol. Two cores (301 and 303) show 40% or more Fe loss at the top of the preserved section. Another core (302) shows no corresponding Fe loss. Rye and Holland (1998) suggested that the most heavily weathered section was missing from core 302, and that interpretations of a lack of iron

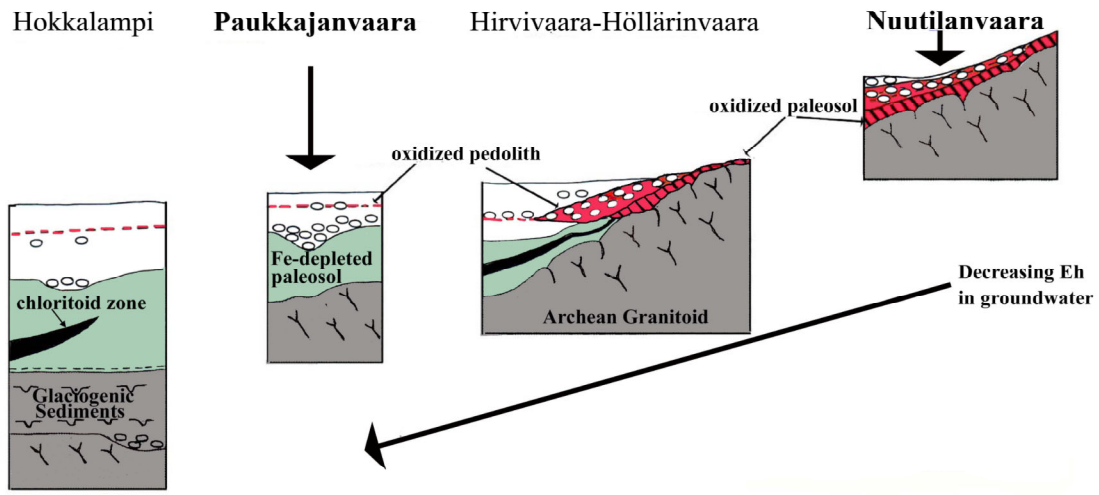

Figure 2.2: Working model of the paleogeography of the Hokkalampi area (from Marmo, 1992) to explain the chemical and sedimentary features observed in the Hokkalampi paleosol. In this model, the more oxidized profiles (i.e. Nuutilanvaara) are inferred to have formed in well-drained conditions, probably in contact with the atmosphere. The more reduced profiles (i.e. Paukkajanvaara) are interpreted to be progressively waterlogged, having formed in topographically lower areas, and they may or may not have been in contact with the atmosphere.

mobility could be compromised as a result. Ohmoto (1996) noted that leaching of Fe^{3+}-rich minerals at low temperatures (<~300°C) requires reductive dissolution by organic acids, and suggested that the loss of ferric and ferrous irons from paleosols is an excellent indicator of an extensive development of biomass on land surface during soil formation. The Hekpoort paleosols in South Africa formed at about the same time and share many similarities with the Hokkalampi paleosols (Beukes *et al.*, 2002). Beukes et al. (2002) argue that the Hekpoort paleosols are groundwater-type paleolaterites, which are characterized by an Fe-depleted zone and an underlying ferric iron enriched zone. Their model proposes the leaching of iron from soil zones

by organic acids and the formation of Fe^{2+}-rich groundwater aquifers during rainy seasons. Additionally, their model proposes additions of O_2 molecules to the groundwater during dry seasons to precipitate ferric hydroxides in the groundwater table.

We have obtained new geochemical and isotopic data from a reduced profile (Paukkajanvaara) and an oxidized profile (Nuutilanvaara) to better constrain the age of the weathering event and to assess the preservation of pedogenic signatures despite subsequent greenschist metamorphism. We also explore alternate processes for major and trace element mobility, including leaching by organic acids and hydrothermal-metamorphic mobilization.

2.3 METHODS IN THE HOKKALAMPI STUDY

Drill core samples (Core 303) from the Nuutilanvaara locality were retrieved from the Geological Survey of Finland drill core archives. Outcrop samples were collected during the summer of 2000 from the Paukkajanvaara locality using a hammer or portable saw. The weathering profiles in both locations formed on Archean granitoid. Three basement rock samples from the Paukkajanvaara site were obtained to determine the average composition of the parent material granitoid, which is relatively homogenous in the study area.

Most samples were prepared for geochemical analyses at the University of Pittsburgh, with the exception of the three parent material samples, which were powdered at the Geologic Survey of Finland. Whole-rock samples were crushed using a jaw crusher, powdered using a tungsten-carbide mixer-mill, and split to aliquots ranging from tens of milligrams to ~1 g.

Whole rock geochemistry was determined by ACME Analytical Laboratories, Ltd., in Vancouver, BC; major elements were analyzed by ICP-AES, trace elements were analyzed by ICP-MS, and FeO was determined by dichromate titration.

Rubidium-strontium and samarium-neodymium chemistry were carried out under clean laboratory conditions at the University of Pittsburgh. Whole rock samples of 50 to 200 mg were dissolved in Teflon© bombs using ultrapure hydrofluoric (HF), perchloric ($HClO_4$), and hydrochloric (HCl) acids. An aliquot of 1-5 mg was removed and spiked with a mixed ^{87}Rb-^{84}Sr-^{147}Sm-^{150}Nd tracer solution, and rough concentrations were determined using isotope dilution thermal ionization mass spectrometry. Based on these results, the remaining sample was spiked with mixed, isotopically pure ^{87}Rb-^{84}Sr and ^{147}Sm-^{150}Nd tracer solutions. Following addition of the tracer solutions, Rb, Sr, and the REE were separated from the remaining matrix using cation exchange columns. Samarium and neodymium were separated from the other REE and each other in quartz columns containing LNSpec® resin.

Rubidium was loaded on a single rhenium filament and its concentration determined by isotope dilution on a Finnigan MAT 262 thermal ionization mass spectrometer (TIMS) at the University of Pittsburgh. Strontium (~250 ng) was loaded on a single Re filament with Ta-oxide powder, and the concentration and isotope composition were determined simultaneously by TIMS. For each sample, 100 ratios were measured at an intensity of 2-4 x 10^{-11} amperes (A), and mass fractionation was corrected using an exponential law with $^{86}Sr/^{88}Sr = 0.1194$. Ratios of $^{87}Rb/^{86}Sr$ are good to $\leq$1% of the measured value. Strontium standard SRM 987 was run continually throughout the measurement period, and all measured $^{87}Sr/^{86}Sr$ ratios are consistent with SRM 987 = 0.71024.

Both neodymium and samarium were loaded on double Re filaments. Concentrations of Sm were determined by isotope dilution, and the concentration and isotopic composition of Nd were determined simultaneously by TIMS, with 100 ratios measured at an intensity of 0.5-2 x 10^{-11} A. $^{143}Nd/^{144}Nd$ ratios were corrected for mass fractionation using an exponential law and normalizing to $^{146}Nd/^{144}Nd = 0.724134$. The maximum uncertainty in the $^{147}Sm/^{144}Nd$ measurements is 0.2% of the measured value. The University of Pittsburgh value for chondritic $^{143}Nd/^{144}Nd$ is 0.511847, based on multiple analyses of the La Jolla Nd standard. The reported uncertainties for all isotope analyses ($^{87}Sr/^{86}Sr$ and $^{143}Nd/^{144}Nd$) reflect both in-run and external reproducibility.

2.4 HOKKALAMPI RESULTS

2.4.1 Petrology of the Hokkalampi Profiles

2.4.1.1 Mineralogy and Micromorphology of Pedogenesis

Both the Paukkajanvaara ("reduced") and Nuutilanvaara ("oxidized") sections exhibit a gradational increase in weathering upward from the parent granitoid. The lowermost sections (zone 3 of Marmo, 1992) of both profiles contain granitic rock fragments with primary quartz and twinned plagioclase grains (e.g., PK 43, 14 m depth; **Figure 2.3c**). These lithorelicts (sensu Brewer, 1976, p. 146) are surrounded by a matrix of finer-grained quartz and secondary sericite and carbonate; grain boundaries contact sporadically (agglomeroplasmic microfabric, sensu Brewer, 1976, p. 170). Minerals most susceptible to chemical weathering (plagioclase, biotite,

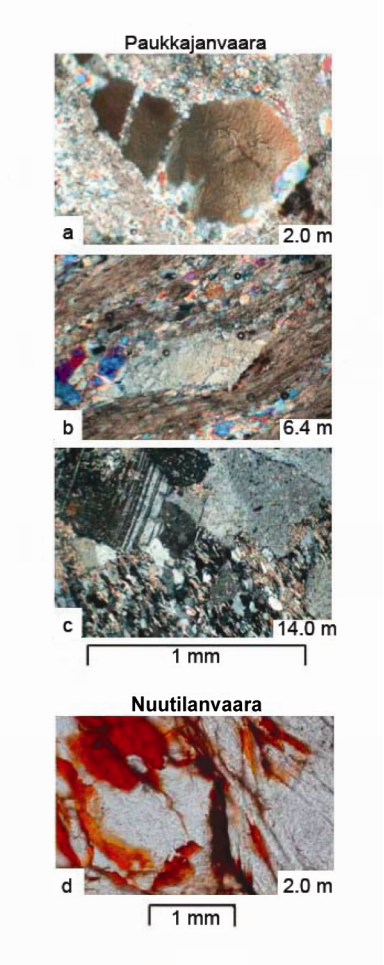

Figure 2.3: Photomicrographs of weathering and post-pedogenic alteration textures in the Hokkalampi paleosol: (1) Paukkajanvaara profile- (a) Quartz grain coated by sericite, (likely replacement for kaolinite) cutan and indicative of *in situ* weathering (highly weathered, zone 1; PK 36); (b) Recrystallized quartz floating in fine-grained sericite matrix (agglomeroplasmic microfabric) and overprinted by metamorphic foliation (moderately weathered, zone 2; PK 30); (c) Island of granitoid (upper part of photograph) surrounded by matrix of sericite, carbonate and quartz with sporadically touching grains (intertexic microfabric) (partially weathered, zone 3; PK 43). (2) Nuutilanvaara profile- (d) Quartz grains coated by ferrans (iron oxide cutans), which could indicate exposure to oxygen prior to burial and are indicative of *in situ* weathering (moderately weathered, zone 2: N 66.5). Depths (m) below the unconformity are shown.

potassium feldspar) are mottled and contain pits filled with sericite and carbonate. Sericite is likely a metamorphic replacement for kaolinite, a common 1:1 product of subaerial weathering (Delvigne, 1998). Alteration apparently initiated in mineral fractures and progressively widened outward, leaving islands of protolith surrounded by matrix. In both profiles, zone 3 (which corresponds to a weathered C soil horizon) transitions upward to one with textures more indicative of B horizon pedogenic processes (zone 2 of Marmo, 1992). Here rare remnant plagioclase and potassium feldspar grains are intensely altered, although resistant quartz grains show no signs of chemical attack (e.g., PK 30, depth= 6.4 m; **Figure 2.3b**; corresponding to lower B horizons**)**. Clumps and accordion shapes of sericite could reflect the flocculation and swelling of clay minerals prior to metamorphism. An increase in sericite (presumed to be metamorphically altered clay) and chloritized, exfoliating biotite is correlated with increased chemical weathering intensity up profile. Quartz grains are recrystallized, occur mainly in pockets and stringers, and are occasionally coated by sericite grains (agglomeroplasmic fabric; possibly metamorphosed argillans (clay cutans); e.g., PK 36, 2.0 m depth; **Figure 2.3a**) or ferrans (iron oxyhydroxide cutans; e.g., N 66.5, 2.0m depth; **Figure 2.3d**). Iron oxide coatings are found in soils and paleosols in which Fe has been mobilized and deposited locally (Delvigne, 1998). The ferrans found at the top of the Nuutilanvaara profile could indicate exposure to oxygen prior to burial by overlying sediment (Jackson and Sherman, 1953); these are observed in early Paleozoic paleosols (e.g., Capo, 1993).

Where weathering is most intense (zone 1 of Marmo, 1992; absent in the Nuutilanvaara profile), even quartz exhibits pitting and corrosion. Quartz grains are isolated and surrounded by fine-grained matrix (porphyroskelic microfabric, sensu Brewer, 1976, p. 170). This zone corresponds to an upper B soil horizon. The presence of embayed grains, mineral coatings,

spalling grains and intertextic, agglomeroplasmic and porphyroskelic microfabrics throughout the two profiles are indicative of *in situ* changes due to pedogenesis, preserved even after metamorphism.

2.4.1.2 Post-Pedogenic Alteration Fabrics

The minerals and textures preserved in both profiles are consistent with subaerial weathering that was followed by a greenschist metamorphic event that produced schistosity. The present mineral assemblage is likely the result of the alteration of primary minerals such as biotite to chlorite and iron oxides, and the recrystallization of weathering products, such as kaolinite to sericite. Microcrystalline quartz and epidote or carbonate produced by the breakdown of plagioclase during weathering apparently remained intact during metamorphism. Larger grains of primary quartz survived and preserve spalling and evidence of dissolution. Most of the sericite appears to have formed synmetamorphically, as it follows the foliation direction. However, some may have formed pre-metamorphically, as evidenced by its crenulated texture (e.g., Philpotts, 1989). Chloritized biotite appears to be both prograde and retrograde, as some of the grains cut across the schistose fabric. From the bottom to the top of each profile, there is a general increase in schistosity, quartz recrystallization, and amount of strained quartz. This could be the result of weathering-induced porosity, which would enhance fluid flow in the upper, more pedogenically altered portions of the profiles relative to the parent granitoid during metamorphism.

2.4.2 Major and Trace Element Concentrations in the Hokkalampi Profiles

2.4.2.1 Major Elements in the Hokkalampi Profiles

Bulk-sample elemental data are summarized in **Table 2.1**. Major elements are reported as oxides, with the partitioning between FeO and Fe_2O_3 based on the dichromate titration. In soils and paleosols, elemental data are generally normalized to a relatively immobile element, such as aluminum (Al), titanium (Ti), zirconium (Zr), niobium (Nb) or hafnium (Hf), to account for volume changes during weathering and for concentration or dilution due to gain and loss of other

Table 2.1: Whole rock major element concentrations (in wt%) of Hokkalampi samples.

Sample Name	Depth (m)	SiO_2	Al_2O_3	Fe_2O_3	FeO	MnO	MgO	CaO	Na_2O	K_2O	TiO_2	P_2O_5	Cr_2O_3	LOI[b]	Total[c]	C_{total}	S_{total}
Paukkajanvaara																	
00 PK 42	-1.0	71.8	16.37	1.36	0.4	0.02	1.04	0.27	3.52	3.52	0.26	0.06	0.001	2.2	100.8	0.03	<0.01
00 PK 39	0.3	76.5	17.18	0.03	0.1	<0.01	0.02	0.01	0.05	1.14	0.14	<0.01	0.001	5.1	100.2	0.01	<0.01
00 PK 38	0.6	74.7	18.34	0.15	0.1	<0.01	0.02	0.01	0.13	1.80	0.45	0.02	0.003	4.7	100.4	0.04	<0.01
00 PK 37	1.0	75.6	18.44	0.13	0.1	<0.01	0.01	0.01	0.10	1.24	0.32	<0.01	0.001	4.3	100.2	0.03	0.02
00 PK 36	2.0	76.8	18.19	0.11	0.1	<0.01	0.01	0.04	0.06	1.19	0.19	0.05	<0.001	3.3	100.0	0.07	0.02
00 PK 41	3.0	75.9	17.92	0.09	0.1	<0.01	0.01	0.02	0.10	1.64	0.27	0.02	<0.001	4.0	100.1	0.02	0.01
00 PK 40	3.4	75.7	17.93	0.05	0.1	<0.01	0.04	0.04	0.15	1.79	0.63	0.04	0.016	3.4	99.9	<0.01	0.01
00 PK 33	3.7	75.9	16.79	0.19	<0.1	<0.01	0.03	0.02	0.24	3.26	0.27	<0.01	0.005	3.1	99.8	<0.01	0.01
00 PK 32	4.9	75.2	17.12	0.49	0.1	<0.01	0.14	0.07	0.25	4.74	0.39	0.04	0.006	2.6	101.2	0.05	0.02
00 PK 31	5.4	76.1	15.91	0.42	0.1	<0.01	0.15	0.10	0.28	4.49	0.30	0.06	<0.001	2.3	100.2	0.03	0.01
00 PK 30	6.4	77.5	15.37	0.27	0.1	<0.01	0.12	0.08	0.23	4.34	0.26	0.05	<0.001	2.2	100.5	0.01	<0.01
00 PK 22	10.0	77.1	13.26	1.70	0.1	0.01	0.95	0.03	0.14	4.89	0.15	<0.01	<0.001	1.5	99.9	0.01	0.01
00 PK 43	14.0	76.0	13.71	0.67	0.5	0.02	1.11	0.17	5.18	1.96	0.10	<0.01	<0.001	0.3	99.8	0.02	0.02
Nuutilanvaara																	
R303 N 59.0	-1.0	83.9	10.69	0.78	0.2	<0.01	0.13	0.02	0.17	2.64	0.24	<0.01	0.006	1.7	100.5	0.02	<0.01
R303 N 66.5	2.0	60.2	23.78	2.41	0.1	<0.01	0.47	0.44	0.45	8.00	1.01	0.31	0.001	2.4	99.6	<0.01	0.01
R303 N 70.3	5.8	72.1	13.89	0.98	0.5	0.02	0.62	2.94	2.30	2.94	0.11	0.05	<0.001	4.0	100.4	0.57	0.03
R303 N 76.5	11.0	75.4	12.95	1.00	0.6	0.02	0.71	1.60	2.26	2.99	0.14	0.05	<0.001	2.2	99.9	0.32	0.01
R303 N 80.1	15.0	68.7	15.66	1.71	1.5	0.02	1.43	1.08	0.42	5.26	0.29	0.16	0.006	3.4	99.7	0.17	0.03
Parent Material																	
Parent 1A	>15.0	71.5	15.56	1.05	0.6	0.02	1.64	0.30	4.63	2.68	0.22	0.06	n/a	1.5	99.7	0.01	<.01
Parent 2	>15.0	74.5	14.27	1.07	0.4	0.02	1.12	0.24	4.17	2.55	0.13	0.02	n/a	1.3	99.8	0.04	0.01
Parent 4	>15.0	71.1	16.05	1.30	0.4	0.01	0.86	0.53	4.53	2.86	0.43	0.17	n/a	1.4	99.6	0.05	<.01
Average Parent (1A, 2, 4)	>15.0	72.4	15.29	1.14	0.5	0.02	1.21	0.36	4.44	2.70	0.26	0.08	n/a	1.4	99.7	0.03	n/a

[a] ACME Analytical Laboratories LTD.; Method: $LiBO_2$ Fusion, Analysis by ICP-ES. FeO by dichromate titration. Total C and S measured by LECO CNS Analyzer.
[b] LOI = loss on ignition
[c] Total includes LOI; excludes C_{total} and S_{total}.

elements during weathering processes (Chadwick *et al.*, 1990). These elements are typically chosen for normalization purposes according to criteria such as abundance, homogeneity of distribution, and relative chemical immobility (Rye and Holland, 1998; Driese *et al.*, 2000; Kurtz *et al.*, 2000). For the Hokkalampi profile samples, only the ratio of Ti/Nb varies by less than 40% from the granitoid parent material in either profile (**Figure 2.4a**), consistent with the distribution of immobile elements in modern soil profiles (Maynard, 1992). The other normally immobile elements measured in this study (Al and Zr) vary from the parent material by >40%

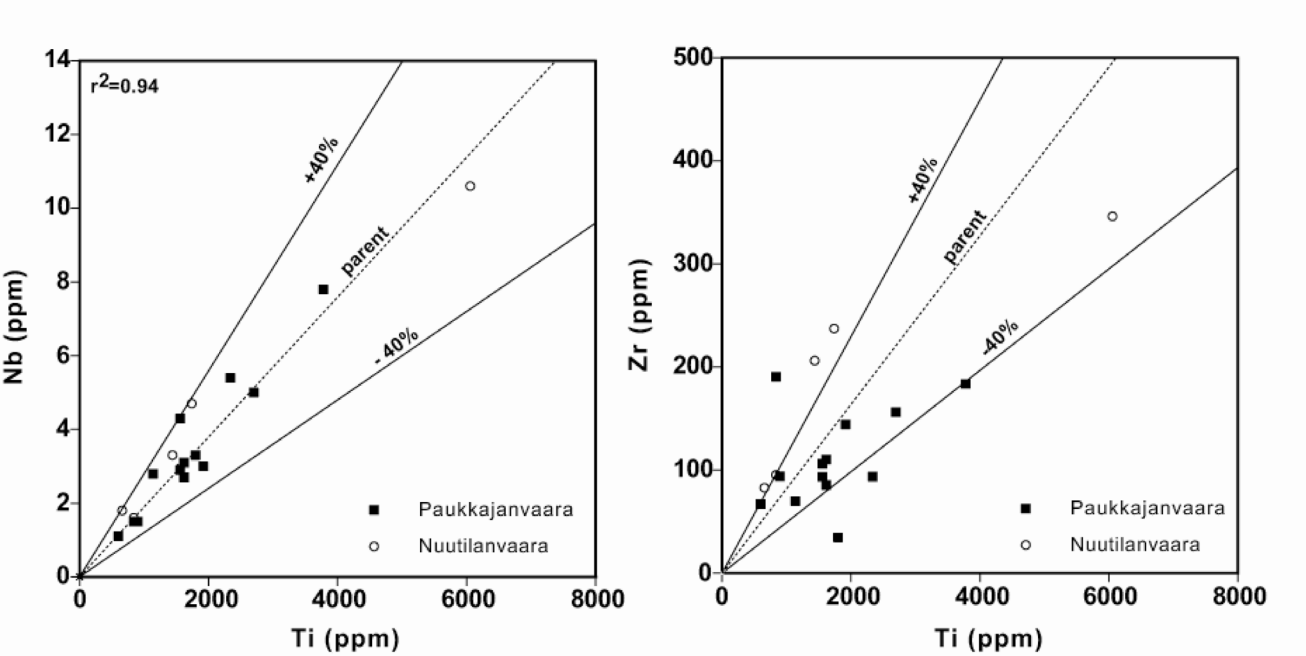

Figure 2.4: Variation of Ti with Nb and Zr for the Nuutilanvaara and Paukkajanvaara sections of the Hokkalampi paleosol.

when plotted against each other or against Ti and Nb (e.g., Zr vs. Ti, **Figure 2.4b**). The Variation in Zr/Ti ratios probably reflects the heterogeneity of parental rocks, rather than the dissolution/reprecipitation of Zr. Therefore, we use Ti for normalization of elemental data due to

its abundance (relative to Nb) and relatively homogeneous distribution throughout both profiles. The Ti/Nb ratios in the conglomerate overlying the paleosol were also within 40% of the parent, suggesting that the conglomerate could be derived from reworked paleosol material and granitoid, as suggested by Marmo (1992). The relative gain or loss of an element in a weathering profile can be calculated by comparing element/Ti ratios of the profile to that of the parent material. This mass balance is expressed by $100[(R_W-R_P)/R_P]$, where R_W is the ratio of an element to Ti in the weathered sample and R_P is the ratio of the element to Ti in the unweathered parent (Nesbitt, 1979; Nesbitt and Markovics, 1997). Elemental ratios from the Paukkajanvaara and Nuutilanvaara profiles and the overlying conglomerate (containing transported paleosol) of the Hokkalampi area show significant differences from the underlying granitoid (**Figure 2.5**).

Most samples from the moderate to highly weathered portions of the paleosol (zones 1 and 2) of both profiles, as well as the conglomerate above both profiles, show significant depletion of the mobile elements calcium (Ca), magnesium (Mg), and sodium (Na) relative to parent material (**Figure 2.5**). This loss of base cations from both weathering profiles is typical for intensively weathered soils and paleosols (e.g., Nesbitt *et al.*, 1980; Rainbird *et al.*, 1990; Nesbitt and Markovics, 1997; Panahi *et al.*, 2000; Chadwick *et al.*, 2003). Concentrations of Ca and Mg increase significantly in the lower portions (zone 3) of both profiles. In particular, the extreme enrichment of Ca in zone 3 of the Nuutilanvaara profile (to nearly 2000% of the parent value) suggests accumulation of pedogenic carbonate. Potassium (K) deviates from the trend of the other alkalis and the alkaline earth metals in that it is significantly enriched relative to the parent through most of the profile (**Figure 2.5**). This kind of enrichment is not expected from pedogenic processes, and it suggests later addition of K to the profile, either through diagenesis or metamorphism/metasomatism.

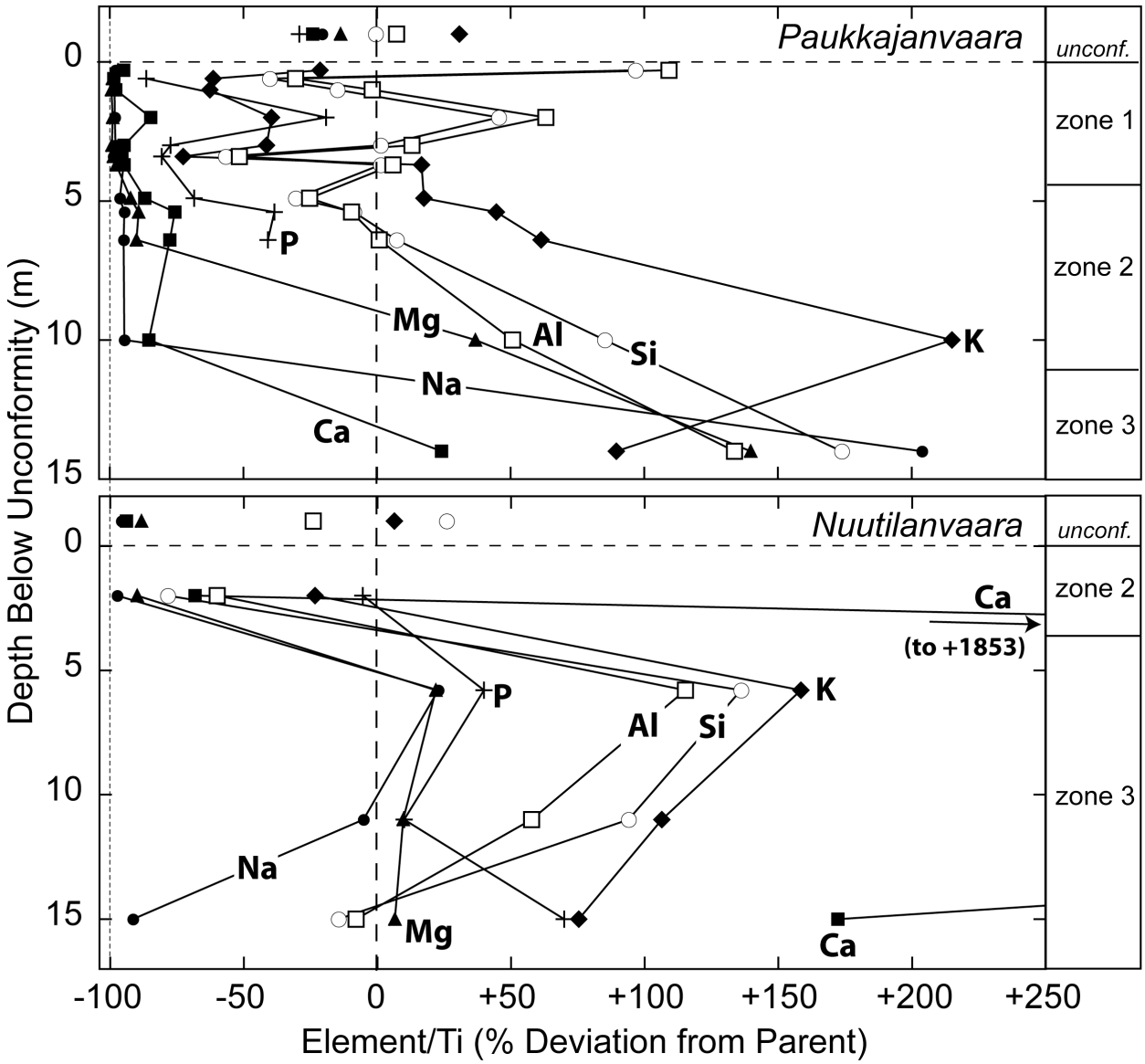

Figure 2.5: Percent deviation of major elements (Ti-normalized) from parent granitoid with depth in the Paukkajanvaara and Nuutilanvaara profiles. Note that Ca is off-scale in the Nuutilanvaara profile, reaching +1853% at 5.8 m and +735% at 11 m depth.

Variation of Ti-normalized total Fe (Fe_T), Fe^{2+}, and Fe^{3+} from average parent material with depth for both profiles is shown in **Figure 2.6**. In the Paukkajanvaara profile, Fe_T is significantly depleted (-96%) in zone 1, but increases in zone 2 and exhibits enrichment over parent of up to +95% in zone 3. Fe^{3+} shows more enrichment than Fe^{2+} in the mid to lower profile, reaching enrichments as high as +159% relative to parent material at the base of zone 2. At the bottom of the profile, Fe^{2+} is more enriched (+187%) than Fe^{3+} (+54%). At the top of the Nuutilanvaara profile, which represents the lower part of zone 2 (moderately weathered), Fe_T is depleted by 60% compared to the parent granitoid. Fe_T increases to +122% over parent in zone 3. In this zone, Fe^{2+} is more enriched than Fe^{3+} (up to +197% compared to up to +105%). In the sedimentary deposits immediately overlying the profiles, thought to represent paleosol-derived material (Marmo, 1992), Fe^{3+} is less depleted than Fe^{2+}, and in fact shows a slight enrichment over the Paukkajanvaara profile (+19%).

2.4.2.2 Trace Elements in the Hokkalampi Profiles

Rare earth element (REE) and selected trace element data are reported in **Table 2.2**. Chondrite-normalized REE plots for samples from each profile, along with the range in parent material, are presented in **Figure 2.7**. Different samples of parent material (shaded region) vary in their REE concentrations by as much as a factor of ~24, but all show the strong enrichment in light rare earth elements (LREE: La to Sm) relative to chondrites expected from a granitic parent lithology (**Figure 2.7a,b**). Paleosol samples from the Paukkajanvaara profile (**Figure 2.7a**) generally fall in the range of parent material values, although they show considerably more variation in LREE than in the heavy rare earth elements (HREE: Gd to Lu), with some LREE falling below the lowest parent concentrations measured. In contrast, most of the weathered samples from the Nuutilanvaara profile (**Figure 2.7b**) tend to have relatively high HREE

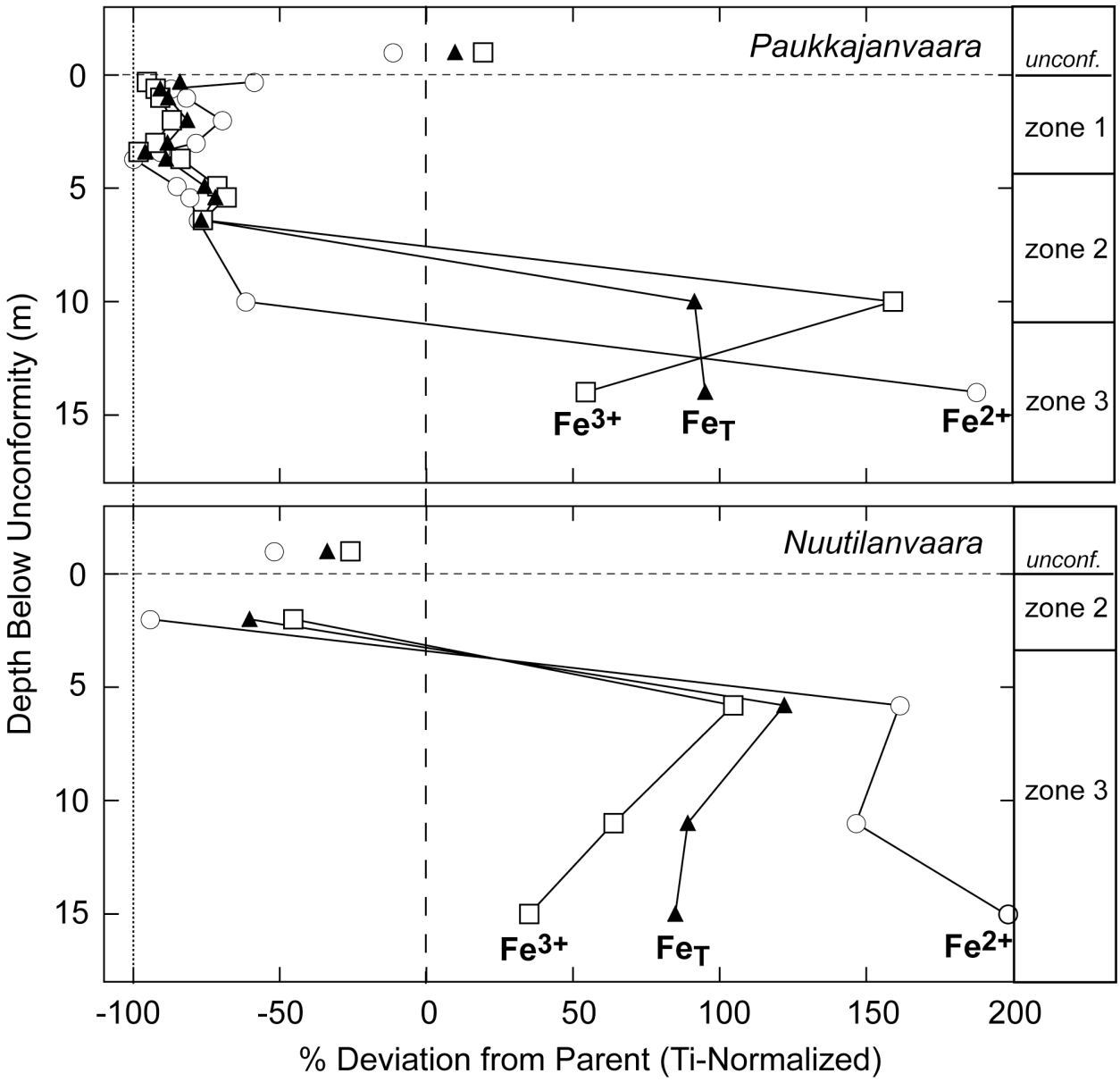

Figure 2.6: Percent deviation of Ti-normalized Fe_T, Fe^{2+} and Fe^{3+} from parent granitoid (calculated as $100[Fe_{sample}/Fe_{parent} - 1]$) with depth in the Paukkajanvaara and Nuutilanvaara profiles.

Table 2.2: Whole rock analysis of trace elements for the Hokkalampi paleosol.

Sample Name	Nb	Zr	U	Th	Rb	La	Ce	Pr	Nd	Sm	Eu	Gd	Dy	Er	Yb	Lu
Paukkajanvaara																
00 PK 42	4.3	106	4.4	0.7	139	1.3	5.7	0.54	2.8	0.6	0.33	0.97	0.50	0.32	0.26	0.08
00 PK 39	1.5	191	1.6	4.2	31.0	17.7	30	2.65	9.5	0.8	0.17	0.40	0.44	0.28	0.48	0.10
00 PK 38	5.0	156	0.7	4.5	48.9	33.2	54.3	5.16	15.6	1.4	0.39	0.90	0.30	0.19	0.24	0.05
00 PK 37	3.0	144	1.0	4.1	33.0	19.9	31.7	2.89	7.8	0.7	0.19	0.61	0.63	0.45	0.48	0.09
00 PK 36	2.8	70	0.6	15.7	30.3	102	220	27.3	110	15.8	3.32	6.48	1.16	0.19	0.34	0.03
00 PK 41	2.7	111	1.3	0.7	40.1	31	56.8	6.05	22.9	2.6	0.57	0.91	0.58	0.32	0.41	0.09
00 PK 40	7.8	184	1.5	8.3	44.3	125	246	25.7	85.5	10.1	2.22	4.26	2.68	1.50	1.41	0.22
00 PK 33	3.1	86	1.0	0.9	75.3	19.7	30.8	3.35	12.5	1.7	0.56	1.10	0.92	0.51	0.41	0.06
00 PK 32	5.4	94	2.8	3.9	117	55.6	110	13.6	52.3	7.0	1.01	3.15	0.81	0.17	0.29	0.03
00 PK 31	3.3	35	1.0	1.7	107	5.5	12.7	1.46	6.3	1.0	0.15	1.27	0.70	0.39	0.27	0.04
00 PK 30	2.9	94	3.0	0.9	98.8	2.5	4.8	0.47	2.0	0.4	<.05	0.80	0.48	0.20	0.24	0.03
00 PK 22	1.5	94	7.9	0.8	159	1.5	3.9	0.62	3.4	1.0	0.00	0.64	0.32	0.18	0.20	0.03
00 PK 43	1.1	67	3.6	0.4	74.4	7.2	20.6	2.13	8.6	1.3	0.40	0.68	0.44	0.23	0.22	0.03
Nuutilanvaara																
R303 N 59.0	3.3	206	1.2	20.0	97.4	28.3	55.6	6.13	19.8	3.3	0.56	2.66	1.54	0.82	0.69	0.12
R303 N 66.5	10.6	346	2.4	40.3	258	86.9	143	24.3	96.6	18.6	3.06	15.09	12.68	7.08	4.83	0.65
R303 N 70.3	1.8	83	1.0	11.3	126	26.9	49.4	5.35	16.3	2.5	0.59	1.52	1.15	0.50	0.39	0.07
R303 N 76.5	1.6	95	0.6	1.8	123	9.1	16.8	1.88	6.8	1.1	0.27	0.65	0.55	0.35	0.39	0.05
R303 N 80.1	4.7	237	4.0	31.6	211	85.3	171	18.4	64.3	10.6	2.56	6.53	4.77	2.25	1.67	0.21
Parent Material																
Parent 1A	2.3	100	1.2	2.5	112	11.2	32.4	3.22	12.4	1.6	0.40	0.98	0.50	0.24	0.26	0.04
Parent 2	1.5	60	0.7	0.7	99.1	5.7	10.7	1.02	3.70	0.5	0.28	0.31	0.15	0.08	0.13	0.02
Parent 4	5.8	286	4.8	33.2	111	87.2	247	23.9	87	11.1	2.66	5.30	2.39	0.86	0.92	0.11
AVG PARENT (1a, 2, 4)	3.2	149	2.2	12.1	108	34.7	96.6	9.39	34.4	4.4	1.11	2.20	1.01	0.39	0.44	0.06

[a] ACME Analytical Laboratories LTD.; Method: $LiBO_2$ fusion, analysis by ICP-MS

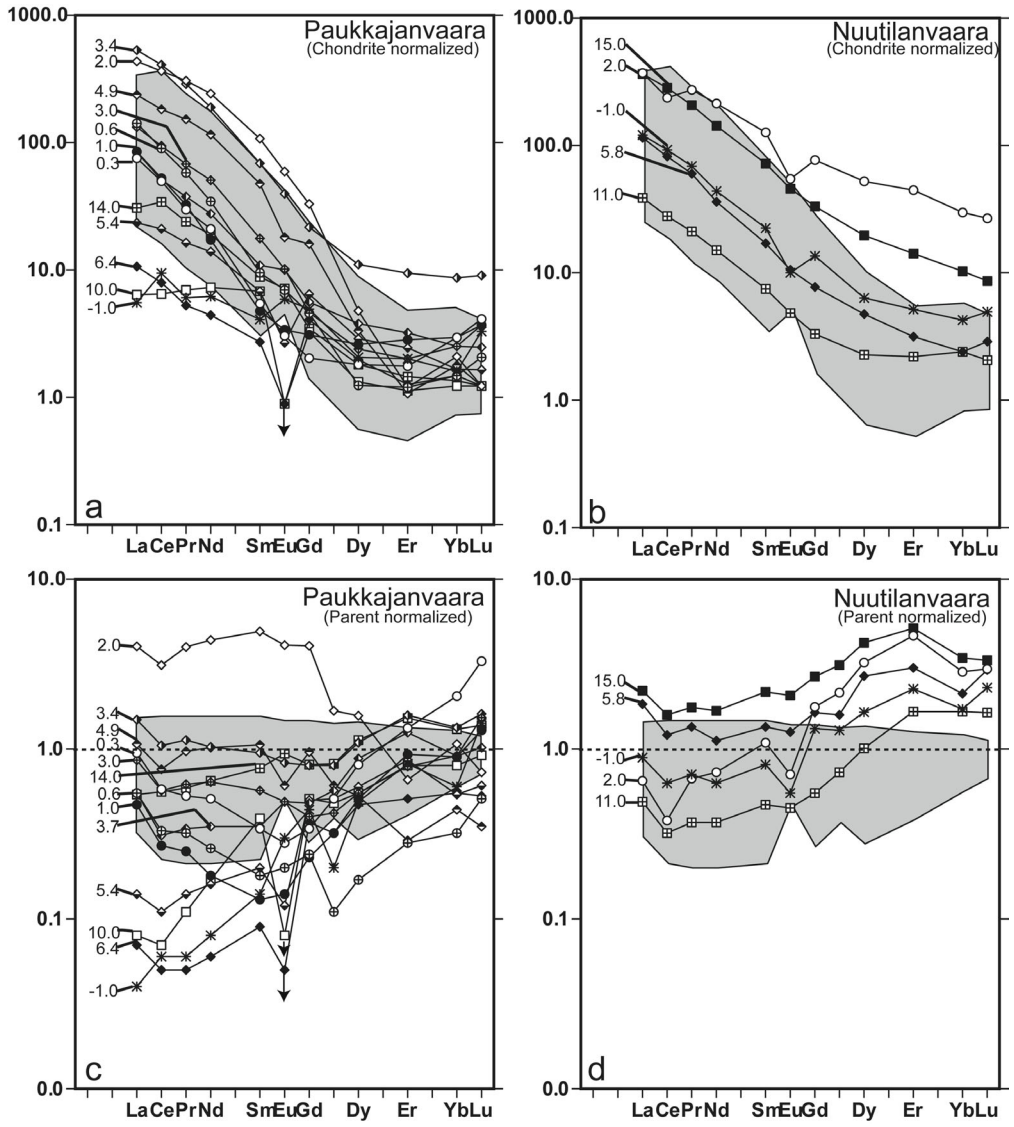

Figure 2.7: Normalized rare earth element concentrations for Hokkalampi samples. Shaded areas reflect the range of parent material values. (a) REE concentrations of the Paukkajanvaara samples normalized to chondrites. (b) REE concentrations of the Nuutilanvaar Nuutilanvaara samples normalized to chondrites. (c) REE concentrations of the Paukkajanvaara samples normalized to average parent material. (d) REE concentrations of the Nuutilanvaara samples normalized to average parent material. Depths below the unconformity for each sample are noted on the left side of each plot.

contents and LREE patterns subparallel to those of the parent material samples. Two samples show measurable Ce anomalies (**Figure 2.7a, b**): Sample 00 PK 42 from the conglomerate overlying the Paukkajanvaara profile (positive anomaly), and Sample R303 N 66.5 from 2 m below the unconformity in the Nuutilanvaara profile (negative anomaly).

To facilitate comparison of weathered samples to the parent material, we plot the paleosol REE normalized to both the immobile element Ti and the average parent material REE (Figure 2.7c, d). This not only allows evaluation of weathering effects on REE patterns, but also allows us to quantify absolute gain or loss of REE during soil development. When normalized to Ti, the maximum spread in parent material REE concentrations decreases by about a factor of three. As shown in **Figure 2.7c**, most of the weathered Paukkajanvaara profile samples fall below the average parent material value, and are indicative of leaching of REE. In some cases LREE in some cases show a greater depletion than HREE. These patterns indicate that fluids leached rare earth elements in many parts of the profile. In contrast, the REE patterns from the Nuutilanvaara profile (**Figure 2.7d**) straddle the parent material values, with enrichment in HREE suggesting some accumulation of REE in the profile. Nearly all parent-normalized REE patterns show a small negative Ce anomaly. This reflects a small positive Ce anomaly measured in the parent material, rather than pedogenic depletion of Ce.

2.4.3 Radiogenic Isotopes in the Hokkalampi Profiles

Results from Rb-Sr and Sm-Nd analyses of selected samples from the Paukkajanvaara and Nuutilanvaara profiles are presented in **Table 2.3**. The data show a significant spread in the $^{87}Rb/^{86}Sr$ (2.7 to 38.4) and present-day (measured) $^{87}Sr/^{86}Sr$ (0.7870 to 1.6946). The $^{147}Sm/^{144}Nd$ values range between 0.0725 and 0.1761, commensurate with the various degrees of LREE

Table 2.3: Rb-Sr and Sm-Nd data for the Hokkalampi paleosol. Concentrations (by isotope dilution TIMS) are in ppm.

Sample Name	Depth (m)	Rb	Sr	Sm	Nd	$^{87}Rb/^{86}Sr$	$^{87}Sr/^{86}Sr(0)$	$^{147}Sm/^{144}Nd$	$\varepsilon_{Nd}(0)^a$	$\varepsilon_{Nd}(T)^b$
Paukkajanvaara										
00 PK 40	3.4	44.2	47.2	9.7	81.0	2.73	0.787029 ± 11	0.0725	-41.79 ± 0.27	-4.07 ± 0.32
00 PK 33	3.7	76.5	22.9	1.9	12.8	9.85	0.913362 ± 15	0.0894	-37.43 ± 0.31	-4.85 ± 0.37
00 PK 22	10.0	161.5	13.4	0.9	3.0	38.4	1.694540 ± 27	0.1761	-10.98 ± 0.31	-4.75 ± 0.42
00 PK 43	14.0	79.1	42.0	1.1	6.5	5.55	0.876046 ± 12	0.1021	-34.05 ± 0.33	-5.33 ± 0.40
Nuutilanvaara										
R303 N 66.5	2.0	247.7	72.3	16.5	87.7	10.2	0.980635 ± 18	0.1137	-28.45 ± 0.31	-3.23 ± 0.38
R303 N 76.5	11.0	122.3	87.5	0.9	5.8	4.10	0.832192 ± 12	0.0988	-35.62 ± 0.27	-5.89 ± 0.33
R303 N 80.1	15.0	212.0	53.2	10.3	60.9	11.9	1.020872 ± 74	0.1019	-33.41 ± 0.29	-4.63 ± 0.36

[a] Chondritic $^{143}Nd/^{144}Nd(0) = 0.511847$

[b] Corrected to an age of 2.35 Ga ago (see *Section 5.1.1*).

enrichment observed in the samples (**Figure 2.7a, b**). The neodymium isotope ratio calculated for any time in the past (time T in years before present) is presented in equation 2.1 using the standard ε notation:

$$\varepsilon_{Nd}(T) = 10^4 \frac{^{143}Nd/^{144}Nd_{sample}(T)}{^{143}Nd/^{144}Nd_{CHUR}(T)} - 1 \qquad (2.1)$$

where CHUR is the chondritic meteorite value. Present-day (measured) values, $\varepsilon_{Nd}(0)$, for the paleosol samples range from -11.0 to -41.8 (**Table 2.3**), reflecting the age and wide range in Sm/Nd of different portions of the weathering profile.

2.5 DISCUSSION OF HOKKALAMPI DATA

2.5.1 Chronology of Pedogenesis and Post-Pedogenic Processes of the Hokkalampi Paleosol

2.5.1.1 Dating Soil Formation with the Sm-Nd Isotope System

Application of the Sm-Nd isotopic system to Precambrian paleosols provides possible temporal constraints on soil formation and a better evaluation of element mobility during pedogenesis. The nuclide ^{147}Sm decays to ^{143}Nd with a half-life of 106 Ga, allowing this system to be used for geochronology, primarily of igneous rocks. Pedogenesis is unlikely to rigorously satisfy the requirements for the Sm-Nd geochronologic system particularly due to the requirement of uniform initial $^{143}Nd/^{144}Nd$. However, pedogenic fractionation of REE (as discussed in the last section) leads to the possibility of achieving a significant spread in Sm/Nd ratios during soil formation, and this may constrain the timing of pedogenesis. In addition, any initial $^{143}Nd/^{144}Nd$ variations in the soil profile can provide information about pre-weathering processes and possible multiple sources of profile parent material.

In order to track possible variations in $\varepsilon_{Nd}(T)$ of the soil, we require an age to which the Nd isotope values can be corrected for decay of ^{147}Sm. Cross-cutting relations show that the Hokkalampi paleosol formed between 2.2 Ga (overlying sedimentary rock cut by dikes; Marmo, 1992; Vuollo *et al.*, 1992) and 2.44 Ga ago (gabbro cut by weathering event; (Sturt *et al.*, 1994), a ~240 Ma window that allows for considerable variation in initial ε_{Nd} values. If the parent material for the paleosol was relatively isotopically homogeneous at the time of soil formation, and pedogenesis resulted in significant fractionation of Sm from Nd, then the possibility exists to

use the Sm-Nd data to better constrain the time of soil formation. In **Figure 2.8**, we plot the Sm-Nd data from both profiles in an isochron diagram and use the least squares regression method and error analysis of York (1969) to calculate an age. Provided the above conditions were met, the apparent isochron gives the time of soil formation as 2.35 ± 0.19 Ga (2σ). As can be seen, much of the spread in the isochron is created by one sample, 00-PK-22. Even when this point is excluded, the data yield an identical age but with a larger uncertainty (2.35 ± 0.49 Ga).

When corrected to this apparent age, $\varepsilon_{Nd}(T)$ values from both profiles range from -3.2 to -5.9, with a mean of -4.7 (**Table 2.3**). This is consistent with a parent granodiorite derived from a depleted mantle source 300-600 Ma before pedogenesis (i.e., 2.7-3.0 Ga ago). While this "age" does not necessarily narrow down the time frame of pedogenesis within its 95% confidence interval, it does fall in the center of the geologically allowable interval for Hokkalampi pedogenesis, suggesting that pedogenic REE fractionation could be the primary cause of the spread in Sm/Nd. Moreover, it opens up the possibility that the Sm-Nd system could be used elsewhere for paleosol geochronology in the Precambrian, particularly for those paleosol profiles with more uniform parent material.

In **Figure 2.9**, we present a schematic model for the Sm-Nd evolution of the Hokkalampi paleosol and its granitoid parent. In this model, the granitoid is derived from depleted mantle 2.85 Ga ago, with an initial ε_{Nd} of +3, which is reasonably close to the mantle evolution curves of DePaolo (1981) and Goldstein *et al.* (1984). Whole rock samples of the granitoid (shaded region between 2.85 and 2.35 Ga) evolve within a very restricted range of values, based on parent material Sm/Nd ratios measured in this study. However, individual minerals within the granitoid, while starting out with identical $\varepsilon_{Nd}(T)$ values, are expected to diverge widely over the ~500 Ma between granitoid crystallization and Hokkalampi pedogenesis. Evolution curves for

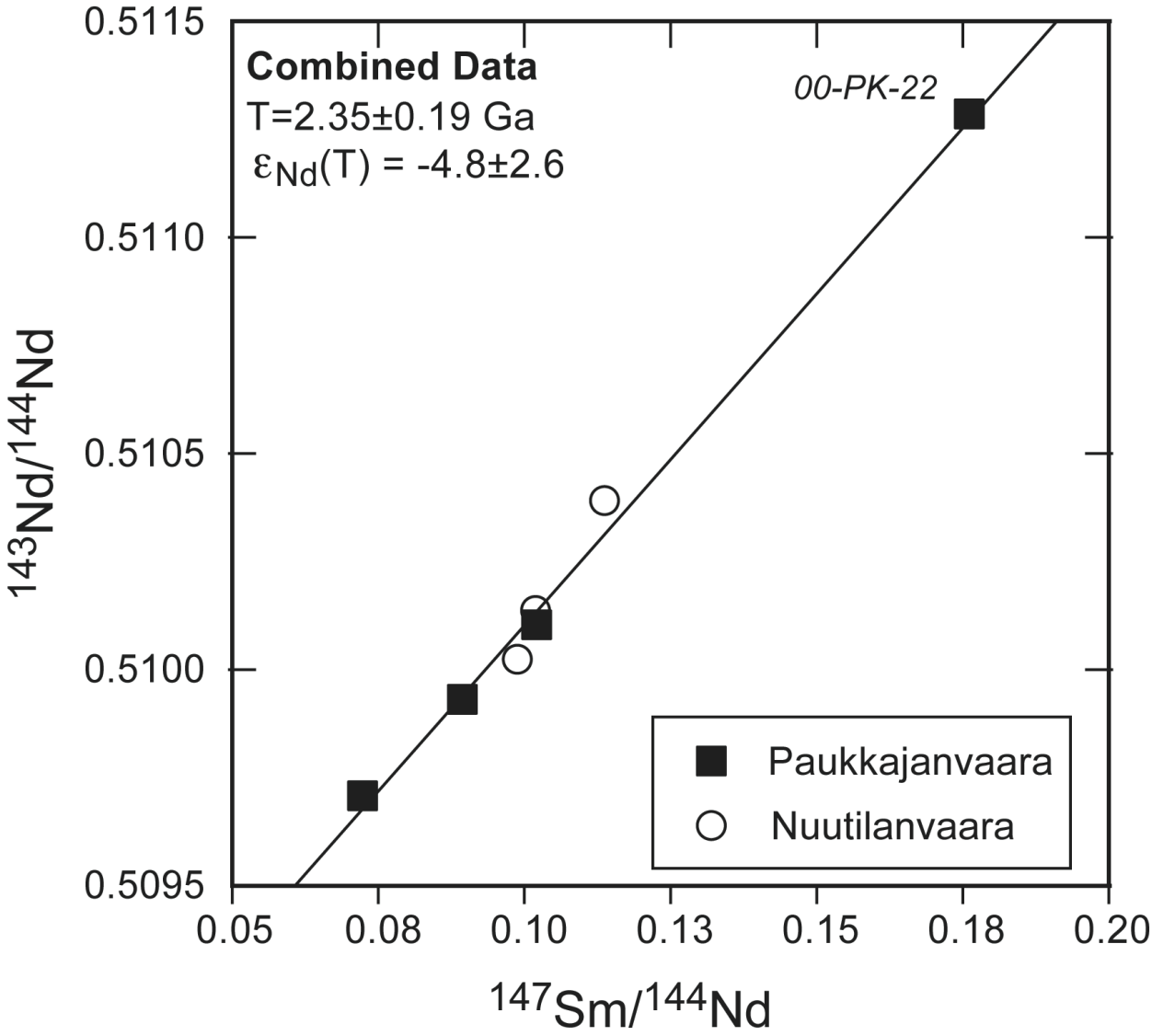

Figure 2.8: $^{143}Nd/^{144}Nd$ **variation with** $^{147}Sm/^{144}Nd$ **for Paukkajanvaara and the Nuutilanvaara sections of the Hokkalampi paleosol. The combined data plotted form an apparent isochron reflecting a model age of 2.35 ± 0.19 Ga ago (2σ).**

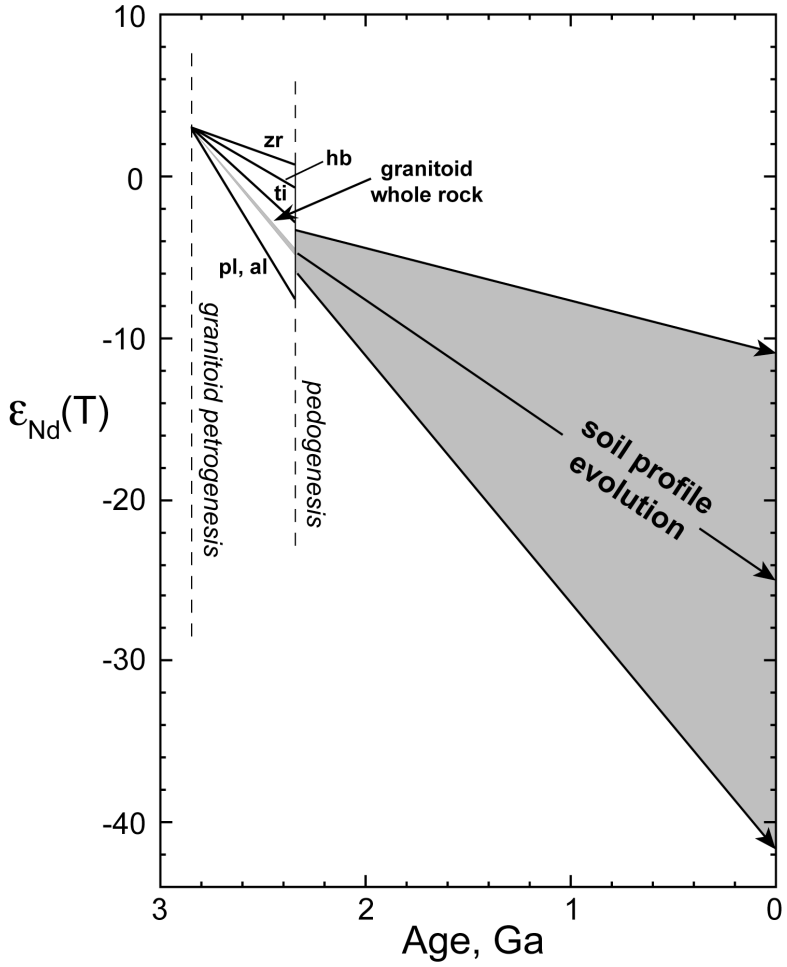

Figure 2.9: Schematic model of Sm-Nd evolution for the Nuutilanvaara and Paukkajanvaara sections of the Hokkalampi paleosol. In this model, the granitoid is derived from depleted mantle 2.85 Ga ago, with an initial εNd of +3. Whole rock samples of the granitoid (shaded region between 2.85 and 2.35 Ga) evolve within a very restricted range of values, based on parent material Sm/Nd ratios measured in this study. Evolution curves for zircon (zr), hornblende (hb), titanite (ti), plagioclase (pl) and allanite (al) are shown based on Sm/Nd ratios of minerals in a granodiorite from the Peninsular Ranges Batholith (Gromet and Silver, 1983). Pedogenesis at ~2.35 Ga partially homogenizes the granitoid, and subsequent evolution paths of the profile. Whole-rock samples fall within the shaded region, based on data from this study.

zircon (zr), hornblende (hb), titanite (ti), plagioclase (pl) and allanite (al) are shown in **Figure 2.9**, based on Sm/Nd ratios of minerals in a granodiorite from the Peninsular Ranges Batholith (Gromet and Silver, 1983). During soil formation at ~2.35 Ga, the rare earth elements (including Sm and Nd) are mobilized throughout the profile, and redistribution of Nd from selective mineral weathering leads to increased isotopic heterogeneity in bulk samples of weathered material. Weathering-induced REE fractionation also creates a greater spread in bulk-rock Sm/Nd than was present in unweathered granodiorite. Therefore, subsequent to pedogenesis, the ε_{Nd} trajectories of bulk paleosol samples diverge significantly from that of the parent, leading to the large range in measured ε_{Nd} values in the paleosol.

The self-consistent model presented in **Figure 2.9** suggests that nearly all of the REE fractionation in Hokkalampi paleosol samples could have taken place during formation of the Paleoproterozoic weathering profile, rather than during later greenschist facies metamorphism or more recent exposure at the Earth's surface. This contrasts with the results of Macfarlane et al. (1994), who suggested that the Sm-Nd systematics of a paleosol developed on the ~2.8 Ga Mt. Roe basalt were disturbed by intense metasomatism at 2.1 Ga. In this event, hydrothermal fluids apparently channeled through the weathered zone of the basalt protolith, and severe alkali depletion was observed (Macfarlane and Holland, 1991; Macfarlane *et al.*, 1994). While the Hokkalampi paleosol shows some degree of alkali metasomatism, the Nd isotope systematics from this study suggest that its REE fractionations reflect Precambrian weathering processes.

2.5.1.2 Rb-Sr Constraints on Post-Pedogenic Metamorphism of the Hokkalampi Paleosol

The rubidium-strontium system, in which the nuclide ^{87}Rb decays to ^{87}Sr with a half-life of 48.8 Ga, has long been used for geochronology of igneous rocks. It is well known, however, that the Rb-Sr systematics of igneous rocks are easily disturbed or reset by weathering and metamorphic processes due to the relatively high mobility of Rb (an alkali element) and Sr (an alkaline earth element). This propensity for resetting makes the Rb-Sr system potentially attractive for examining the timing of pedogenesis and/or later metamorphic disturbances of paleosols. Macfarlane and Holland (1991) found that the Rb-Sr system produced a precise "age" for the Mt. Roe weathering profile that was coincident with post-pedogenic metamorphism and metasomatism.

The Rb-Sr isotope data from the Hokkalampi paleosol (**Table 2.3**) form a linear array on an isochron diagram (**Figure 2.10**). When all samples are used in the calculation, the "isochron" yields an age of 1.75 ± 0.28 Ga (calculated after the method of (York, 1969); if sample 00-PK-33 is excluded (outlier on **Figure 2.10**), the calculated age is 1.82 ± 0.15 Ga. In either case, the Hokkalampi Rb-Sr data clearly indicate a disturbance to the Rb-Sr system well after pedogenesis. The most likely culprit is the regional greenschist-grade metamorphism associated with the Svecofennian Orogenic event that reached its peak around 1.9 Ga ago (Marmo, 1992), but continued until about 1.77 Ga (Kouvo and Tilton, 1966; Kuovo *et al.*, 1983; Wilson *et al.*, 1985; Patchett *et al.*, 1987; Huhma *et al.*, 1990). In this case, the Rb-Sr system might be dating the waning phase of this metamorphic event. Similar metamorphic resetting of the Rb-Sr system at this time is observed in granitoids and gneisses in eastern Finland (Vidal *et al.*, 1980; Martin, 1989).

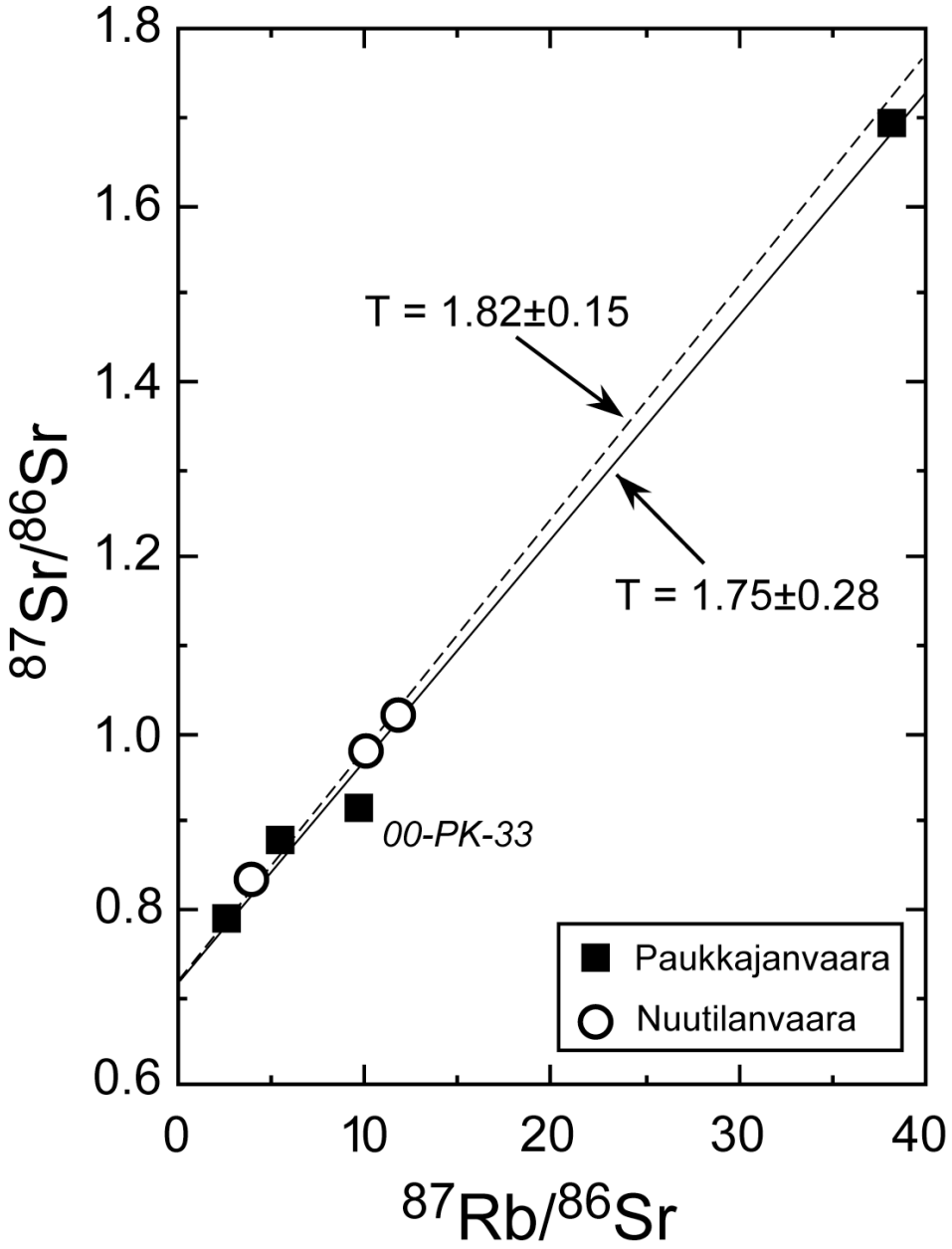

Figure 2.10: Variation of $^{87}Sr/^{86}Sr$ with $^{87}Rb/^{86}Sr$ for the Nuutilanvaara (open circles) and Paukkajanvaara sections (closed squares) of the Hokkalampi paleosol. These data form a linear array on an isochron diagram (solid line). When all samples are used in the calculation, the "isochron" points to an age of 1.75 ± 0.28 Ga; if sample outlier 00-PK-33 is excluded, the calculated age is 1.82 ± 0.15 Ga (dashed line).

The observed resetting of the Rb-Sr system requires at least limited exchange of Sr on a scale of meters, which could have been aided by fluid flow accompanying metamorphism. In addition, it is likely that Rb was selectively added to portions of both profiles during K-metasomatism, which could significantly increase the spread in Rb/Sr ratios. This is demonstrated by a comparison of Ti-normalized Rb and K concentrations in both profiles (expressed as % deviation from parent material, **Figure 2.11**). A regression through all data from both profiles (solid line) yields a significant correlation with $r^2 = 0.91$, and the Nuutilanvaara data alone (dashed line) yield a nearly perfect correlation ($r^2 = 0.9996 \approx 1.00$). The observed correlations strongly suggest that K-metasomatism was synchronous with regional metamorphism at 1.9-1.8 Ga.

2.5.2 Element Mobility During Weathering and Metamorphism of the Hokkalampi Paleosol

2.5.2.1 Major Element Weathering Trends and K Addition

Contrasting patterns of element depletion between the two profiles (**Figure 2.5**) suggest that either the Paukkajanvaara profile is more strongly developed than the Nuutilanvaara profile, or an intensely weathered section at the top of the Nuutilanvaara profile was eroded away. Geographic relationships (Marmo, 1992) and chemical similarity of the overlying sedimentary deposits at the Paukkajanvaara location to the Nuutilanvaara profile support the latter. In either case, the preservation of a highly weathered section in the Paukkajanvaara profile provides an opportunity to study chemical mobility, including redox element mobility, during Proterozoic soil formation.

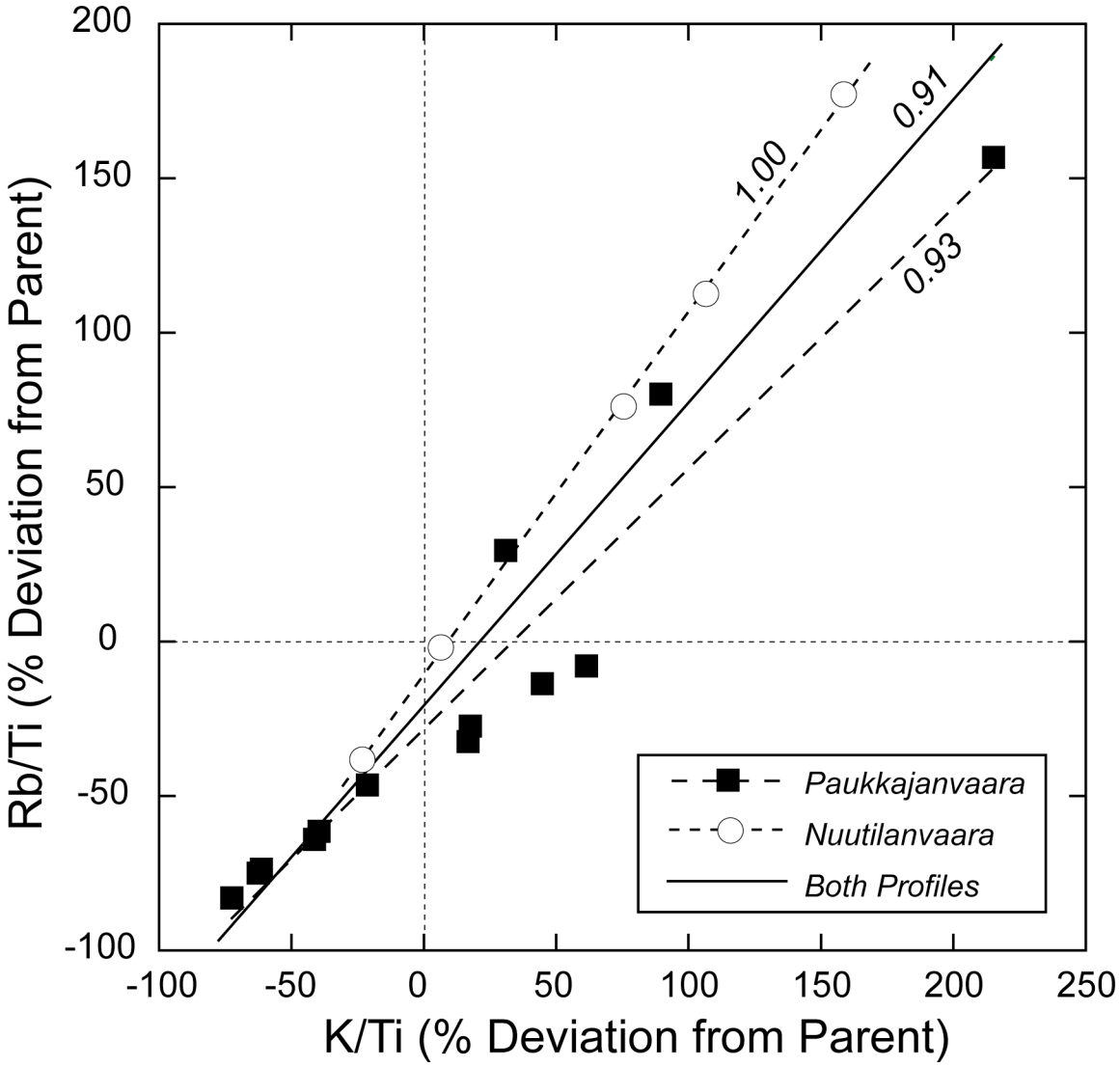

Figure 2.11: Variation of K/Ti (% deviation from parent) with Rb/Ti (% deviation from parent) for the Paukkajanvaara profile (closed squares) and the Nuutilanvaara profile (open circles). The observed correlation strongly suggests that Rb was mobilized and transported into the profile during K-metasomatism.

Nesbitt and Young (1984; 1989) compared thermodynamic and mass balance models for granite weathering to modern granite soil profiles on A-CN-K (Al_2O_3-CaO_{sil}+Na_2O-K_2O) diagrams, where CaO_{sil} represents the CaO only in silicate minerals. The Hokkalampi paleosol data are plotted on such a diagram in **Figure 2.12**, with CaO corrected for carbonate by assuming that all carbon, (C_{total}) is in the form of carbonate, and corrected for Ca-phosphate using P_2O_5. The arrowed path indicates the typical trend for chemical alteration of granite, reflecting weathering initially dominated by plagioclase and then by potassium feldspar, resulting in alteration to kaolinite. On average, the Paukkajanvaara profile (closed squares) exhibits a higher degree of weathering (i.e., samples that plot closer to the Al_2O_3 corner) than the Nuutilanvaara profile (open circles). While the Hokkalampi samples show a general trend of decreasing Ca, Na, and K from the parent material as seen in modern weathering profiles, they are displaced toward more potassium-rich values relative to the normal weathering trend (**Figure 2.12**). This can also be seen in **Figure 2.5**, where K shows less depletion than other mobile elements (e.g., Ca, Mg, Na) in the heavily weathered zone (zone 1) of the Paukkajanvaara profile, and it is in fact enriched in portions of zones 2 and 3 of the Hokkalampi profiles. The observed trend cannot be explained as simple residual enrichment of K during weathering, as this would require preferential removal of Al relative to K during the early stages of pedogenesis, which is unlikely. The data suggest K addition some time after pedogenesis, either during diagenesis or during a later metamorphic/metasomatic event. Circulating groundwaters rich in K could have converted pedogenic kaolinite to illite (e.g., Gay and Grandstaff, 1980; Holland *et al.*, 1989; Rainbird *et al.*, 1990), while metasomatic fluids would have added additional K at temperatures sufficiently high to recrystallize illite into sericite. This recrystallization most likely took place pre- and syn-metamorphically, based on the alteration textures of sericite (*see section 2.4.1.2*). As discussed

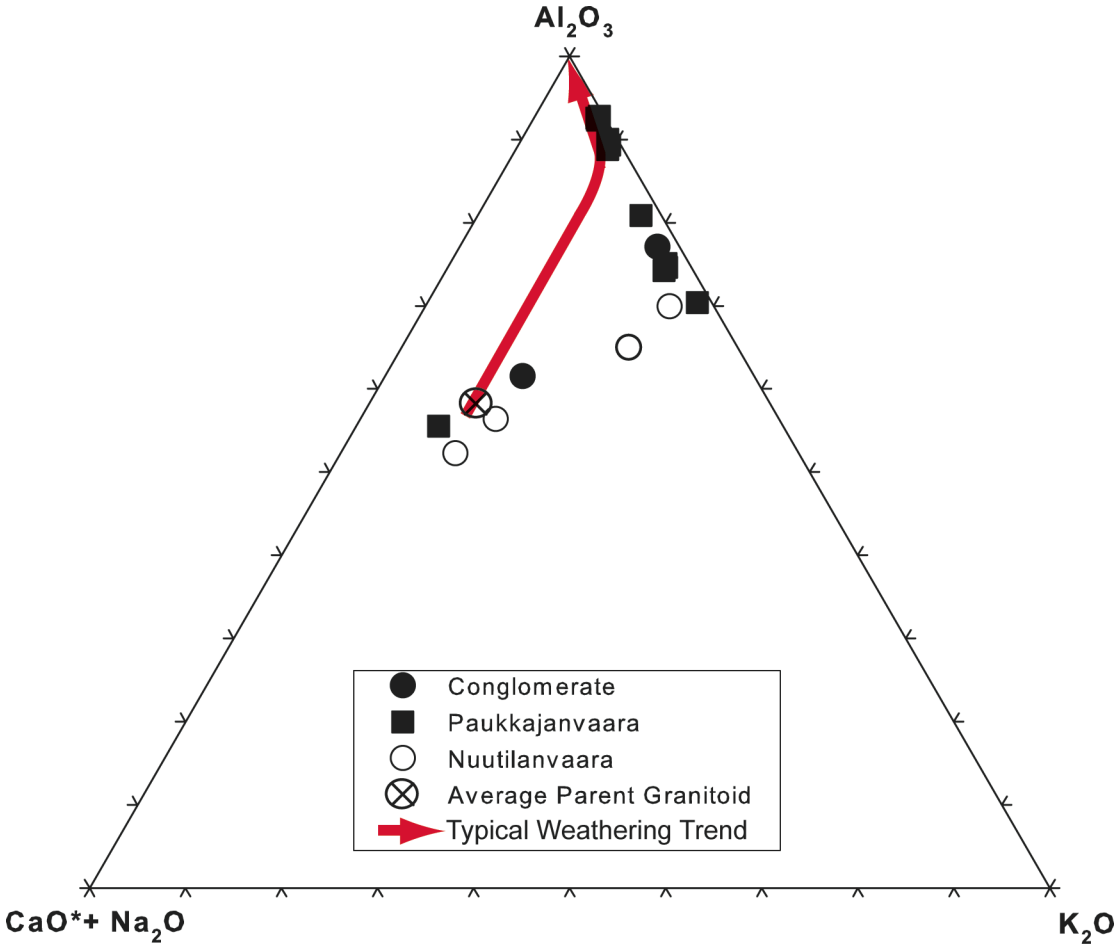

Figure 2.12: A-CN-K diagram showing an idealized model for modern granitic weathering compared to the weathering trend for the Hokkalampi paleosol. The arrows indicate the typical trend for chemical alteration of granite reflecting weathering of plagioclase and potassium feldspar to kaolinite. On average, the Paukkajanvaara profile (closed squares) exhibits more advanced weathering (i.e. samples that plot closer to the Al_2O_3 corner) than does the Nuutilanvaara profile (open circles). While the Hokkalampi samples exhibit decreases in Ca, Na, and K as seen in modern weathering profiles developed on granite, they are clearly displaced toward more potassium-rich values. This implies K addition some time after pedogenesis.

previously, the apparent metamorphic Rb-Sr age for the paleosol (**Figure 2.10**) coupled with the strong correlation of Ti-normalized Rb and K (**Figure 2.11**) argue strongly that the excess K was added to the profile during metamorphism.

2.5.2.2 REE Mobility During Hokkalampi Profile Development

Previous studies have shown that REE can be mobilized and fractionated during pedogenesis (Balashov *et al.*, 1964; Nesbitt, 1979; Schau and Henderson, 1983; Banfield and Eggleton, 1989; Braun *et al.*, 1990; Price *et al.*, 1991; Mongelli, 1993; Macfarlane *et al.*, 1994; Nesbitt and Markovics, 1997; Aubert *et al.*, 2001). This is particularly true under tropical conditions, such as those that produce bauxite, where chemical weathering is intense (Kimberley and Grandstaff, 1986). Paleosols formed in the Archean and Paleoproterozoic undoubtedly formed under very different conditions than modern soils. Vegetation was absent on the terrestrial surface, and the extent of biological activity, most likely in the form of microbial mats, is unknown (e.g., Rye, 1998; Rye and Holland, 2000; Watanabe *et al.*, 2000). A key question is to what extent soil-forming processes in the Precambrian were capable of mobilizing and fractionating REE. However, a potential confounding factor is the effect of metamorphism on REE distribution in a paleo-profile. While most studies suggest that the rare earth elements remain relatively immobile on a whole-rock scale during metamorphism, based on the systematics of the Sm-Nd isotope system (Hamilton *et al.*, 1979; Jahn *et al.*, 1982; Farmer and DePaolo, 1987; Stewart and DePaolo, 1996), rare earth element patterns in some Archean and Paleoproterozoic volcanic rocks in eastern Finland show evidence of disturbance during ca. 1.8-1.9 Ga metamorphism (Huhma *et al.*, 1990; Gruau *et al.*, 1992). The Sm-Nd isotope data discussed earlier (*see section*

2.5.1.1) strongly suggest that the REE patterns displayed by the Hokkalampi paleosol samples are representative of weathering remobilization during pedogenesis and were not substantially affected by later metamorphism.

In both Hokkalampi soil profiles, it appears that weathering and soil development have led to mobilization of rare earth elements, with gains and losses in total REE, as well as significant fractionation of the REE patterns (**Figure 2.7**). In general, the REE budgets of granitoid rocks tend to be controlled by REE-rich accessory minerals such as apatite, allanite, titanite (sphene) and/or zircon (Gromet and Silver, 1983; Condie *et al.*, 1995). While there is no unique set of weathering patterns that can explain up-profile enrichment of LREE, selective weathering of one or more accessory phases is a possibility, along with preferential capture of LREE by secondary minerals. For example, titanite is generally LREE-depleted relative to its igneous parent and this mineral can dominate the REE budget of granitoids (Gromet and Silver, 1983). In the ~3 Ga Steep Rock paleosol, Canada, which has developed on granodiorite parent material, the REE appear to be closely associated with a Ti-rich phase, most likely titanite or its weathering products (Macpherson *et al.*, 2000). Alteration of titanite to a Ti-oxide with concomitant release of its REE could explain the trend in the Paukkajanvaara profile. Titanite is thought to weather readily in soils (Condie *et al.*, 1995; Lång, 2000; Singh and Rajamani, 2001; Girty *et al.*, 2003), and the REE released by weathering near the top of the profile would be subject to the greatest flux of soil water, enhancing its removal. Another possibility for LREE enrichment near the top of the profile would be capture of weathering-released LREE by adsorption onto oxy-hydroxides or clay minerals (Nesbitt, 1979; Schau and Henderson, 1983; Öhlander *et al.*, 1996) or by incorporation into precipitated LREE phosphates. There is, however, no apparent correlation between P_2O_5 content and La/Sm ratios.

In the Nuutilanvaara profile, the modest (to nonexistent) LREE losses, gains in HREE, and limited La/Sm variations (**Figure 2.7d**) most likely reflect limited REE mobility (including REE accumulation from above) during weathering in an unsaturated, and possibly oxygenated, soil profile. The upper portions of the Nuutilanvaara profile, where the strongest weathering and REE fractionation might be expected, have apparently been physically removed by erosion (Marmo, 1992). Because plagioclase commonly displays a strong positive Eu anomaly (Eu concentration elevated significantly above its neighbors in a normalized REE pattern), weathering and removal of plagioclase REE can result in negative Eu anomalies in the bulk residual soil. Negative Eu anomalies corresponding to low total REE at 5-10 m depth in the Paukkajanvaara profile (**Figure 2.7c**, **Table 2.2**) suggest significant removal of plagioclase (and other REE-bearing phases) at this level, possibly related to leaching by groundwaters. The Nuutilanvaara profile shows no such REE-depleted zone, strengthening the argument that it remained above the water table during its formation.

2.5.3 Mobilization of Redox-Sensitive Elements

2.5.3.1 Iron Mobility

The Fe loss in portions of the Hokkalampi profiles (**Figure 2.6**) is much higher than the ≤50% average loss for Paleozoic and younger profiles (Driese, 2004) and is similar to the >75% Fe loss seen in the upper portion of the 2.3 Ga Hekpoort paleosol, although Driese (2004) notes that the calculated Fe loss is much lower in the Hekpoort paleosol if saprolitic basalt is assumed to be its parent material. The trend of iron loss in the upper part of the Hokkalampi profiles and Fe_T gain in the lower part could be due to leaching of Fe under reducing conditions and movement of Fe through the soil profile, followed by deposition at or near the weathering front or the paleo-water

table. Subsequent deposition of Fe near the weathering front could be due to: (1) an increase in cation exchange capacity with the increase of 2:1 clays deeper in the soil profile; (2) an increase in pH due to weathering of feldspars, which produces alkalinity; and/or (3) a decrease in the leaching capacity as inorganic and/or organic acids are naturally neutralized or diluted (Nesbitt, 1979).

However, iron mobility does not necessarily imply that pedogenesis took place under anoxic atmospheric conditions; Driese (2004) documented pedogenic translocation of Fe, with associated depletion and enrichment, in both modern and paleo-vertisols. Waterlogged conditions could reduce and mobilize Fe despite an oxygenated atmosphere. Experimental studies by Neaman *et al.* (2005) indicate that organic ligands could also play a significant role in the mobility of Fe and other redox elements in soil. Both of these mechanisms (waterlogged conditions and organic ligands) require that sufficient organic matter was present in the terrestrial environment to produce reducing solutions and/or organic ligands, which is still an open question (e.g., Ohmoto, 1996; Holland and Rye, 1997; Gutzmer and Beukes, 1998; Rye and Holland, 2000; Watanabe *et al.*, 2000). There has been no experimental verification that reductive dissolution of ferric (hydr)oxides can take place in the *absence* of organic matter at temperatures below ~250°C.

Reductive dissolution of ferric oxides/hydroxides may take place by H_2-rich hydrothermal fluids that are ≥ ~250°C (Ohmoto, 1996). Some redistribution of Fe in the Hokkalampi profiles may have occurred due to the same metamorphic fluids that reset the Rb-Sr system during the Svecofennian Orogeny (*see section 2.5.1.2*). **Figure 2.13** illustrates a strong correlation between Ti-normalized Fe_T and Ti-normalized Rb, expressed as percent deviation from parent granitoid for the Paukkajanvaara (solid squares) and Nuutilanvaara (solid circles)

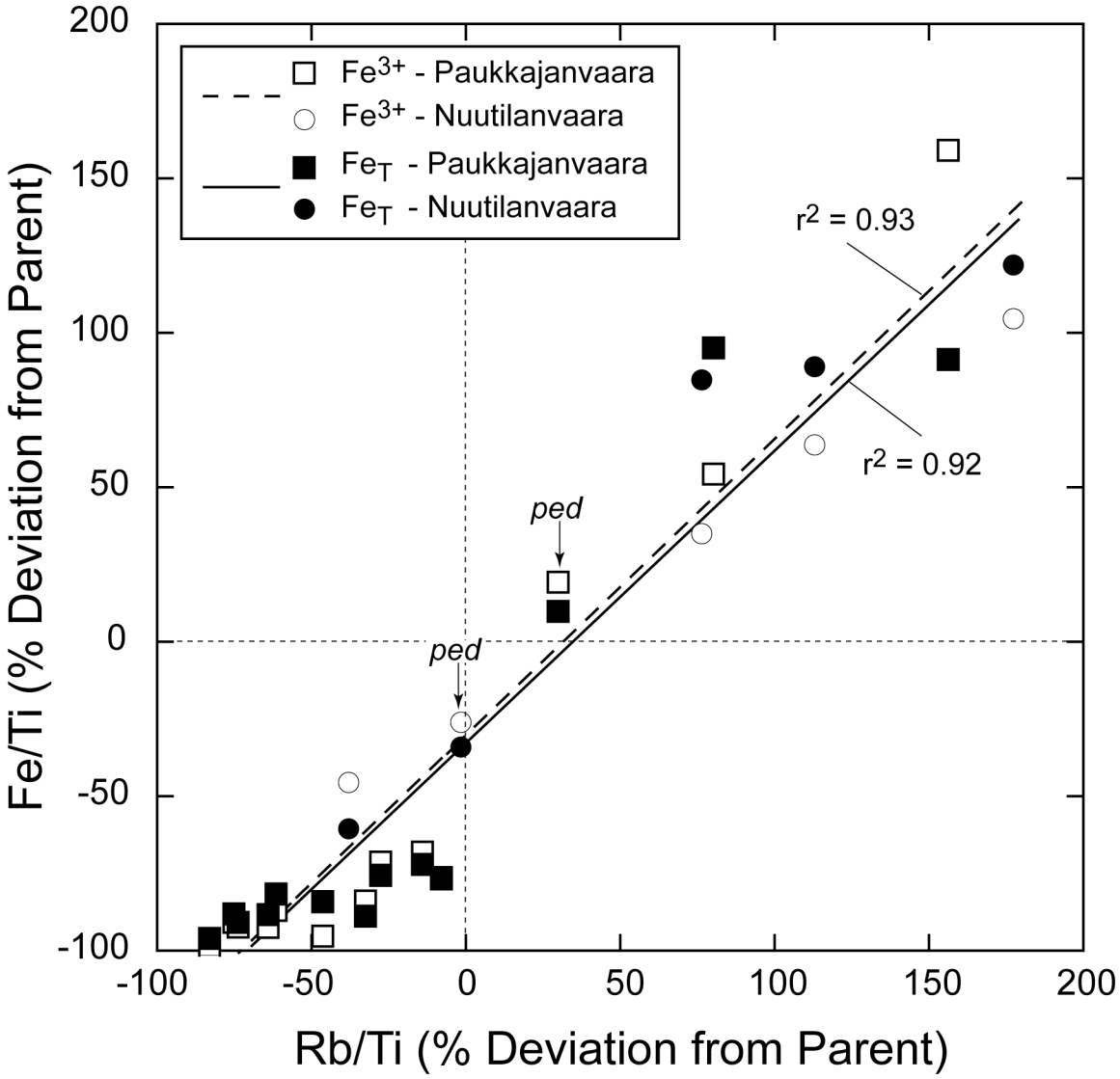

Figure 2.13: Ti-normalized Fe_T and Ti-normalized Rb, expressed as percent deviation from parent granitoid for the Paukkajanvaara (solid squares) and Nuutilanvaara (solid circles) profiles. The solid line ($r^2 = 0.92$) is the best fit for the combined Paukkajanvaara and Nuutilanvaara Fe_T data; the dashed line ($r^2 = 0.93$) is the best-fit line for the combined Paukkajanvaara and Nuutilanvaara Fe^{3+} data. Enrichments of Ti-normalized Fe^{3+} over parent granitoid *(noted by "ped")* imply oxidation of Fe during the pedogenic stage.

profiles. This correlation suggests that metamorphic fluids affected the distribution of Fe_T in the Hokkalampi profiles. However, metamorphic fluids are reducing in nature (e.g., Ohmoto and Kerrick, 1977). Therefore, it is unlikely that the enrichments in Fe^{3+} observed in both profiles were caused by deposition of Fe^{3+} or by oxidation of existing Fe^{2+} during metamorphism. The enrichments of Ti-normalized Fe^{3+} shown in **Figure 2.13** *(noted by "ped")* must have been during the pedogenic stage.

At the top of the eroded Nuutilanvaara profile (zone 2) and in the (paleosol-derived) conglomerate overlying both profiles, Fe^{3+} is less depleted than Fe^{2+} (**Figure 2.6**). This suggests that pedoliths within the conglomerate overlying the Hokkalampi paleosol formed under oxidizing conditions (**Figure 2.2**), as suggested by Marmo (1992).

2.5.3.2 Uranium and Thorium Variations in the Hokkalampi Profiles

Studies of modern weathering profiles show that Th is relatively immobile (Braun *et al.*, 1990), although it may be mobilized by organic acid-rich fluids (Langmuir, 1997). At Earth surface conditions, uranium dissolves in solution when U^{4+} is oxidized to U^{6+} (Brookins, 1988). **Figure 2.14** shows deviations of Ti-normalized U and Th from the parent material as a function of depth in the profile. Thorium is significantly depleted throughout most of the Paukkajanvaara profile, with only one sample showing enrichment relative to the parent material. Ratios of Th/Ti vary to a greater extent in the Nuutilanvaara profile, ranging from significant depletion to ~150% enrichment. The evident mobility of Th suggests the involvement of fluids rich in organic acids during or after pedogenesis. However, we note that Th/Ti ratios vary by an order of magnitude in the different parent material samples, raising the possibility that Th was not distributed uniformly throughout the profile prior to weathering.

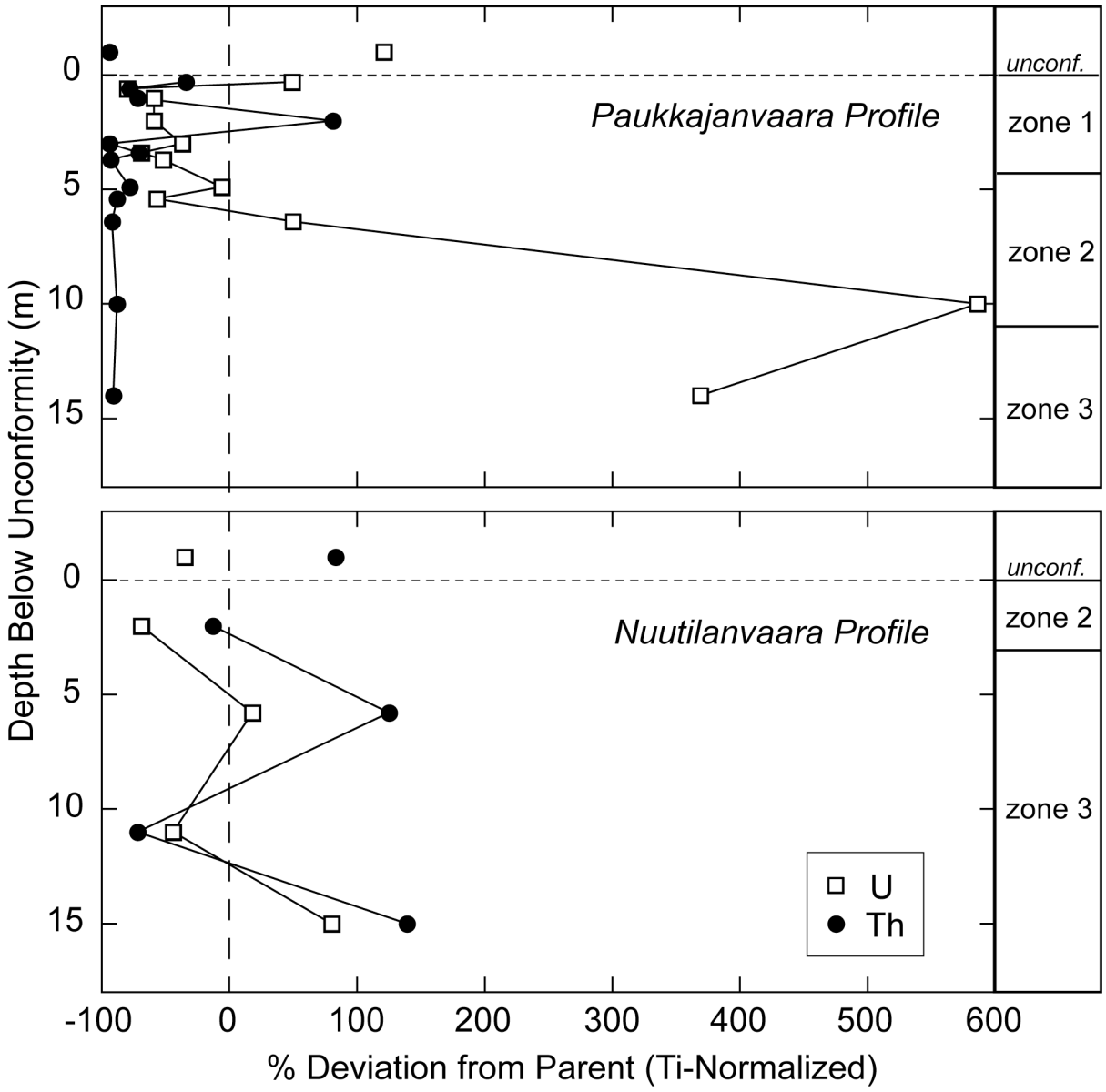

Figure 2.14: Percent deviation of Ti-normalized U (open squares) and Th (closed circles) from parent granitoid with depth for the Paukkajanvaara and Nuutilanvaara profiles.

Uranium is depleted through most of zone 1 and the upper half of zone 2 in the Paukkajanvaara profile, and it shows significant enrichment at the top and especially the bottom of the profile (**Figure 2.14**). In the Nuutilanvaara profile, U varies from somewhat depleted to somewhat enriched. The pattern in the Paukkajanvaara profile is consistent with mobilization of U in the middle to upper portions of the profile by oxygen-rich ground or soil waters, and redeposition of U under reducing conditions at greater depth. The pattern of strong U enrichment at the base of the Paukkajanvaara profile mirrors that of Fe^{3+} (**Figure 2.6**), which suggests that U might have been fixed at this level through adsorption by ferric hydroxides (Ulrich *et al.*, 2006). A possible correlation of Ti-normalized U and Rb concentrations (**Figure 2.15**) suggests an alternate explanation of uranium mobilization and deposition during the apparent metamorphic event that led to potassium enrichment in the profile.

2.5.3.3 Cerium Anomalies

Anomalous concentrations of cerium in soil profiles are significant because these anomalies only develop under oxygenated conditions where Ce3+ can transform to the highly immobile Ce4+. Positive Ce anomalies develop when REE other than Ce are partially removed by weathering, leaving behind a Ce-enriched residuum; negative Ce anomalies form in those regions of the profile where REE have accumulated from an overlying oxygenated zone. Small positive anomalies can be seen in the Paukkajanvaara profile (Figure 2.7a) from a sample at 14 m depth and the overlying conglomerate. A small negative anomaly is apparent in the Nuutilanvaara profile at 2 m depth (**Figure 2.7b**). However, we caution that positive Ce anomalies are observed in two of the three parent material samples used to determine the average parent material composition, suggesting limited post-pedogenic mobility of REE in these samples. This is the likely reason that most of the parent-normalized profile samples appear to

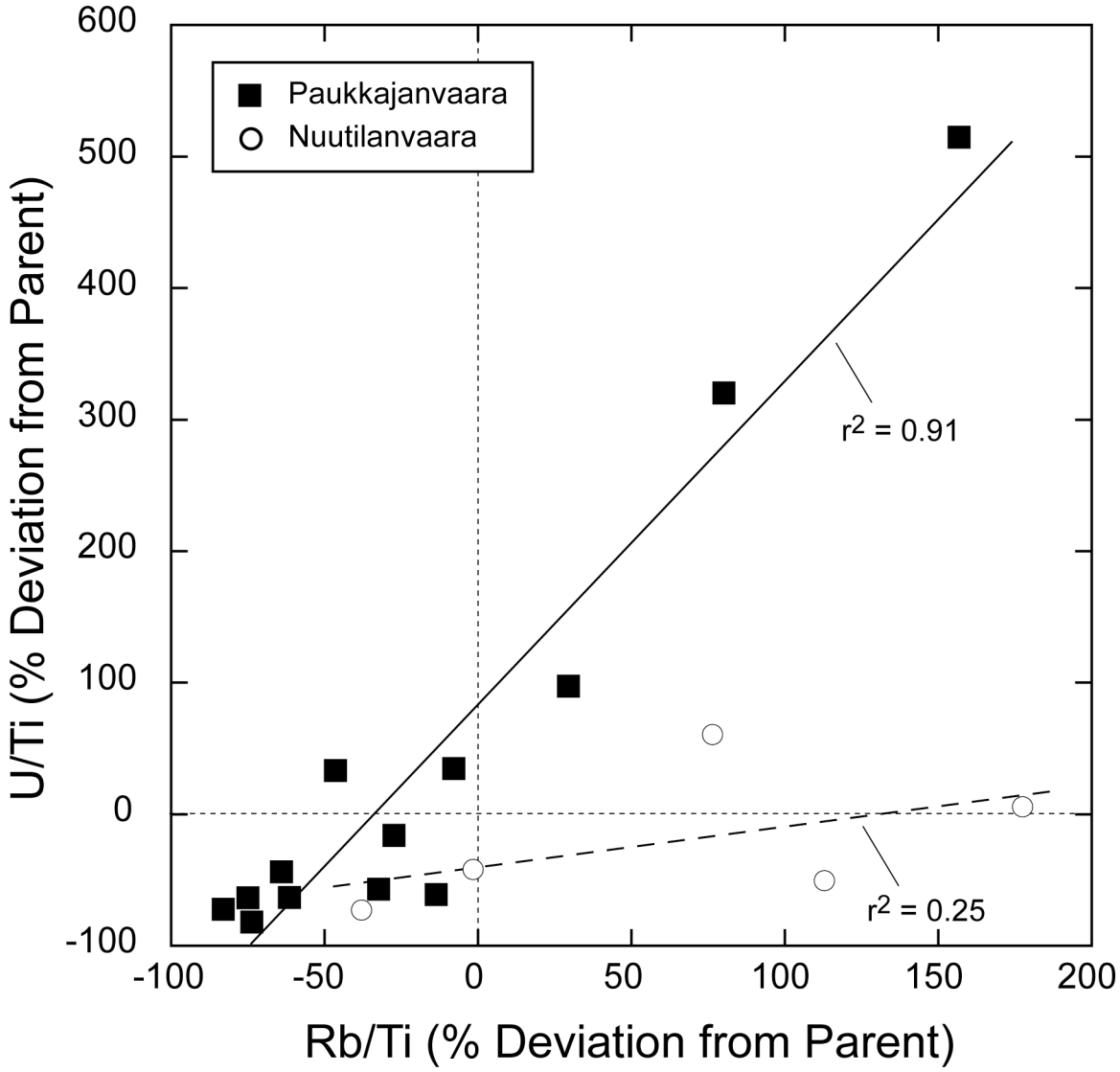

Figure 2.15: Correlation of Ti-normalized U with Ti-normalized Rb, expressed as % deviations from the parent granitoid. The solid line ($r^2 = 0.91$) is the best fit for the combined Paukkajanvaara data; the dashed line ($r^2 = 0.25$) is the best-fit line for the Nuutilanvaara data.

have small negative anomalies (**Figure 2.7c,d**). Given this observation, it would be tenuous to ascribe the small Ce anomalies in either profile to weathering and soil development under oxygenated conditions. With the possible exception of the samples noted above, it appears that the REE were mobilized primarily during movement of *reducing* fluids during pedogenesis of the Hokkalampi paleosol.

2.5.3.4 Redox Model for the Development of the Hokkalampi Paleosols

Data from the redox-sensitive elements, taken together, suggest that the Hokkalampi paleosols developed under conditions that alternated locally between oxic and reducing. During the formation of lateritic soils, the soil water chemistry most likely fluctuated seasonally: organic acid-rich and reducing during wet seasons, and oxic during dry season (i.e., O_2-diffusion through the unsaturated soil zone). Organic-rich water moving through the subsurface under saturated conditions was responsible for mobilization of rare earth elements and perhaps thorium. As suggested for the Hekpoort paleosol (Beukes *et al.*, 2002), iron was mobilized at the mid-levels of the paleosols deposited at depth as Fe^{2+}. During the dry seasons, a portion of this Fe was fixed as Fe^{3+} by oxic soil/ground waters. Some leaching of uranium at shallow to middle levels in the profile by these oxic waters may also have taken place, with subsequent adsorption at depth by Fe hydroxides. This model would suggest that the Paukkajanvaara profile at one time had an oxidized upper zone (analogous to the Hekpoort paleosol; Beukes *et al.*, 2002) that was subsequently eroded away. It is not clear to what extent organic acid-rich waters interacted with the Nuutilanvaara profile, as only the lower portions of the profile are preserved. The smaller degree of Fe depletion in that profile suggests that it was better drained, which is consistent with the paleotopographic model of Marmo (1992, Fig. 2).

Some redistribution of redox-sensitive elements could have taken place during metamorphism, rather than pedogenesis. If the metamorphic fluids were at temperatures >200°C (which is likely, given the apparent resetting of the Rb-Sr system), U could have been transported as well as Fe^{2+}. Because of the reducing nature of most metamorphic fluids (e.g., Ohmoto and Kerrick, 1977) it is unlikely that the enrichments in Fe^{3+} observed at the base of both profiles were caused by deposition of Fe^{3+} or by oxidation of existing Fe^{2+} during metamorphism.

2.6 CONCLUSIONS TO HOKKALAMPI STUDY

Micromorphologic textures and geochemical signatures in two weathering profiles from the Hokkalampi region, Finland, are consistent with intense subaerial weathering in a humid, tropical climate (e.g. ultisol- to oxisol-forming conditions), followed by potassium metasomatism and greenschist metamorphism. The geochronological constraints afforded by the Sm-Nd and Rb-Sr systems present a consistent scenario for the formation and subsequent evolution of the Hokkalampi paleosol. Between 3.1 and 2.44 Ga ago, granitoid plutons intruded mafic volcanics to form the Presvecokarelidic Shield area of eastern Finland. These plutons were unroofed and exposed to subaerial conditions that produced a large sequence of sediments and weathering products, including the Hokkalampi paleosol.

Both the Nuutilanvaara and the Paukkajanvaara profiles contain clear micromorphologic evidence of soil-forming processes and a general trend of increasing degree of weathering toward the paleo-surface. Under warm, low-latitude climate conditions and an atmosphere richer in carbon dioxide, weathering probably could progress quickly on the barren landscape. Ca- and

Na-rich plagioclase weathered first, followed by biotite and K-feldspar. Over time, the profiles became more kaolinite-rich; acid leaching in the upper portions of the soil mobilized cations such as Na, K, Ca, Mg, Al, and Fe as well as the HREE down-profile. Intense chemical weathering leached SiO_2; embayed textures in primary quartz grains are consistent with the mobility of SiO_2. TiO_2, and Nb were relatively immobile. Cations and HREE were precipitated as secondary minerals such as oxy-hydroxides and phosphates in the lower, less weathered section of the profiles.

The weathering profile from the Nuutilanvaara region shows evidence of developing under unsaturated, possibly oxidized conditions, whereas significant element depletions (Fe, LREE) from the Paukkajanvaara profile suggest formation in a (periodically?) saturated and/or organic-rich zone, consistent with the model proposed by Marmo (1992). Pedogenic processes in the Paukkajanvaara profile led to mobilization of rare earth elements (REE) with gains and losses in total REE, as well as significant REE fractionation, comparable to that seen in modern soil profiles. The Nuutilanvaara profile exhibits modest changes in the REE budget; however, the most heavily weathered portions of this profile were probably removed by erosion. Pedogenic fractionation of REE produced a wide range of Sm/Nd ratios at different depths within each profile. When plotted on an isochron diagram, these samples produce an apparent isochron yielding an age of 2.35±0.19 Ga, which falls within the expected time period for pedogenesis of this profile. We suggest that Paleoproterozoic weathering processes effectively reset the Sm-Nd system, and that REE mobility has been minimal since that time. Preserved Ce anomalies indicate that the atmosphere had enough oxygen to oxidize Ce sometime between the apparent age of pedogenesis (~2.35 Ga) and the age of the dikes cross-cutting the paleosol and

the overlying sediment (2.2 Ga). As the thickness of the overlying sedimentary deposits is quite substantial, an oxidizing atmosphere probably existed closer to the model age of pedogenesis (~2.35 Ga).

Whole rock Rb-Sr data from samples throughout the profile yield an apparent age of ~1.8 Ga, which most likely reflects a regional greenschist grade metamorphic event that is thought to have peaked around 1.9 Ga. Correlation of Rb and K concentrations suggests that K-metasomatism of the profile occurred during the waning stages of this metamorphic event, which transformed illite into sericite. Metamorphism affected the more permeable upper sections of the paleosol to a greater extent than the lower, less weathered sections, as evidenced by the texture, mineralogy, and chemistry of the samples. While certain alkali elements and possibly Sr and Ca were mobilized during metamorphism, the Sm-Nd data gathered so far clearly indicate that the REE systematics were largely unaffected, and that they are a reliable record of the Precambrian weathering processes. This study suggests that REE, Rb-Sr and Sm-Nd studies of Precambrian paleosols can assist in constraining the age of pedogenesis, and in evaluating the mobility of selected elements during and after formation of a weathering profile.

3.0 GEOCHEMICAL AND TEXTURAL INVESTIGATION OF THE ARCHEAN STEEP ROCK PALEOSOL, SOUTH ROBERTS PIT, ONTARIO, CANADA

3.1 INTRODUCTION TO THE STEEP ROCK PALEOSOL INVESTIGATION

Paleosols in the Steep Rock area (Ontario, Canada) are significant because they could preserve a paleoenvironmental record of a key part of the Archean, and help constrain age relationships between granitoids and greenstones in the Superior Province. Jolliffe (1966) interpreted the granitoid-greenstone contact at Steep Rock as an unconformity, although other studies suggested that the contact represents an intrusive or faulted relationship (Tanton, 1927; Hicks, 1950; Shklanka, 1972). Schau and Henderson (1983) described an apparent paleosol that developed on the ~3 Ga granodiorite phase of the Marmion Complex in the Steep Rock area (Caland Pit). In a later study of the Steep Rock Group, which is stratigraphically above the Marmion Complex, Wilks and Nisbet (1988) also concluded that the Marmion Complex-greenstone contact was unconformable and presented evidence for a paleosol exposed at South Roberts Pit that developed on the tonalitic phase of the Marmion Complex.

Rye and Holland (1998) evaluated and ranked Precambrian paleosols based on textural, mineralogical, and chemical evidence as well as soft-sediment deformation (e.g. rip-up clasts). In their review, the Steep Rock profiles at the Caland and South Roberts Pits were only

considered "possible" paleosols, primarily because both the Caland and South Roberts Pit profiles lacked sufficient textural evidence, and the SRP profile lacked chemical data.

This study combines micromorphologic examination with major and trace element data, including the rare earth elements (REE), and radiogenic isotope analysis for the Steep Rock SRP profile. The goals of this study are: (1) to provide and evaluate geochemical evidence of pedogenic processes; (2) to identify sedimentary features at the unconformity indicative of subaerial weathering; (3) to characterize the diagenetic and hydrothermal events that could have altered the apparent profile subsequent to exposure at the Earth's surface; (4) to compare the geochemistry of two synchronous weathering profiles (SRP and CP) developed on different parent materials; and (5) to better constrain the age of the unconformity, which has implications for understanding the granitoid-greenstone relationships and the origin of the original continental crust in the Superior Province.

3.2 BACKGROUND OF THE STEEP ROCK STUDY

3.2.1 Geologic Setting of the Steep Rock Profiles

The Steep Rock profiles formed on the Marmion Complex, an Archean granitoid unit located in the western Superior Province, Wabigoon Subprovince (**Figure 3.1**). The unconformities at both South Roberts Pit (SRP) and Caland Pit (CP) are directly overlain by a clastic unit comprising a basal metaconglomerate to sandstone (Wagita Formation), a carbonate platform succession of limestones and dolostones (Mosher Carbonate), a highly altered iron ore zone (Jolliffe Ore Zone), a series of volcanics (Dismal Ashrock), and a sequence of metavolcanics/metasediments

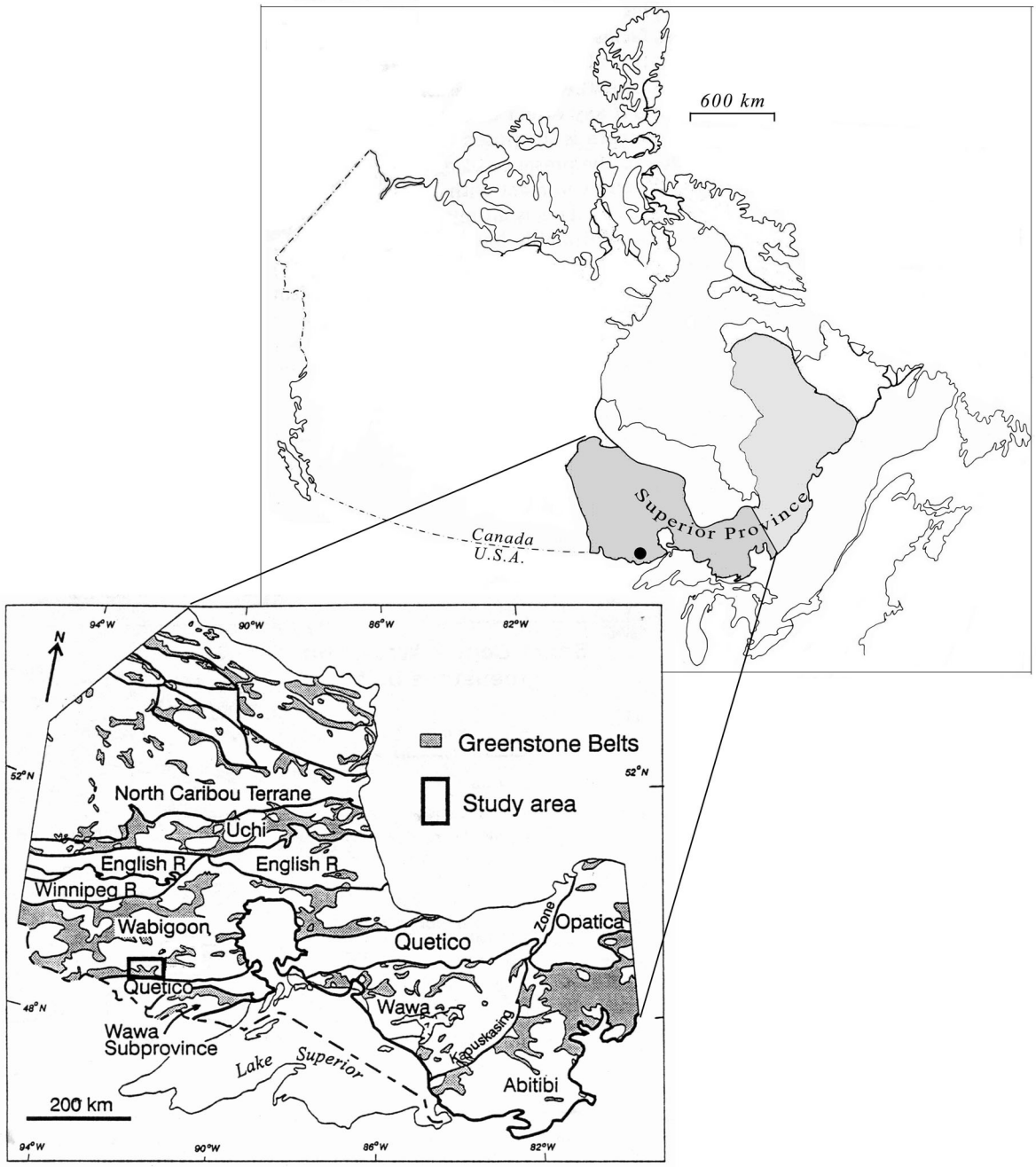

Figure 3.1: Location of Steep Rock Lake, Superior Province, Canadian Shield (modified from Schau and Henderson, 1983) and the geologic setting of the Steep Rock Lake paleosols, Wabigoon subprovince, Ontario (modified from Tomlinson et al., 1999).

(Witch Bay Formation). These units are collectively referred to as the Steep Rock Group (**Figures 3.2 and 3.3**) (Jolliffe, 1966; Wilks and Nisbet, 1988; Kusky and Hudleston, 1999) and are thought to represent a portion of an Archean greenstone belt (Tomlinson *et al.*, 1999).

The Marmion Complex at South Roberts Pit has a generally tonalitic composition, although it exhibits some compositional heterogeneity (Schau and Henderson, 1983; Wilks and Nisbet, 1988). Davis and Jackson (1988) obtained U-Pb zircon ages up to 3003±5 Ma from the tonalite, which they interpreted as the age of emplacement of the Marmion Complex. In work on nearby units, they found evidence for a regional metamorphic event at about 2700 Ma. Discordant titanite U-Pb ages of 2809 Ma from the Marmion complex (Davis and Jackson, 1988) suggest an even earlier disturbance. Titanites yielding U-Pb ages of 2950 Ma could represent hydrothermal deposition concurrent with the formation of the Jolliffe Ore Zone (reported by Tomlinson *et al.*, 1999, as D. Davis, personal communication); if this is the case, then (1) the Marmion Complex crystallized, (2) the unconformity developed, and (3) the Steep Rock Group was deposited in a ~50 Ma window between 3003 and 2950 Ma ago.

3.2.2 REE Mobility during Soil Formation

While the rare earth elements are considered relatively immobile under earth surface conditions, REE redistribution can occur during weathering and soil formation due to alteration of primary minerals, formation of secondary minerals, and transport of REE to other parts of the profile. Nesbitt (1979) demonstrated that subaerial weathering in a granodiorite produced significant fractionation in the REE patterns, ranging from enrichment of heavy rare earth elements (HREE) in incipient and moderately altered rocks, to HREE depletion in heavily weathered rock. Subsequent studies of modern weathering profiles and paleosols have shown that certain REE

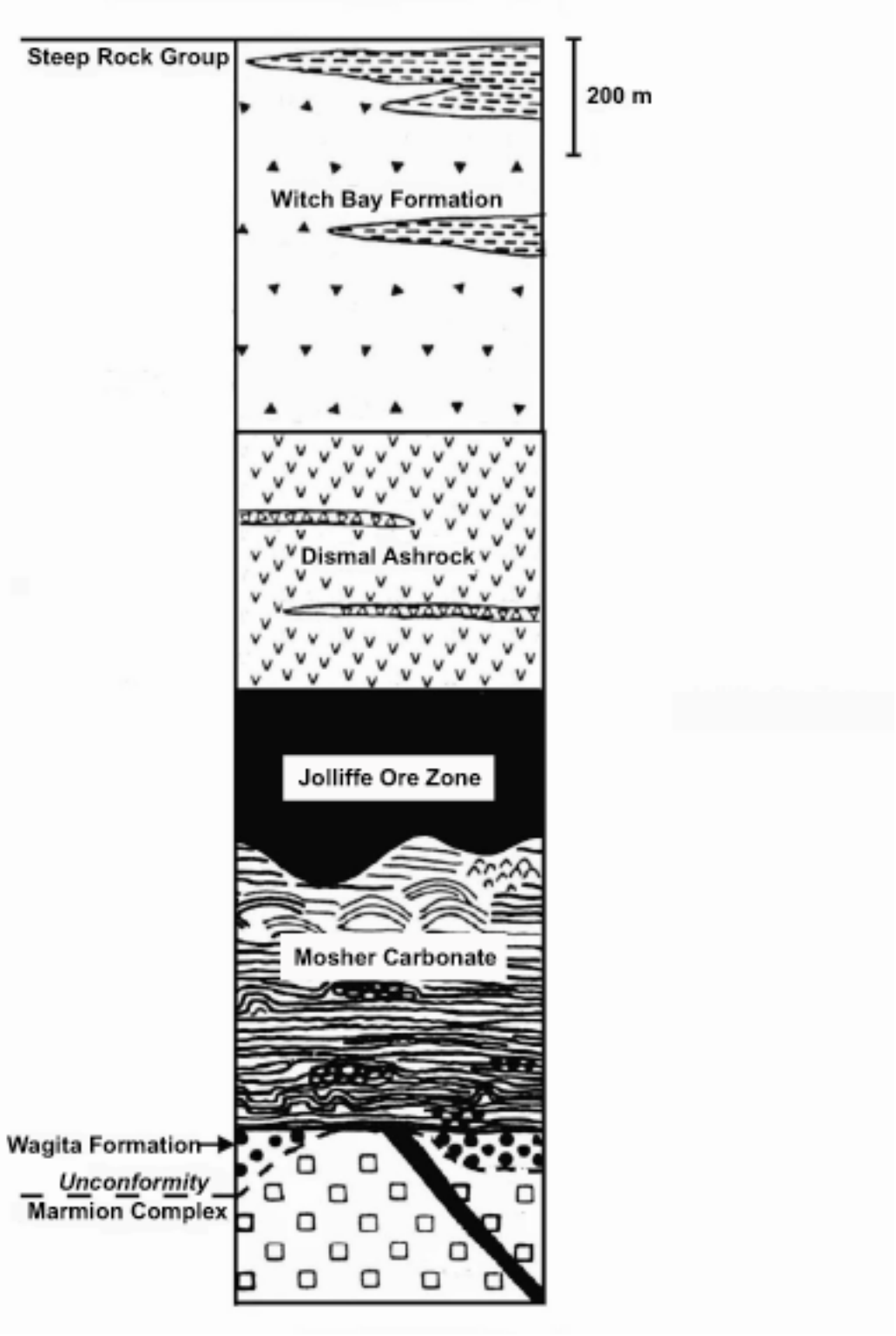

Figure 3.2: Generalized stratigraphy of Steep Rock Group (modified from Wilks and Nesbit, 1988).

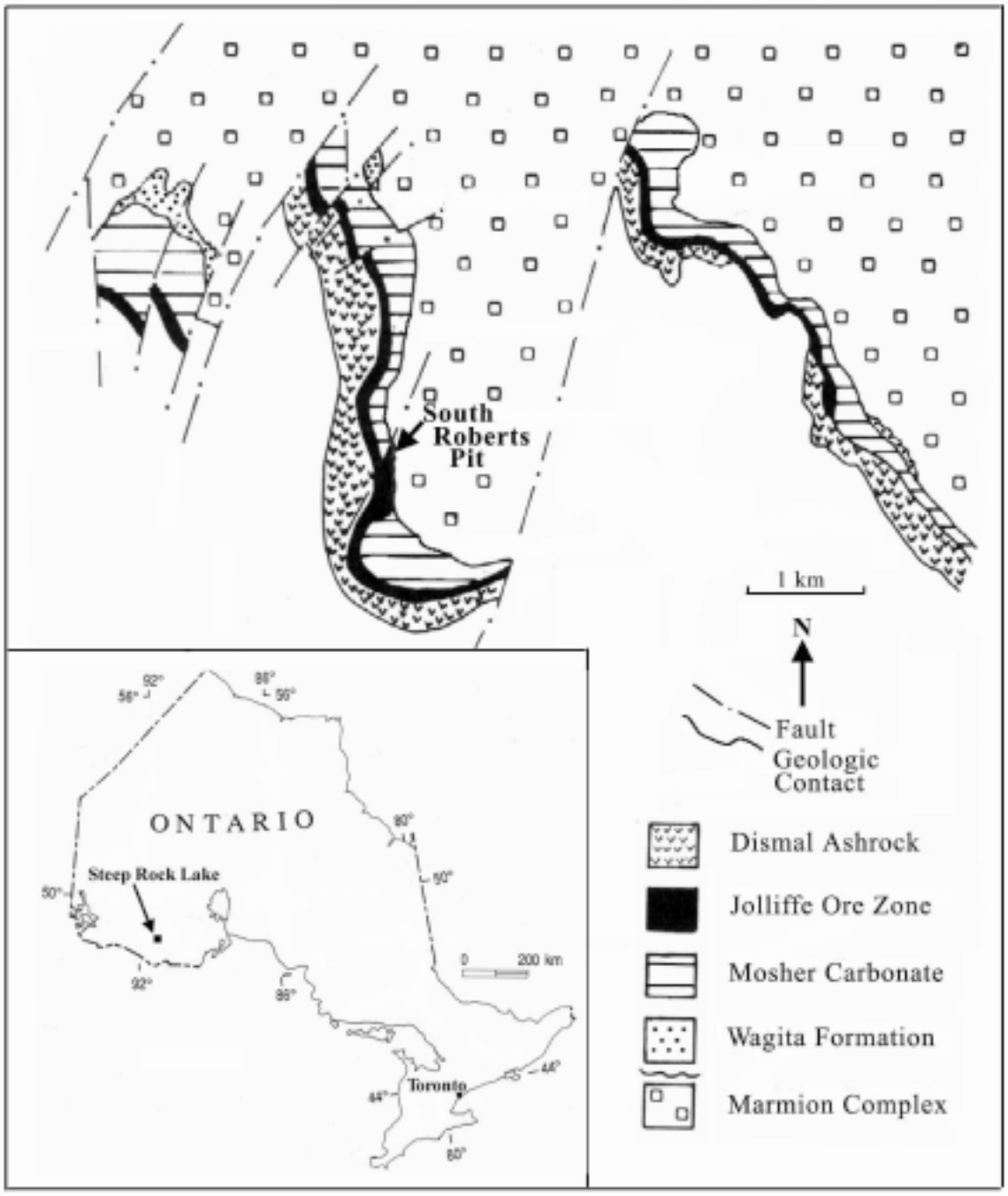

Figure 3.3: Map of Steep Rock area showing the location of South Roberts Pit (SRP) and Caland Pit (CP) (modified from Wilks and Nesbit, 1988).

are mobilized to variable extents when their host mineral is dissolved or altered to a secondary phase (Topp *et al.*, 1984; Middelburg *et al.*, 1988; Macfarlane *et al.*, 1994; Condie *et al.*, 1995; Öhlander *et al.*, 1996; Panahi *et al.*, 2000; Sharma and Rajamani, 2000) and that the redox conditions of soil solution could play an important role in pedogenic REE mobility (Duddy, 1980; Braun *et al.*, 1990). Because REE concentrations and patterns vary greatly among different minerals, weathering redistribution of REE can have widely varying effects in different profiles formed on different parent materials and under different conditions. In many cases, trace minerals (e.g., apatite, monazite, sphene, or zircon) control the overall REE content of the rock or soil, and different solubilities under earth-surface conditions can lead to a wide variety of REE patterns in the weathering products (e.g., Harlavan and Erel, 2002) . For obtaining a Sm-Nd age of weathering, the important factor is that weathering processes can fractionate the Sm/Nd ratio of the parent rock.

3.2.3 Sm-Nd Geochronology Applied to the Steep Rock Profiles

Absolute ages of rocks are obtained by quantifying the natural decay of a radioactive parent nuclide into a stable daughter nuclide. In order to obtain the age of a rock using the isochron method for a particular parent-daughter decay system, the following is required: (1) the half-life of the parent-daughter decay system must be appropriate for the age of the rock; (2) the parent and daughter nuclides must be present in quantities sufficient for accurate measurement by existing technology; (3) the daughter element must have been isotopically homogenized in the rock (at the scale of measurement) when it formed; (4) there must be a spread in the parent: daughter ratio among phases (minerals or whole rock samples) of the rock unit to be dated; and (5) parent and daughter elements must not have been substantially disturbed thereafter.

The Sm-Nd geochronologic system is most commonly used for igneous rocks, which are likely to be isotopically homogeneous at the time of their formation, and which have different, separable phases (minerals) with different Sm/Nd ratios that can be used to generate isochrons. In the Sm-Nd system, the parent ^{147}Sm undergoes alpha decay to ^{143}Nd with a half-life of 106 billion years (Ga). Both the parent and daughter are rare earth elements (REE), a group of elements ($_{57}La$ to $_{71}Lu$) whose members generally behave in a geochemically coherent fashion and are considered relatively immobile during metamorphism and low-temperature alteration. However, recent work has suggested that weathering and diagenesis can affect the distribution of REE in rocks at or near the earth's surface. This can lead to problems when trying to "see through" low-temperature events or recent weathering, but it can also create opportunities for using Sm-Nd as a geochronometer of earth surface processes. In order for the Sm-Nd system to be used successfully to date the time of soil formation in a paleosol, pedogenic processes must be capable of creating a spread in Sm/Nd ratios in different parts of a soil profile.

3.3 METHODS USED IN THE STEEP ROCK INVESTIGATION

3.3.1 Sampling and Sample Preparation of Steep Rock Samples

Samples from the apparent paleosol at South Roberts Pit (SRP), overlying sediments of the Steep Rock group, and the parent tonalite were collected during a field excursion in 1999. **Figure 3.4** shows a schematic geologic column with the stratigraphic position of the samples collected from the weathering profile and the overlying Wagita Formation conglomerate. Samples were ~0.5 kg in size; the samples were cut in the lab and oriented thin sections were prepared. Rock chips

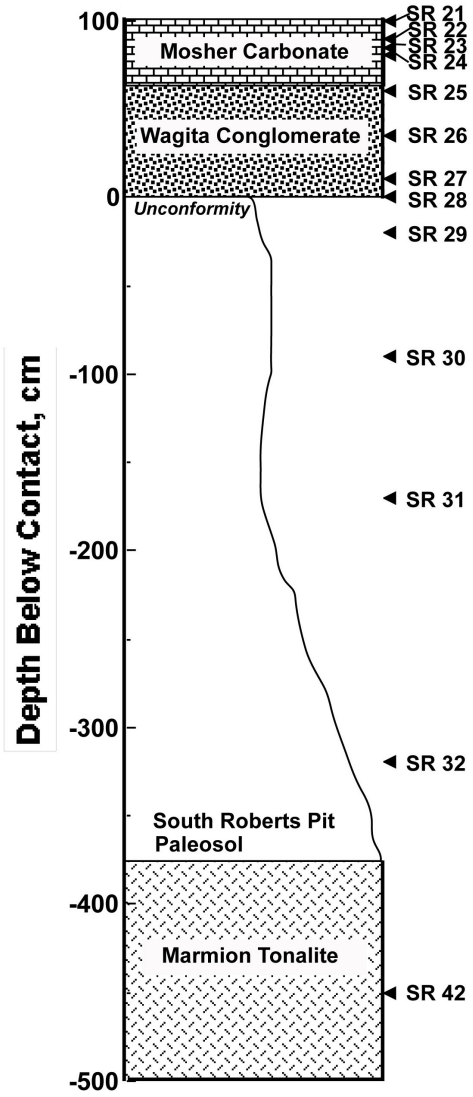

Figure 3.4: Schematic profile of the South Roberts Pit (SRP) paleosol showing sample locations.

free of modern weathering rinds were segregated and ground to a fine powder in a tungsten-carbide ball mill. Splits of ~20 g were set aside for major and trace element analysis, and smaller splits of ~300 mg were set aside for isotopic analysis.

3.3.2 Major and Trace Element Geochemistry of Steep Rock Samples

Major and trace element data for whole rock samples were measured by Activation Laboratories Ltd., in Ontario, Canada. Whole rock powders were dissolved by $LiBO_2$ fusion; major elements were analyzed by ICP-OES and trace elements were analyzed by ICP-MS. FeO was determined by dichromite titration.

3.3.3 Sm-Nd Geochemistry of Steep Rock Samples

Radiogenic isotope chemistry (Rb-Sr and Sm-Nd) was carried out at the University of Pittsburgh under clean laboratory conditions. A portion of the whole rock powder splits (50 to 200 mg) was dissolved in Teflon© bombs using ultrapure acids including hydrofluoric (HF), perchloric ($HClO_4$) and hydrochloric (HCl). An aliquot of 1-5 mg was removed and spiked with a mixed ^{87}Rb-^{84}Sr-^{147}Sm-^{150}Nd tracer solution, and rough concentrations were determined using isotope dilution thermal ionization mass spectrometry. Based on these results, the remaining sample was spiked with mixed, isotopically pure ^{87}Rb-^{84}Sr and ^{147}Sm-^{150}Nd tracer solutions. Following addition of the tracer solutions, Rb, Sr, and the REE were separated from the remaining matrix using cation exchange columns. Samarium and neodymium were separated from the other REE and each other in quartz columns loaded with LNSpec® resin.

Rubidium was loaded on a single rhenium filament and its concentration determined by isotope dilution on a Finnigan MAT 262 thermal ionization mass spectrometer (TIMS) at the University of Pittsburgh. About 250 ng of Sr was loaded on a single Re filament with Ta-oxide powder, and the concentration and isotope composition were determined simultaneously by TIMS. For each sample, 100 ratios were measured at an intensity of 2-4 x 10^{-11} A, and mass fractionation was corrected using an exponential law with $^{86}Sr/^{88}Sr = 0.1194$. The average value for $^{87}Sr/^{86}Sr$ of SRM 987 over the time period of these analyses is 0.71024. Both Nd and Sm were loaded on double Re filaments. Concentrations of Sm were determined by isotope dilution, and the concentration and isotopic composition of Nd were determined simultaneously by TIMS, with 100 ratios measured at a ^{144}Nd beam intensity of 0.5-2 x 10^{-11} A. $^{143}Nd/^{144}Nd$ ratios were corrected for mass fractionation using an exponential law and normalizing to $^{146}Nd/^{144}Nd = 0.724134$. The University of Pittsburgh value for chondritic $^{143}Nd/^{144}Nd$ is 0.511847.

3.4 MINERALOGY AND MORPHOLOGY OF STEEP ROCK SAMPLES

3.4.1 Macromorphology of the SRP Profile

The South Roberts Pit profile formed on tonalitic rock. The parent material (sample SR 42) is black and white with pink and green mottles. The profile (samples SR 32 to 28) is relatively thin (~3m) compared to some paleosols and consists of increasingly altered tonalitic material grading into pistachio green (5G 7/1) rock with up to 35% quartz and a gritty, talc-like sheen. Quartz stringers and buff-colored wispy lineations are apparent on fresh surfaces. The weathered section lacks sedimentary bedding. It is directly overlain by a poorly sorted sandstone (Wagita

Formation) with >75% quartz. The yellow (10Y 8/2) sandstone (SR 27 to 25) contains some dark green (5G 4/2) apparent hydrothermal zones, which contain concentrated stringers of choritized biotite and opaques (mainly pyrite with some ilmenite). The sandstone is ~0.2 m thick in the sampled section, gradually lightens in color and becomes more calcareous upward. Directly above the sandstone is a dark blue-gray to blue gray carbonate sequence (5PB 4/1 to 5PB 6/1) (Mosher Carbonate, SR 24 to 21). The basal carbonate has lineations with minor chloritized biotite and opaques (pyrite). The pyrite in the carbonate is mostly associated with black stringers, which appear to be organic material. The carbonate continues up to 500 meters above the sampled section and contains stromatolite forms ranging from *Stratifera*-like to hemispherical (Wilks and Nisbet, 1988).

3.4.2 Mineralogy and Micromorphology of SRP Samples

The parent tonalite (SR 42) has a relatively homogeneous texture and is composed of interlocking grains (average size ~1 mm) of plagioclase (~55%), quartz (~35%), biotite (9%) and accessory minerals (~1%) including ilmenite, paragonite, titanite, epidote and apatite. Plagioclase in the sampled parent rock is ~30-40% altered to sericite (**Figure 3.5a**) and biotite is partially altered to chlorite.

Moving upward in the outcrop, the plagioclase in sample SR 32 shows a mottled appearance and is more altered to sericite (up to 50%; likely a metamorphic alteration of 2° smectite). Leucoxene (a fine grained alteration product of ilmenite and titanite) appears as white mottles (~1mm) in reflected light. Shadowy grain boundaries and twinning are still apparent in the remnant plagioclase grains (**Figure 3.5b**). The lower profile displays an intertexic texture (from Stoops and Jongerius, 1975), with grain boundaries touching and clay forming between

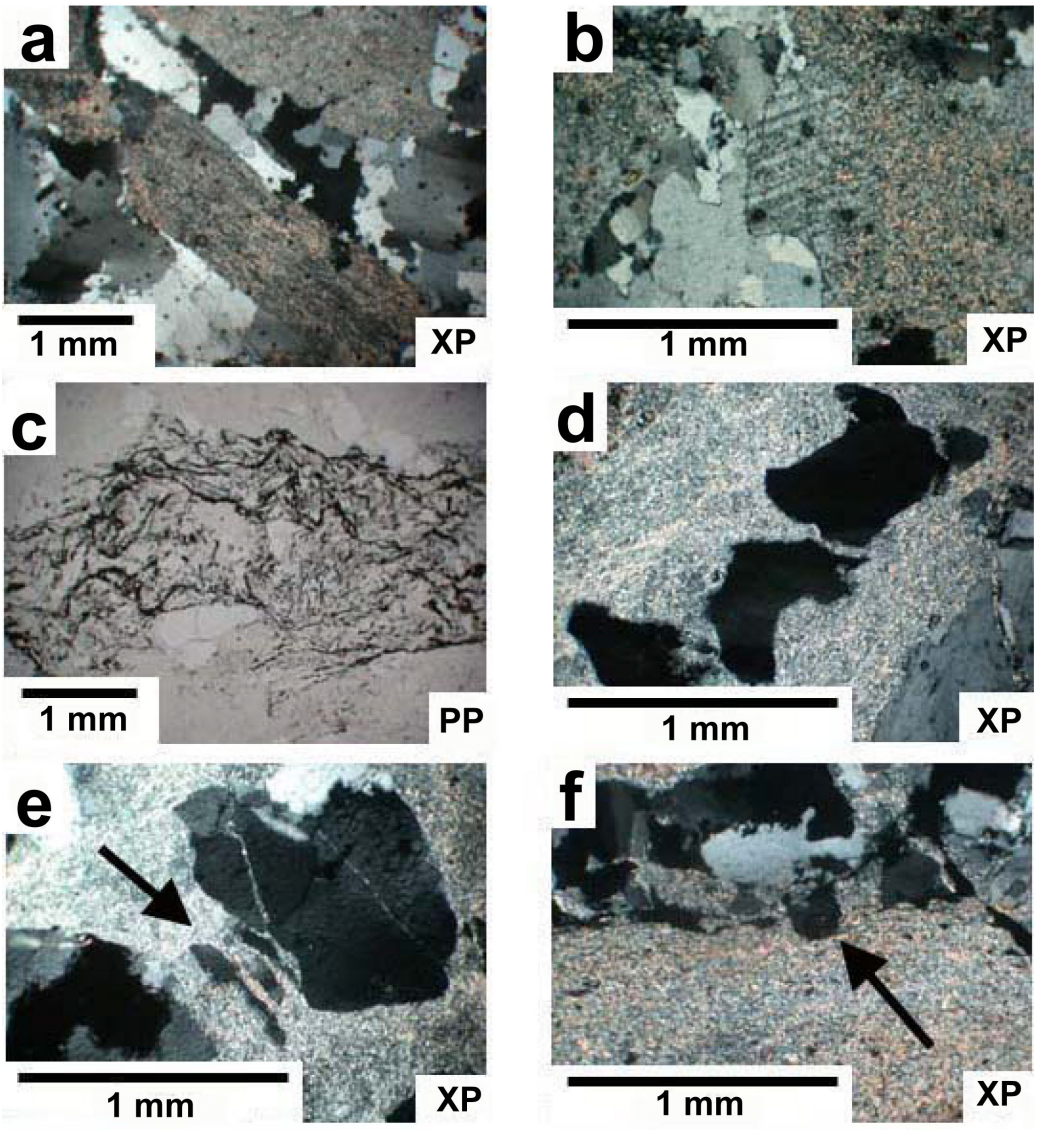

Figure 3.5: (a-f) Photomicrographs of the SRP profile. XP= crossed polars and PP= plain polars. Scale is on each photograph. (a) tonalite parent (SR-42); (b) remnant twinned plagioclase in paleosol (SR-29); (c) weathered biotite in paleosol (SR-29); (d) embayed quartz in paleosol (SR-28); (e) spalling quarts grain in paleosol (SR-28); (f) soft sediment deformation at unconformity (SR-27). Photomicrographs of the SRP profile. XP= crossed polars and PP= plain polars. Scale is on each photograph.

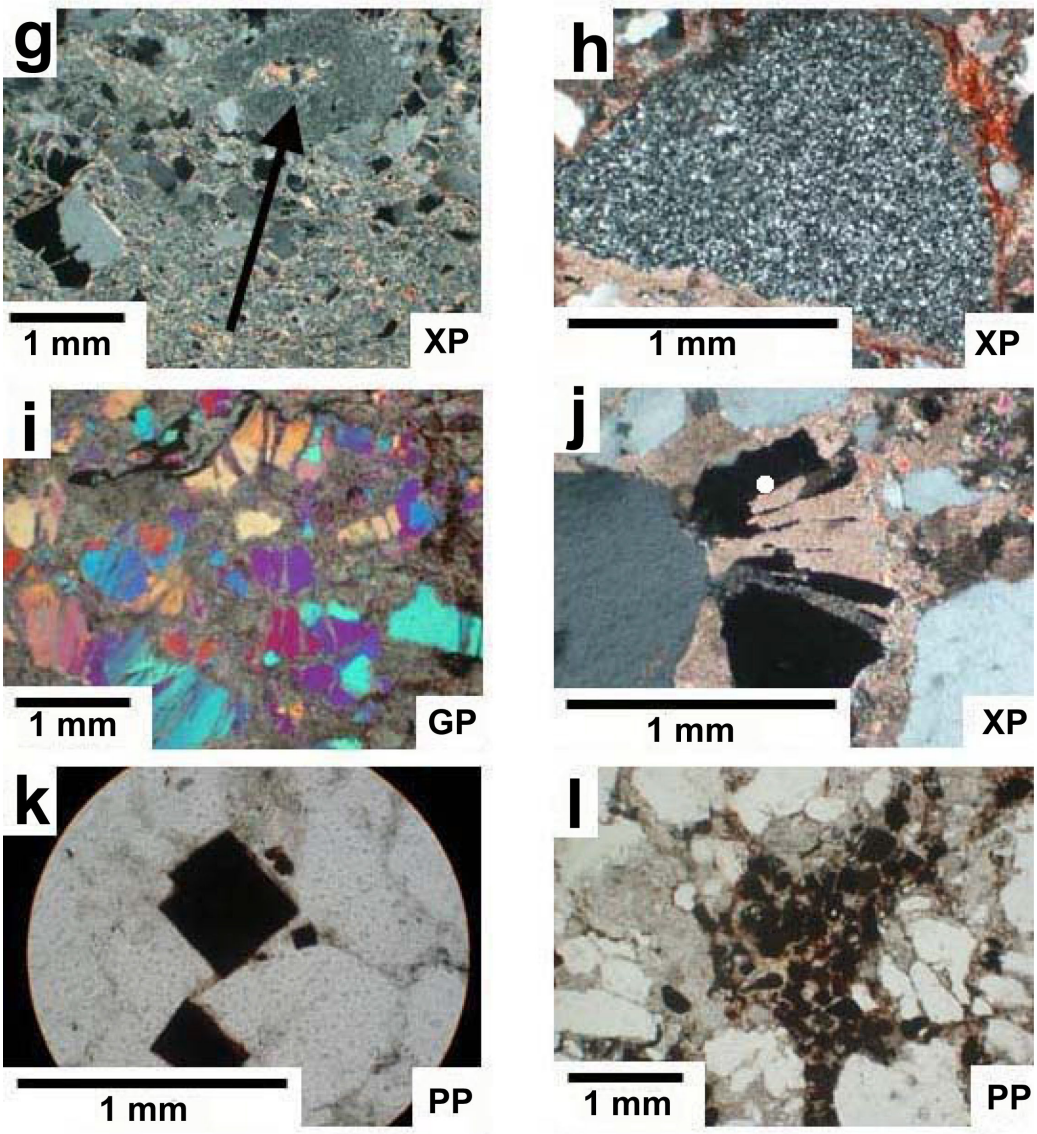

Figure 3.5 (cont'd): (g-i) (g) rip up clast with feldspar in the Wagita conglomerate (SR-27); (h) cutan of clay and iron oxide (post-pedogenic alteration of iron hydroxide) surrounding recrystallized quartz in Wagita conglomerate (SR-26); (i) spalled quartz grains (SR-24, with gypsum plate) in Wagita Conglomerate; (j) carbonate replacing clay in spalled quartz grain in Wagita Conglomerate (SR-25); (k) post pedogenic pyrite in Wagita Conglomerate (SR-26); (l) opaque minerals including pyrite and ilmenite in vein cutting Wagita conglomerate (SR-26).

some grains. Plagioclase boundaries decrease upward and are rare at the top of the profile (SR 31 to SR 29), as the samples become increasingly matrix-supported (agglomeroplasmic texture). Sericite increases up the profile to the unconformity, eventually forming a massive felt-like texture near the unconformity. The brown wispy lineations apparent in hand sample (SR 32 to SR 28) are weathered and chloritized biotites mixed with leucoxene (**Figure 3.5c**). As a crystal of biotite weathers to clay (kaolinite or smectite), it takes on a bloated appearance, expanding and splitting into sub-parallel layers (Folk and Patton, 1982; Capo, 1994). If the biotite weathers to smectite, the Fe content is generally accommodated in the smectite structure (Delvigne, 1998); if the biotite weathers to kaolinite, the Fe content is typically associated with iron oxide or secondary chlorite (Delvigne, 1998). In the Steep Rock samples, the Fe may be related to smectite and/or chlorite.

Dissolution textures found at the top of the profile include pitted and corroded quartz grains (SR 28; **Figure 3.5d**). Corroded and dissolved quartz has been documented in modern soils (Delvigne, 1998). Spalling of quartz mineral grains is also apparent at the top of the profile (SR 29; **Figure 3.5e**). Spalling is typically associated with biotite or clay expansion during weathering as in the Cambrian Squaw Creek paleosol (Capo, 1994). It may be caused by differential thermal expansion or preferential fracturing along weak cleavage planes (Begle, 1978). Preservation of delicate spalled grain textures probably indicates that weathered material has not undergone significant post-pedogenic sedimentary transport.

The boundary between the SRP profile and the overlying Wagita sandstone is very apparent in thin section (SR 27; **Figure 3.5f**). Along this boundary, quartz grains from the overlying sandstone appear to sink into the "softer" weathering profile. Paleosol clasts composed of feldspar grains altered to sericite (some with remnant twinning) and sericite (altered

smectite) are encased in the overlying sandstone (SR 27; **Figure 3.5g**). These rip-up clasts indicate erosion and entrainment of soil material into the transgressing sands. Rip-up clasts are considered an important identification criterion for paleosols (Retallack, 1988; Gall, 1992; Rye and Holland, 1998).

Some quartz grains just above the unconformity are coated with sericite and remnant clay indicative of *in situ* weathering and minimal transport during deposition of the overlying sandstone (SR 26; **Figure 3.5h**). Other quartz grains have been split apart by the expansion of clay (e.g., smectite, now altered to sericite) grains during weathering (SR 24; **Figure 3.5i**) as discussed earlier. Some of the expansion features in the quartz grains are now filled by carbonate (SR 25; **Figure 3.5j**). These features, combined with the geochemical trends discussed below, confirm that the profile exposed at South Roberts Pit is indeed a paleosol.

Spalling quartz, rip-up clasts and cutans (sensu Brewer, 1964) indicate that the sandstone overlying the SRP profile was at least partially derived from the underlying paleosol. Some of the cutans and spalling quartz preserved in the sandstone may also have formed after chunks of paleosol were transported a short distance and mixed with fluvial or nearshore deposits. The minerals in these deposits, which were most likely exposed to atmospheric process at least intermittently, would have continued to weather. Wilks and Nesbit (1988) concluded from the paleotopography of the unconformity that the Steep Rock depositional environment was most likely a mature erosional surface with no strong relief change. This strengthens the argument that transportation of eroded paleosol was most likely proximal. Eventually, the nearby sea transgressed, inundating and burying the newly formed soils and covering them with a carbonate platform. The carbonate mineralogy present in the sandstone (SR 27 to SR 25; increasing up from ~10% to 50%) was most likely introduced during the formation the carbonate platform or

during burial and diagenesis of the sandstone. Changes in mineralogy and micromorphology up the SRP profile are consistent with *in situ* subaerial weathering followed by erosion, transgression, and carbonate deposition.

3.4.3 Post-pedogenic Alteration Fabrics in SRP Samples

In the parent tonalite (SR 42), biotite is partially chloritized, even in the freshest samples; chlorite is present as green mottles. Rare 1 mm diameter pink mottles in the parent material are probably paragonite. The trend of the paragonite, parallel with the metamorphic grain, suggests that it formed syn-metamorphically. During regional metamorphic events, platy minerals generally form normal to directed stress resulting in schistosity (Philpotts, 1989). Within the SRP, biotite is ~50% altered to chlorite; chloritization gives the profile its characteristic green color. Sericite is likely a metamorphic alteration of smectite produced from the weathering of plagioclase. It increases upward, ultimately forming a felted texture. Quartz at the base of the SRP is recrystallized into weakly developed stringers (2- 10 mm long) with slightly strained extinction. Quartz grains are increasingly strained and recrystallized up the profile. This, and the presence of muscovite as the unconformity is approached (SR 30 to SR 28), could be due to increased porosity at the top of the preserved profile (upper C horizon/lower B horizon?), which would have enhanced interaction with hydrothermal fluids.

Minor (1-4 mm diam.) carbonate veins cut both the tonalite and the apparent paleosol. Larger (up to 1 cm diam.) dark green to brown veins cut across the overlying sandstone and carbonate. The minerals include pyrite, chlorite and microcrystalline quartz and minor ilmenite (**Figure 3.5k-l**). Some of the pyrite grains are euhedral, while others appear hollow and altered, possibly indicative of more than one thermal event that affecting the profile or the alteration of

sedimentary pyrite produced in localized reducing conditions related to organic material. The minerals and textures preserved in the Steep Rock profile are consistent with subaerial weathering followed by hydrothermal/greenschist grade metamorphic event(s).

3.5 GEOCHEMISTRY OF THE SRP PROFILE

3.5.1 Major Element Geochemistry of the SRP Profile

To account for concentration or dilution due to volume changes during pedogenesis, data were normalized to a relatively immobile element (see Nesbitt, 1979; see Chadwick *et al.*, 1990; Kurtz *et al.*, 2001). Titanium (Ti) is commonly used to normalize geochemical data in paleosols. However, in a study by Stone *et al*. (1992) of Precambrian geology in the Steep Rock area, Ti showed a relatively heterogeneous distribution in the tonalitic parent whole rock samples; TiO_2 concentrations ranged between 0.14% and 0.88% (see **Table 3.1**). In addition, Macpherson *et al.* (2000) found that in the SRP samples hafnium (Hf), tantalum (Ta), and zirconium (Zr), sometimes used to normalize paleosol data, co-reside with Ti in the accessory mineral titanite . For the SRP whole rock samples, aluminum (Al) was chosen for normalization because of its abundance and relatively homogeneous distribution throughout the profile compared to these other immobile elements.

Whole rock elemental data are reported in **Table 3.2**. The percent change of elements in the SRP profile and the overlying sandstone, normalized to Al and to parent tonalite (parent=100), is shown in **Figure 3.6**. Sandstone samples are shown to illustrate the distinct change in rock chemistry above the unconformity.

Table 3.1: Whole rock geochemical statistics for the "old" tonalite (1b) (Stone et al., 1992)

Oxide (%)	Minimum	Maximum	Median	Mean	Std dev.
SiO_2	57.3	73.4	71.4	68.42	5.78
TiO_2	0.14	0.88	0.26	0.34	0.22
Al_2O_3	12.8	17.1	15.0	14.96	1.35
Fe_2O_3	0.3	4.1	0.5	1.05	1.12
FeO	0.0	4.2	1.7	2.08	1.31
MnO	0.02	0.11	0.05	0.06	0.03
MgO	0.40	4.03	0.85	1.47	1.31
CaO	0.37	7.46	2.63	3.17	2.03
Na_2O	1.59	5.90	4.40	4.33	1.16
K_2O	0.26	3.56	1.27	1.29	0.88
P_2O_5	0.04	0.28	0.08	0.11	0.08
H_20	0.6	2.4	1.1	1.22	0.64
CO_2	0.0	4.5	0.4	0.86	1.33
S	0.00	0.03	0.00	0.00	0.01

Table 3.2: Whole rock major element analysis of Steep Rock paleosol samples and parent tonalite.

	Depth	Weight %													
Sample	(cm)	SiO_2	Al_2O_3	Fe_2O_3	FeO	MnO	MgO	CaO	Na_2O	K_2O	TiO_2	P_2O_5	LOI	Total	CIA
Conglomerate															
99-SR-26	35	74.19	3.57	0.84	1.94	0.236	3.39	5.90	0.06	0.98	0.246	0.02	8.81	100.18	-
99-SR-27	10	80.91	3.36	1.91	1.33	0.201	1.79	4.37	0.03	0.76	0.256	0.02	5.39	100.33	-
Paleosol															
99-SR-28	0	69.83	17.81	1.14	0.43	0.010	0.94	0.08	0.08	6.25	0.160	0.02	2.77	99.52	75
99-SR-29	-20	70.16	17.70	1.04	0.45	0.006	0.96	0.07	0.07	6.33	0.758	0.05	2.61	100.20	75
99-SR-30	-90	68.20	18.81	0.97	0.69	0.008	0.95	0.18	0.08	6.76	0.433	0.07	3.06	100.21	75
99-SR-31	-170	68.09	18.73	0.98	0.62	0.010	0.88	0.41	0.12	6.43	0.784	0.04	3.31	100.40	74
99-SR-32	-320	59.93	22.24	1.57	0.98	0.012	1.17	0.62	0.24	8.62	0.598	0.06	3.99	100.03	72
Parent Material															
99-SR-42	-450	69.75	14.14	1.16	1.62	0.041	0.99	2.57	1.46	4.09	0.215	0.08	4.20	100.32	59

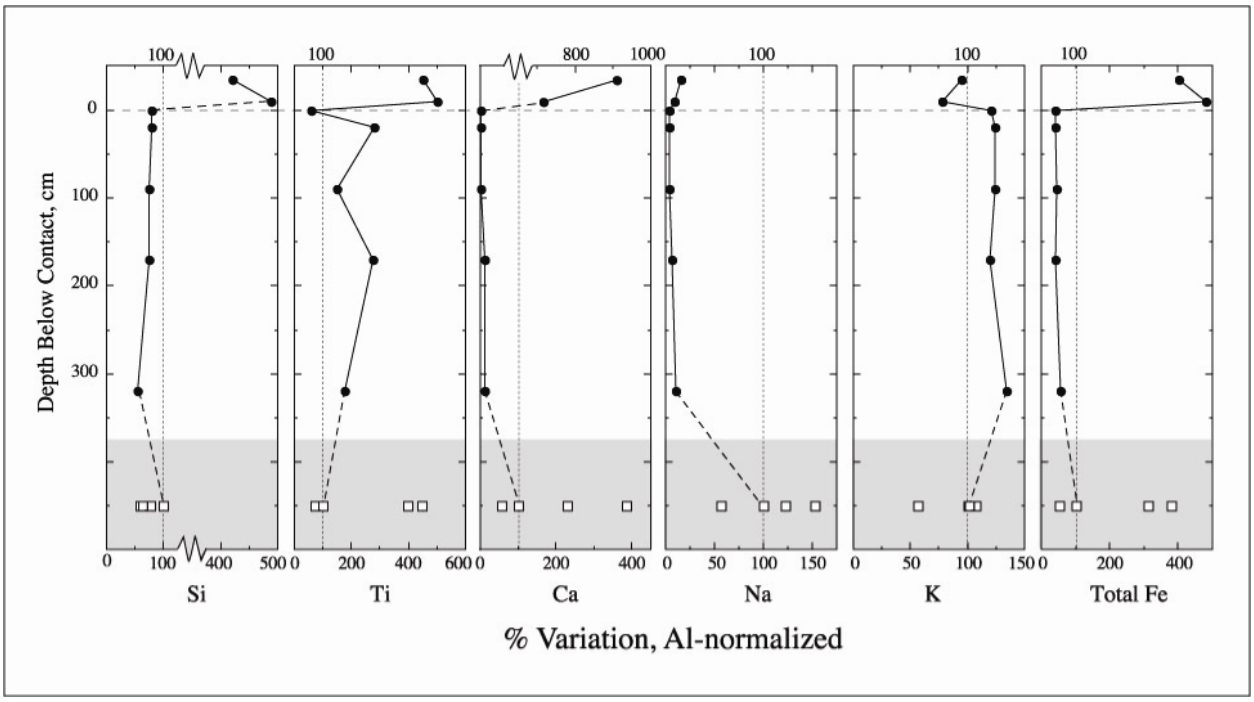

Figure 3.6: Aluminum-normalized percent variation in major elements relative to parent material (parent = 100) for the Steep Rock Paleosol.

The slight depletion of silicon (Si) (average loss of 27%) suggests dissolution of quartz and the breakdown of plagioclase during weathering and/or hydrothermal activity. The large increase (~300%) in silicon just above the unconformity is due to the change from matrix-supported soil to quartz grain supported sandstone. The profile shows significant depletion of alkali and alkaline earth elements including calcium (Ca; up to 98%) and sodium (Na; up to 96%) relative to parent material. The decrease in Ca and Na upward reflects increasing loss of plagioclase feldspar. The upper horizons of modern soils are often affected by leaching agents, which can be inorganic (e.g. carbonic acid) or organic (e.g. humic or fulvic acid). The acidity increases the mobility of cations (Nesbitt *et al.*, 1980). Additionally, in well-developed soils, the presence of low cation exchange capacity 1:1 clays such as kaolinite inhibits retention of cations (Nesbitt *et al.*, 1980). Although only the lowermost part of the SRP profile is preserved, the

pervasive gradational loss of base cations suggests that the profile represents a soil developed in an area with high chemical weathering rates. The loss of base cations in the SRP profile is typical in modern ultisols, soils that form in warm, moist environments conducive to chemical weathering.

However, some base cations are relatively less depleted. Magnesium (Mg), which is only slightly depleted (<35%), was most likely incorporated in the smectite structure (Rye and Holland, 1998); potassium (K) is enriched. Both were likely affected by post-pedogenic alteration, and the overall geochemical trends are consistent with *in situ* subaerial weathering followed by greenschist metamorphism.

Sharma and Rajamani (2000) plotted weathering trends for tonalites and granites on A-CN-K (Al_2O_3-$CaO_{silicate}$+Na_2O-K_2O) diagrams, where $CaO_{silicate}$ represents only the Ca in silicate minerals (**Figure 3.7**). The solid line indicates the typical trend for chemical alteration of granitoid, which reflects weathering of plagioclase and then K-bearing phases (K-spar, illite, and muscovite) and finally results in alteration to kaolinite. The weathering trend for the Steep Rock profile is defined in **Figure 3.7** by open squares. The parent tonalite is plotted as a closed square. While the Steep Rock samples exhibit decreases in Ca and Na as seen in the early stages of modern weathering of granitoid profiles, the samples are clearly shifted toward more potassium-rich values. This implies K addition after pedogenic processes, which is discussed in the following section.

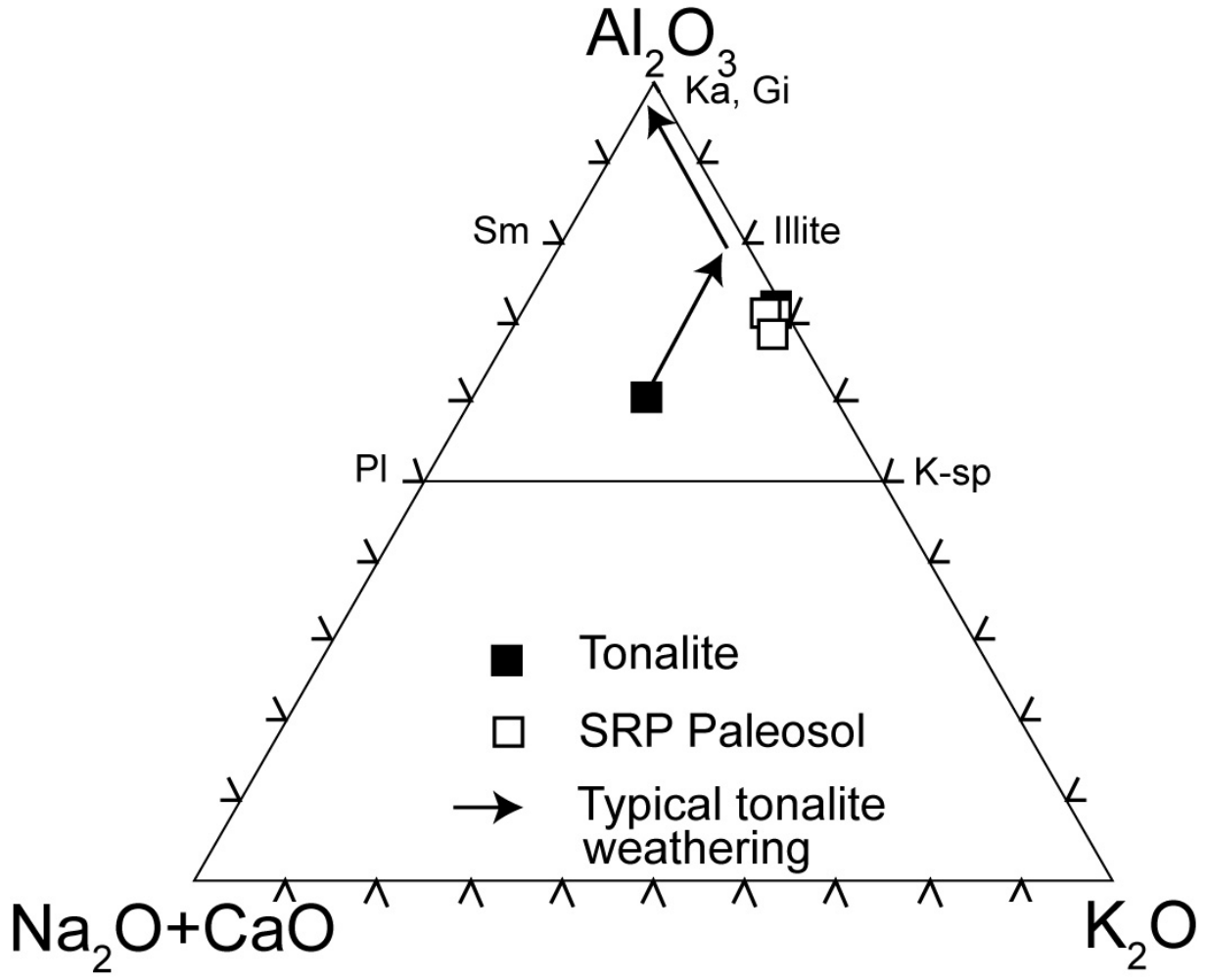

Figure 3.7: ACNK diagram showing parent tonalite (closed square), and paleosol (open squares) samples for SRP profile. The black arrows indicate a typical weathering trend for tonalite. Note the offset of the SRP profile towards K.

3.5.2 Diagenetic, Metasomatic/Metamorphic and Hydrothermal Alteration of the SRP

Post-depositional potassium addition can result in a change in mineralogy from smectite to illitic, chloritic and/or sericitic phases, or to potassic feldspar (for examples see Gay and Grandstaff,

1980; Feakes *et al.*, 1989; Holland *et al.*, 1989; Rainbird *et al.*, 1990). Schmitt (1999) suggested that kaolinite and K-feldspar are unstable in near-surface environments when water is present, and re-equilibrate over time to form assemblages of K-feldspar + muscovite or muscovite + kaolinite. Nesbitt and Young (1984; 1989) theorized that K leached from surface soils provides the source of potassium during late diagenesis. Rainbird et al. (1990) suggested that K addition occurs in buried soils in subsiding basins where continental groundwaters have high K/Na ratios.

Archean continental crust, which mainly consists of komatiite, tholeiitic basalt, and tonalite, is relatively K depleted (Condie, 1981). Tonalite, in particular, is thought to have formed in granitoid-greenstone terranes by partial melting of amphibolite or similar K-poor rocks during collapse of rift-generated greenstone belts or subduction of mafic ocean crust. K-granites in Late Archean terranes typically occur post-tectonically and are related to long periods of cooling during magmatism and deformation when only small melts are generated through partial melting (Condie, 1981). Thus potassium addition in the SRP paleosol was most likely due to post-pedogenic K-metasomatism. Hydrothermal fluids would have added additional K at temperatures sufficiently high to recrystallize kaolinite or smectite produced during weathering into sericite or even paragonite. This metasomatic event could have been related to the 2.95 Ga hydrothermal event concurrent with the formation of the Jolliffe Ore Zone (reported by Tomlinson *et al.*, 1999, as D. Davis, personal communication), but was most likely during the regional greenschist metamorphic event that took place ~2.7 Ga (Davis and Jackson, 1988) related to the Kenoran orogenic event.

Although Mg typically behaves as Ca in weathering profiles (leached in humid environments with high chemical weathering rates or retained in dry climates with low chemical weathering rates), Mg is less depleted in the Steep Rock profile than Ca. Mg is a common

constituent in chlorite. Low-grade metamorphic events associated with Mg and Fe addition can convert clays like smectite ($R_{0.33}Al_2Si_4O_{10}(OH)_2 \bullet H_2O$ where R= Na^+, K^+ Mg^{2+}, or Ca^{2+}) to chlorite (Mg, Fe^{2+}, Fe^{3+})$AlSi_3O_{10}$. The geochemical trends in the SRP profile are consistent with subaerial weathering followed by K-metasomatism and/or greenschist metamorphism.

3.5.3 Chemical Index of Alteration

The chemical index of alteration (CIA= $100 \bullet Al_2O_3/[Al_2O_3+CaO_{silicate}+Na_2O+K_2O]$, all in moles) measures the breakdown of feldspar and mica and the loss of base cations during weathering (Nesbitt, 1979; Schau and Henderson, 1983; Öhlander *et al.*, 1996). A complicating factor in calculating the CIA is the addition of potassium to the Steep Rock profile after soil forming processes. A K correction was made to adjust the values for post-pedogenic K added to the profile using the following formula: $K_2O_{corr}= [m \cdot Al_2O_3 + m \cdot (CaO_{silicate}+Na_2O)]/(1-m)$ where m= $K_2O/(Al_2O_3+CaO_{silicate}+Na_2O+K_2O)$ for the parent material (Panahi *et al.*, 2000) and $CaO_{silicate}$=CaO corrected for apatite using $CaO_{silicate}$=mole CaO-[3.3·mole P_2O_5] (Deer *et al.*, 1966).

The CIA_K increases from 59 to 75% upward from the tonalitic parent to the unconformity (**Figure 3.8**). Although the spread of CIA_K values is not large, the general increase in the CIA_K values from the partially altered parent tonalite at the bottom of the profiles through the weathering profiles to the erosional contact (at 0 meters) reflects the increase in weathering with the progressive breakdown of feldspars and mica to clays. The values are consistent with parent

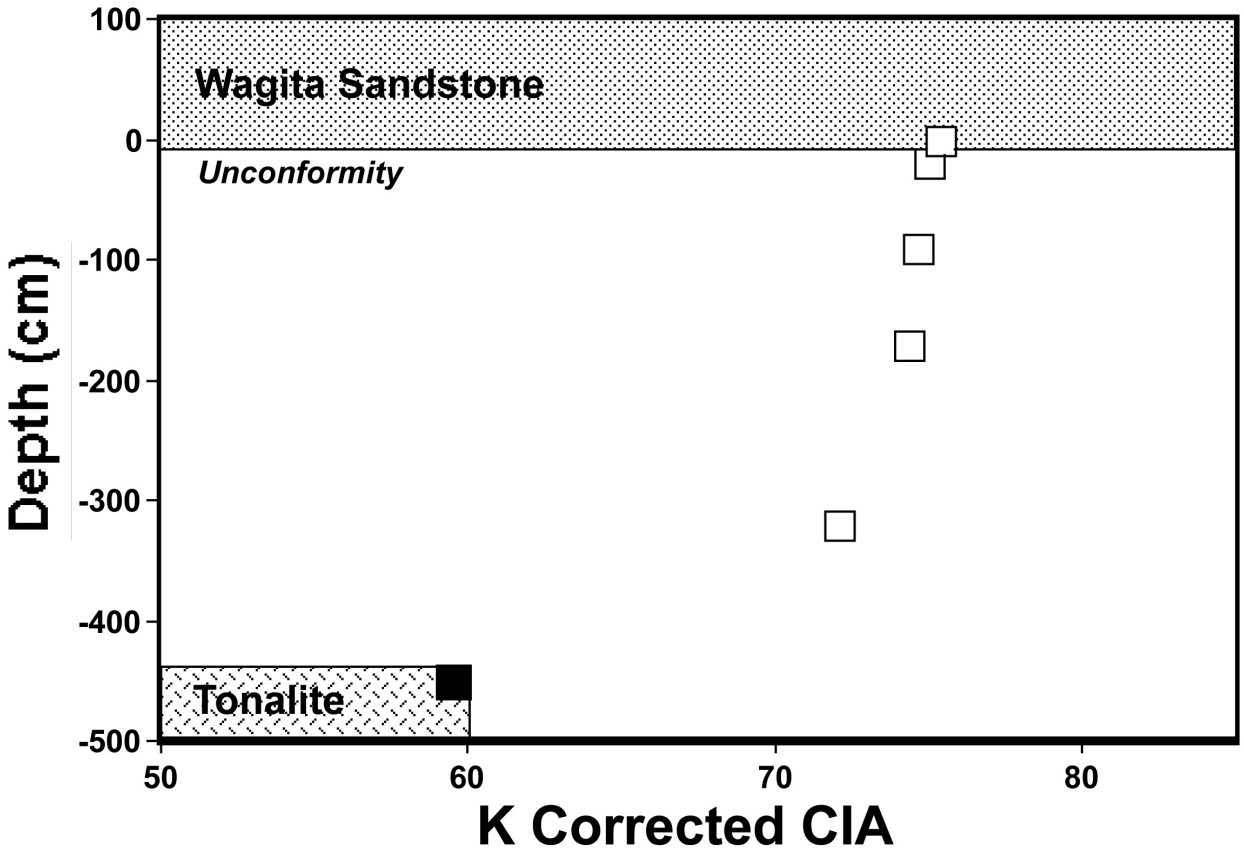

Figure 3.8: K-corrected CIA weathering index for the SRP profile. Parent tonalite=closed square and soil=open square.

tonalite grading into a partially altered soil or "C" horizon or lower "B" horizon (equivalent to Zone 2 of Marmo and Kohonen, 1992; CIA >70 and <80). The lack of CIA_K values of greater than 80% suggests either an immature soil or that the more weathered horizons (i.e. "A" and most of "B" horizon; equivalent to Zone 1 of Marmo and Kohonen, 1992; CIA≥80) found in modern, well developed soils were mostly eroded away.

3.5.4 Iron Mobility in the SRP Profile

Variation of Al-normalized total Fe (Fe_T), Fe^{2+}, and Fe^{3+} from the parent tonalite (p=0) with depth for the SRP paleosol is shown in **Figure 3.9a**. Fe_T loss ranges from 43 to 58%. Fe^{3+} shows less depletion (up to 37%) than Fe^{2+} (up to 79%). Like the SRP paleosol, the CP profile (developed on granodiorite) also exhibits Fe^{3+} values greater than Fe^{2+} (Schau and Henderson, 1983) (**Figure 3.9b**). However, Fe^{3+} shows relative enrichment compared to the parent and total Fe increases (72%) in the middle of the profile. Fe loss occurs only at the top of the profile.

The Fe_T loss at the top of the preserved Steep Rock profiles is slightly more than the Fe_T loss of modern and paleosols, which is ≤50% (Driese, 2004). Only the bottom parts of the Steep Rock profiles are preserved; Fe_T loss may have been higher in the unpreserved upper horizons of the paleosols. Loss of Fe_T is prevalent at the top of pre-2.2 Ga paleosols and has been suggested as evidence for a reducing atmosphere (Holland, 1984; Holland *et al.*, 1989; Kirkham and Roscoe, 1993). Fe loss at the top of the profiles with Fe_T gain in the lower part of the profiles could be due to leaching of Fe under reducing conditions (local or global) and movement of Fe through the soil profile followed by deposition at or near a weathering front or the paleo-water table.

Iron movement does not require an anoxic atmosphere; Driese (2004) documented translocation of Fe within modern and Paleozoic paleo-vertisol profiles despite forming under oxygenated conditions. Waterlogged conditions in modern soils are also capable of reducing and moving Fe despite an oxygen-rich atmosphere (Dia *et al.*, 2000). Alternatively, the experimental work by Neaman *et al*. (2005) shows that organic ligands can also mobilize redox elements such as Fe in soil environments. Subsequent deposition of Fe near the weathering front could be due to: (1) an increase in cation exchange capacity associated with an increase of 2:1 clays deeper in

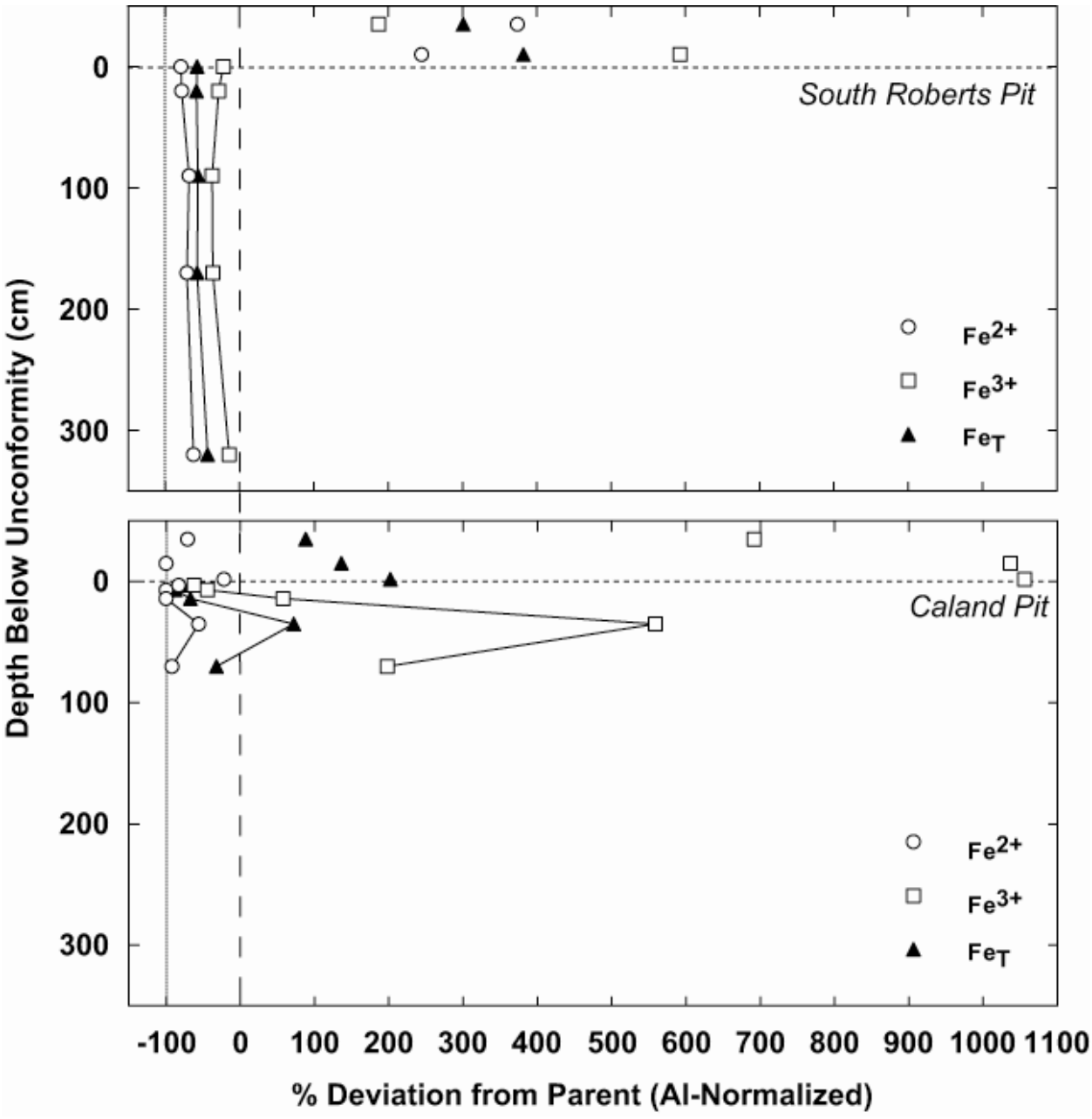

Figure 3.9: Aluminum-normalized percent variation in Fe_T, Fe^{2+}, and Fe^{3+} relative to parent material (parent = 100) for the SRP and CP profile.

the soil profile; (2) a decrease in the leaching capacity as inorganic and/or organic acids are naturally neutralized or diluted; or (3) an increase in pH due to weathering of feldspars, which produces alkalinity (Nesbitt *et al.*, 1980). In addition, the evaluation of Fe^{3+} relative to Fe^{2+} has resulted in alternative interpretations for Fe loss in paleosols, such as oxidation followed by alteration due to reductive fluids (mixed-type paleosol; Ohmoto, 1996).

Relative to average parent material, both Steep Rock weathering profiles show an increase in normalized Fe^{3+} down profile. Schau and Henderson (1983) interpreted the enrichment of Fe^{3+} in the middle of the CP profile as an indication that there was enough pO_2 to oxidize Fe, but qualified the interpretation as a local phenomenon and not necessarily an indication of atmospheric conditions during the Archean. The profiles also have a Fe^{3+}/Fe^{2+} ratio of >1. The loss of Fe_T coupled with amounts of Fe^{3+} greater than Fe^{2+} in both Steep Rock paleosols could indicate that the soils interacted with oxidizing fluids to form Fe hydroxides, but were stripped of Fe by syn-pedogenic organic fluids or during post-pedogenic alteration by hydrothermal fluids (Ohmoto, 1996), resulting in a Fe^{3+}/Fe^{2+} ratio of >1 (**Figure 3.10**).

3.5.5 REE Patterns in the SRP Profile

Rare earth element data are reported in **Table 3.3**. Chondrite-normalized plots for SRP paleosol samples are presented in **Figure 3.11a**. The parent rock (SR42; 450 cm) shows enrichment in light rare earth elements (LREE: La to Sm), which is expected for a tonalite (Condie, 1981). Paleosol REE patterns are subparallel to the parent material and show considerable variation in LREE above and below the parent, but retain the LREE-enriched, flat heavy rare earth (HREE: Gd to Lu) trend of the tonalite.

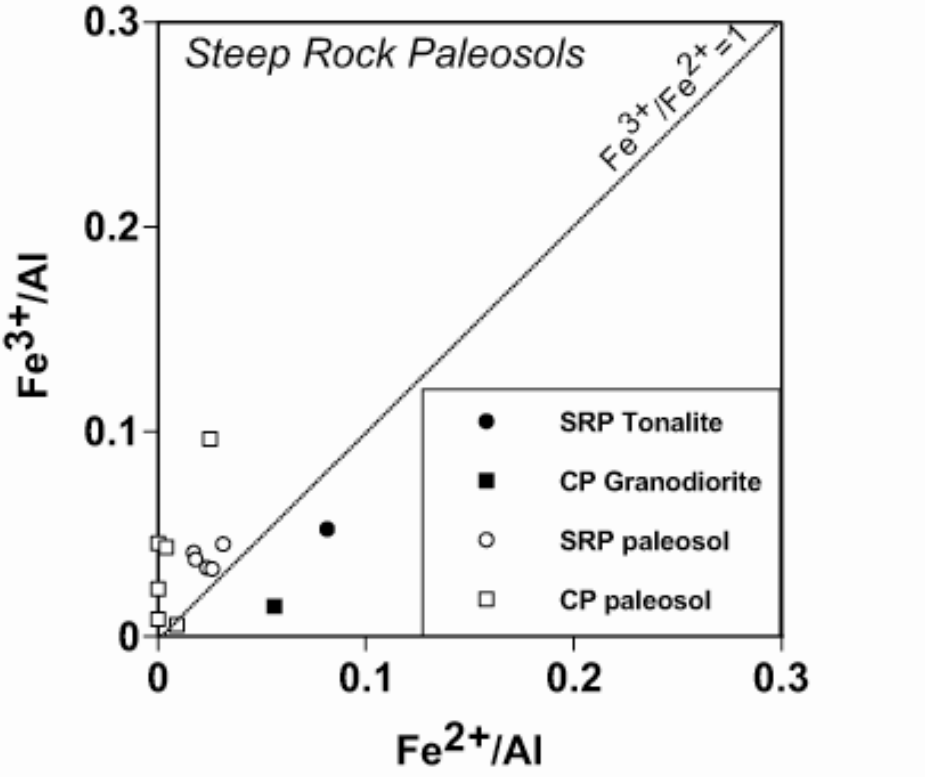

Figure 3.10: Aluminum-normalized Fe^{2+} vs. Fe^{3+} for the SRP and CP profile showing that the $Fe^{3+}/Fe^{2+}>1$.

Table 3.3: Whole rock analysis of trace elements for the Steep Rock paleosol.

Sample Name	Depth (m)	ppm										
		La	Ce	Pr	Nd	Sm	Eu	Gd	Dy	Er	Yb	Lu
Conglomerate												
99-SR-26	35	6.4	11.3	1.1	4.4	0.8	0.26	0.80	0.90	0.60	0.09	0.08
99-SR-27	10	6.8	11.9	1.2	5.0	1.0	0.35	1.00	1.00	0.60	0.60	0.10
Paleosol												
99-SR-28	0	2.9	6.0	0.6	2.7	0.6	0.14	0.60	0.50	0.30	0.40	0.07
99-SR-29	-20	9.9	19.2	2.1	9.2	1.8	0.45	1.60	1.10	0.60	0.40	0.06
99-SR-30	-90	12.3	24.4	2.4	9.3	1.6	0.52	1.20	0.80	0.50	0.50	0.08
99-SR-31	-170	13.7	26.0	3.0	12.3	2.6	0.69	2.00	1.20	0.50	0.40	BDL
99-SR-32	-320	3.7	7.1	0.8	3.5	0.7	0.29	0.80	0.70	0.40	0.30	BDL
Parent Material												
99-SR-42	-450	9.2	17.0	1.6	5.8	0.9	0.33	0.80	0.70	0.50	0.50	0.08

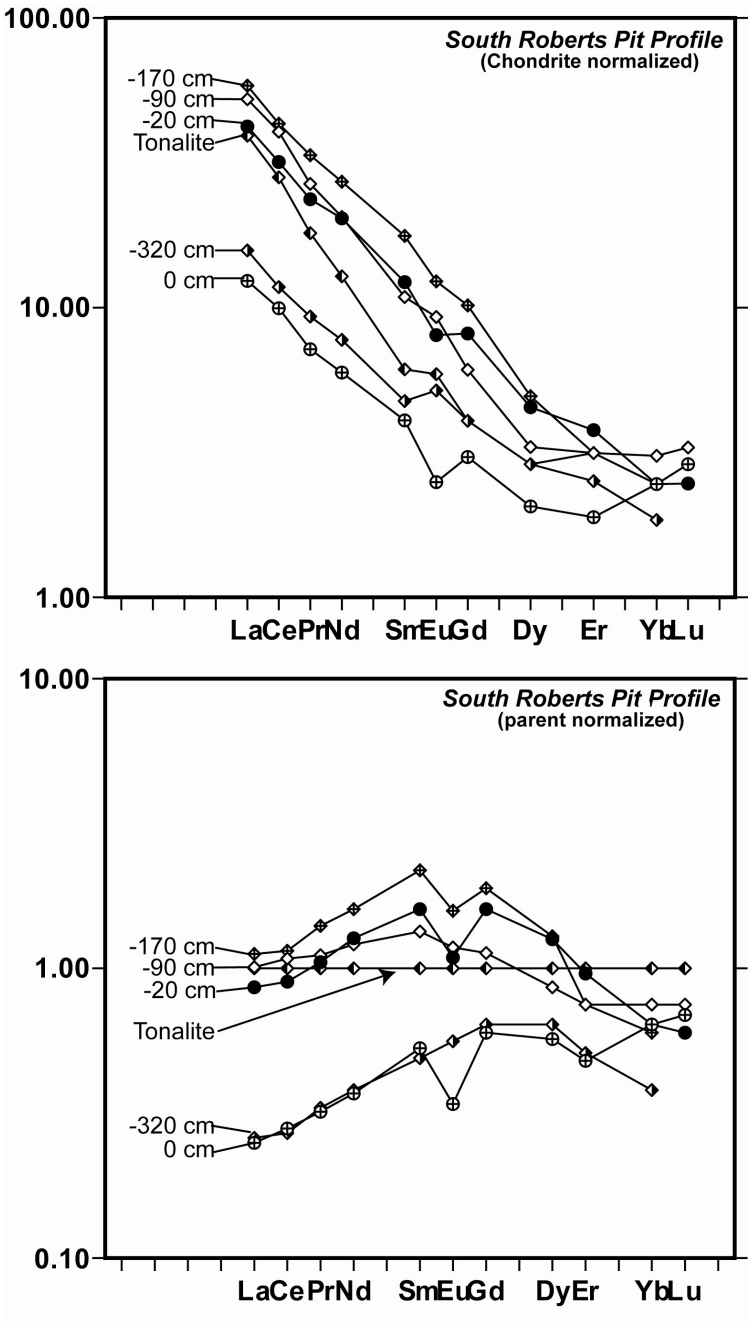

Figure 3.11: (a) REE plot of SRP normalized to chondrite. (b) REE plot of the SRP samples normalized to average parent material (=1). Depths below the unconformity for each sample are noted on the left side of each plot.

To determine the weathering effects on the REE patterns and to quantify absolute gain or loss of REE during pedogenesis, REE abundances were normalized to both Al (a relatively immobile element) and the parent tonalite (**Figure 3.11b**). There is no correlation between depth in the profile and overall REE enrichment or depletion relative to the parent tonalite. Instead there is an overall pattern of increasing LREE (La-Sm), decreasing HREE (Gd-Lu), and negative Eu anomalies. Europium is associated with plagioclase, which is abundant in the parent tonalite; weathering-related removal of plagioclase could produce a negative anomaly (Lipin and McKay, 1989). REE budgets of granitoid rocks tend to be controlled by REE-rich accessory minerals such as apatite, allanite, titanite (sphene) and/or zircon (e.g., Gromet and Silver, 1983; Condie *et al.*, 1995). In the Steep Rock profile, common accessory phases are titanite and ilmenite, which are generally LREE-depleted relative to its igneous parent (Gromet and Silver, 1983). Both can weather readily in soils to secondary minerals such as leucoxene (Condie *et al.*, 1995; Lång, 2000; Singh and Rajamani, 2001; Girty *et al.*, 2003). Peaked middle REE (MREE) patterns may be related to preferential complexation of MREE with Fe oxy-hydroxides. A study by Negrel *et al.*, (2000) documented preferential MREE enrichment on Fe oxide coated sediment in the Loire River. The slight HREE depletion may be due to the weathering of biotite, which is HREE-enriched relative to the parent (Condie *et al.*, 1995).

3.5.6 Cerium (Ce) Anomalies in the SRP Profile

Anomalous concentrations of cerium in soil profiles are significant because these anomalies only develop under oxidizing conditions where Ce^{3+} can transform to highly immobile Ce^{4+} (Lipin and McKay, 1989). Positive Ce anomalies develop when REE other than Ce are partially removed by weathering, leaving behind a Ce-enriched residuum; negative Ce anomalies form in

the regions of the profile where REE have accumulated from an overlying oxidized zone. Only two slightly negative Ce anomalies (calculated as $Ce/Ce^{*}=[Ce]_{N,C}/([La]_{N,C}[Pr]_{N,C})^{0.5}$, where the subscript "N,C" denotes normalization to chondrites) occur in the SRP profile (samples -170 and -320 cm) **(Figure 3.11a)**. Because the zone where these samples occur is not enriched in REE, the negative anomalies are probably not significant. The absence of a significant Ce anomaly does not require pedogenesis under an anoxic atmosphere; modern soils, especially waterlogged profiles, formed under oxygenated atmospheric conditions frequently lack Ce anomalies (Braun *et al.*, 1990; Dia *et al.*, 2000). This suggests that there could have been sufficient oxygen to oxidize Fe, but not Ce *(see section 4.4.2)*.

3.5.7 Radiogenic Isotope Systems Applied to the SRP Profile

3.5.7.1 Samarium-Neodymium Isotope Systematics in Soil

Once the Sm-Nd system has been fractionated by weathering or pedogenesis, it must resist further alteration in order to provide a useful age. Sedimentary processes such as diagenesis can result in REE fractionation and partial or complete resetting of the Sm-Nd system (McDaniel *et al.*, 1994; Ohr *et al.*, 1994; Schaltegger *et al.*, 1994; Bouch *et al.*, 1995; Bouch *et al.*, 2002; Ehrenberg and Nadeau, 2002; Uysal and Golding, 2003). However, burial and diagenesis of a soil profile occurs over a geologically short period following pedogenesis, and so should not significantly shift the age of an Archean paleosol. On the other hand, metamorphism can occur millions or billions of years later, and thus has the potential to overprint the soil formation age. The Sm-Nd system has long been recognized for its relative (although not universal) resistance to metamorphic resetting - this makes it one of the more useful systems for developing Precambrian chronology. High grade thermal metamorphism can have the effect of

redistributing Sm and Nd among minerals at a 10^{-3}-10^{-2} m scale (Gromet and Silver, 1983), but is less likely to redistribute the REE among different lithologic units at a cm-scale, as demonstrated by Nd isotope studies of Precambrian layered mafic intrusions that have suffered significant metamorphism (DePaolo and Wasserburg, 1979; Lambert, 1994; Stewart and DePaolo, 1996). Even when metamorphism is accompanied by fluid flow, the REE can remain relatively immobile at the scale of $>10^{-1}$ m, although this may not always be the case (e.g., Alibert and McCulloch, 1993; Macfarlane *et al.*, 1994).

3.5.7.2 Sm-Nd Isotope Systematics in the SRP Profile

The ten whole-rock samples analyzed for Sm-Nd (including two dissolutions of parent rock 99-SR-42 (**see Table 3.4**) show a strong correlation ($r^2 = 0.998$) on an isochron diagram (**Figure 3.12**). A standard linear correlation after York (1969) yields an age of 3018±90 Ma. This age is indistinguishable from that of the Marmion Complex on which the profile formed and suggests either that weathering took place very soon (less than ~60 my.) after emplacement of the intrusive complex or that the Sm-Nd systematics were only slightly affected on a hand-sample scale by weathering processes. These data also show that the REE systematics were impervious to the ~2.7 Ga greenschist metamorphic event (Davis and Jackson, 1988).

3.5.7.3 Rubidium-Strontium Isotope Systematics in Soil

The rubidium-strontium system, in which the nuclide ^{87}Rb decays to ^{87}Sr with a half-life of 48.8 Ga, has long been used for geochronology of igneous rocks. It is well known, however, that the Rb-Sr systematics of igneous rocks are easily disturbed or reset by weathering and metamorphic processes due to the relatively high mobility of Rb (an alkali element) and Sr (an alkaline earth element). This propensity for resetting makes the Rb-Sr system potentially

Table 3.4: Nd isotope values for the Steep Rock paleosol.

Sample Name	Depth (m)	Sm (ppm)	Nd (ppm)	$^{147}Sm/^{144}Nd$[a]	$^{143}Nd/^{144}Nd(0)$[b]	$\varepsilon_{Nd}(T)$[c]
Conglomerate						
99-SR-26	35	0.6	3.3	0.1157	0.510300 ± 0.000008	1.33 ± 0.248
99-SR-27	10	0.8	3.9	0.1220	0.510436 ± 0.000008	1.54 ± 0.253
Paleosol						
99-SR-28	0	0.4	1.9	0.1290	0.510475 ± 0.000011	-0.44 ± 0.318
99-SR-29	-20	1.4	7.0	0.1238	0.510486 ± 0.000009	1.81 ± 0.274
99-SR-30	-90	1.1	6.6	0.0997	0.509993 ± 0.000007	1.57 ± 0.216
99-SR-31	-170	2.3	11.2	0.1226	0.510461 ± 0.000007	1.79 ± 0.234
99-SR-32	-320	0.7	3.0	0.1310	0.510596 ± 0.000007	1.15 ± 0.241
Parent Material						
99-SR-42	-450	1.2	3.7	0.1973	0.511934 ± 0.000009	1.48 ± 0.332
99-SR-42 D2	-450	1.2	3.7	0.1966	0.511948 ± 0.000014	2.03 ± 0.430
99-SR-44	-450	1.3	4.0	0.1893	0.511765 ± 0.000009	1.29 ± 0.326

[a] uncertainty estimated at 0.2% of the measured value

[b] Uncertainty equals 2s analytical error

[c] Chondrite $^{143}Nd/^{144}Nd(0)= 0.511847$, $^{147}Sm/^{144}Nd=0.1967$

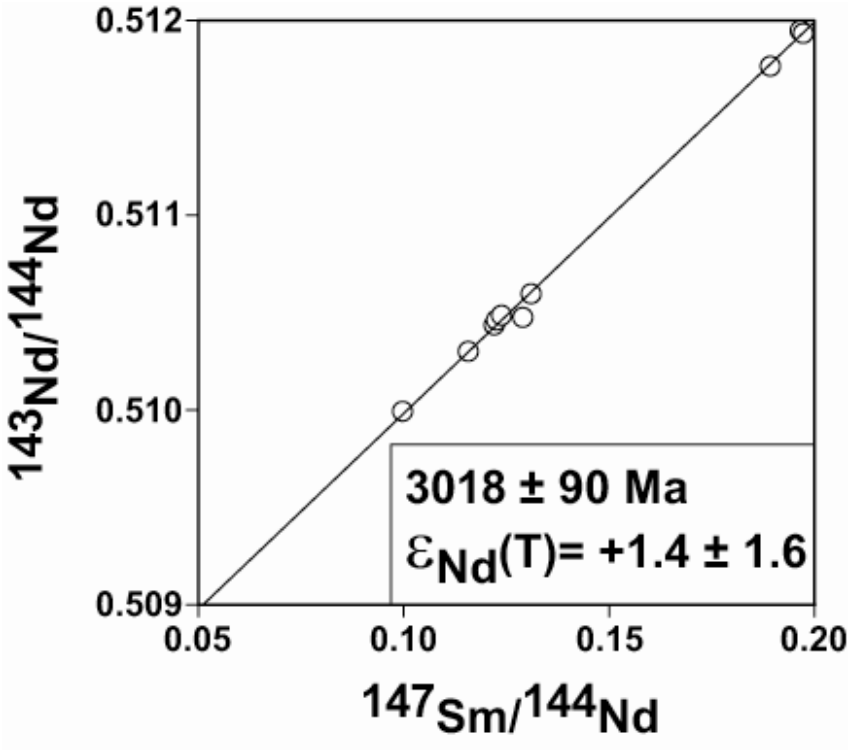

Figure 3.12: $^{143}Nd/^{144}Nd$ variation with $^{147}Sm/^{144}Nd$ for the SRP paleosol. The combined data plotted form an apparent isochron reflecting a model age of 3.018 ± 0.90 Ga ago (2σ) for the apparent age of pedogenesis.

attractive for examining the timing of pedogenesis and/or later metamorphic disturbances of paleosols. Macfarlane and Holland (1991) found that the Rb-Sr system produced a precise "age" for the Mt. Roe weathering profile that was coincident with post-pedogenic metamorphism.

3.5.7.4 Rb-Sr Systematics in the SRP Profile

Results from Rb-Sr analyses of selected samples from the SRP are shown in **Table 3.5**. The data show $^{87}Rb/^{86}Sr$ ranging from 0.0881 to 67.5426, with a corresponding spread in $^{87}Sr/^{86}Sr$ from 0.70535 to 2.97665. We plot the data on an isochron diagram to determine if it yields a meaningful age (**Figure 3.13**). When all samples are used in the calculation, the isochron yields an age of 3.139 ± 0.421 Ga (calculated after the method of York, 1969). This age is greater than the age of the parent tonalite and clearly indicates that the Rb-Sr data was disturbed during one or more events. The most likely culprit is the regional greenschist-grade metamorphism associated with the Kenoran Orogenic event that reached its peak ~2.7 Ga ago.

The observed disturbance of the Rb-Sr system requires at least limited exchange of Sr on a scale of meters, which could have been aided by fluid flow accompanying metamorphism. However, in contrast to observations in the Hokkalampi paleosol, it is clear that the Rb-Sr system was not completely reset by these events. In addition, it is likely that Rb was selectively added to portions of the SRP profile during K-metasomatism, which could significantly increase the spread in Rb/Sr ratios. This demonstrated by a comparison of Rb and K_2O concentrations (**Figure 3.14**).

Table 3.5: Sr isotope values for the Steep Rock paleosol.

Sample Name	Depth (m)	Rb (ppm)	Sr (ppm)	^{87}Rb	^{86}Sr	$^{87}Rb/^{86}Sr$[a]	$^{87}Sr/^{86}Sr(0)$[b]
Conglomerate							
99-SR-26	35	17.8	26.1	58.2	29.2	1.99	0.775756 ± 10
99-SR-27	10	13.9	11.4	45.2	12.7	3.56	0.833517 ± 10
Paleosol							
99-SR-28	0	9.6	5.7	242.6	5.3	45.66	2.903914 ± 26
99-SR-28B	0	76.1	5.9	247.8	5.5	45.46	2.891265 ± 29
99-SR-29	-20	109.7	5.7	357.5	5.3	67.54	2.976653 ± 24
99-SR-30	-90	62.5	6.6	203.7	6.2	33.03	2.769972 ± 75
99-SR-31	-170	85.4	6.9	278.2	6.5	42.49	2.550068 ± 36
99-SR-32	-320	99.5	10.9	324.2	10.8	29.96	2.061469 ± 39
Parent Material							
99-SR-42	-450	25.3	409.1	82.3	460.5	0.18	0.708075 ± 9
99-SR-42B	-450	23.0	408.0	74.8	459.3	0.16	0.708027 ± 13
99-SR-44	-450	21.1	693.9	68.8	781.2	0.09	0.705316 ± 12

[a] Estimated uncertainty 2% of measured value (SR 28=10%)

[b] Uncertainty equals 2s analytical error and is shown as last two decimal places

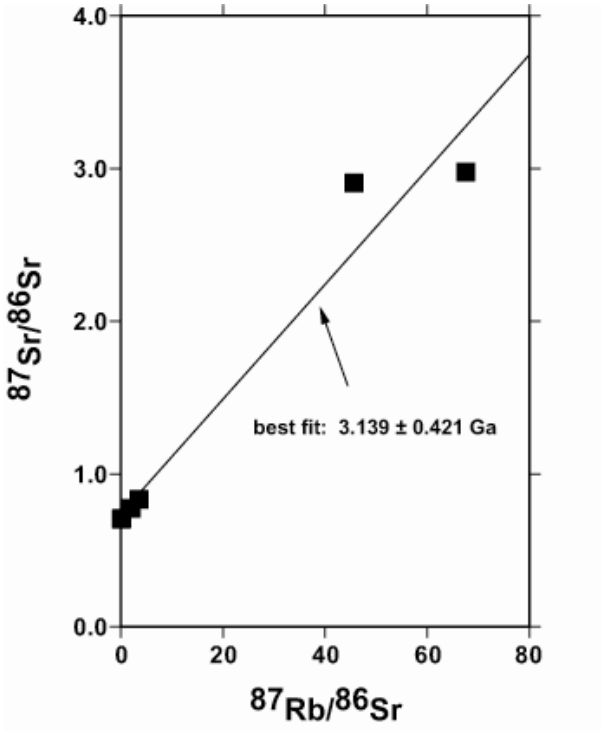

Figure 3.13: Variation of $^{87}Sr/^{86}Sr$ with $^{87}Rb/^{86}Sr$ for the SRP paleosol. These data form a linear array on an isochron diagram. When all samples are used in the calculation, the isochron points to an age of 3.139 ± 0.421 Ga indicating that the Rb-Sr system has been disturbed.

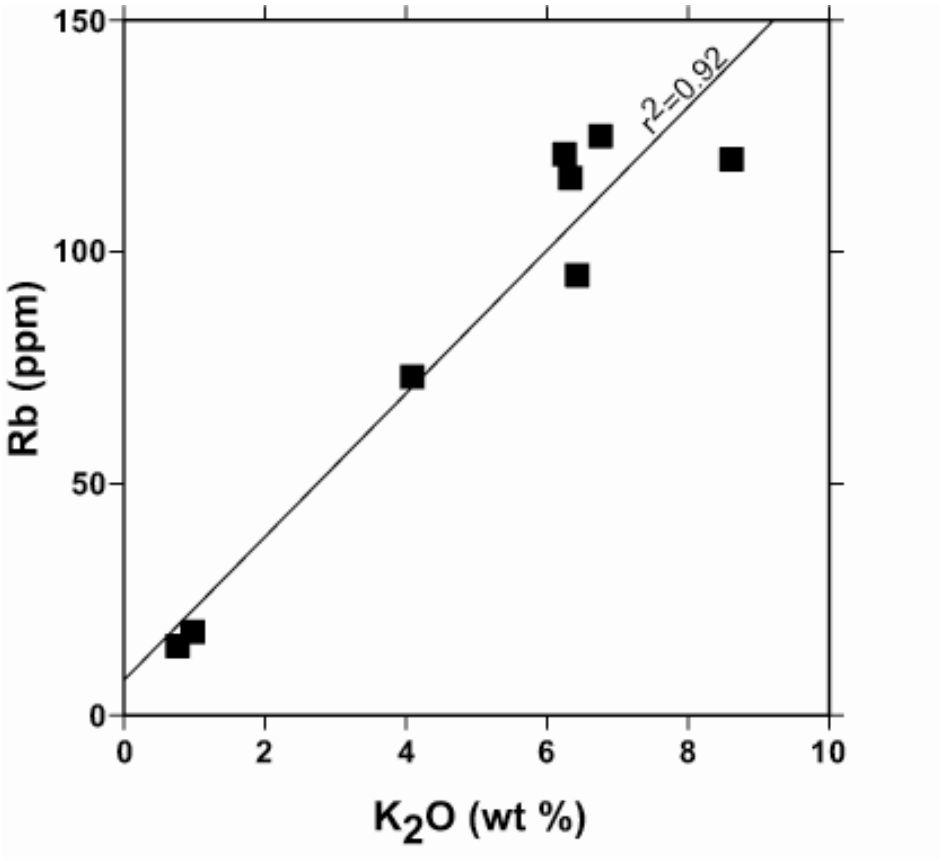

Figure 3.14: Variation of K_2O (wt %) with Rb (ppm) for the parent tonalite (closed circles) and the SRP profile (open circles). The observed correlation strongly suggests that K-metasomatism was synchronous with regional metamorphism at ~2.7-2.5 Ga.

3.6 CONCLUSIONS TO STEEP ROCK STUDY

The textures and geochemistry of the South Roberts Pit profile are consistent with *in situ*, subaerial weathering followed by potassium metasomatism and greenschist metamorphism. There is an increase in the degree of weathering from the tonalite toward the unconformity. Weathering of plagioclase, biotite, ilmenite, titanite, epidote, and apatite likely produced clays such as kaolinite/smectite (now altered to sericite and paragonite) and leucoxene.

Micromorphologic evidence of soil forming processes including intertexic and agglomeroplasmic fabric, spalling quartz grains, and clay cutans. At the unconformity, rip-up clasts are present.

Loss of base cations indicates that the soil formed in a warm, moist environment conducive to chemical weathering. Pedogenic processes led to slight mobilization of REE with slight fractionation similar to newly developed modern soils. A ratio of $Fe^{3+}/Fe^{2+} > 1$ suggests oxygenated soil conditions. However, the lack of Ce anomalies indicates that there was not enough oxygen in the soil to oxidize Ce. A low CIA_K and only small changes in the overall REE budget indicate that either the profile was not well developed or that the most heavily weathered sections were eroded away.

Fractionation of Sm/Nd apparently caused by pedogenic processes produced a slight spread in Sm/Nd ratios; the samples form an isochron with an apparent age of 3.018 ± 0.090 Ga. This age is indistinguishable from that of the Marmion Complex on which the profile formed, and suggests that either weathering took place very soon (less than ~60 my.) after emplacement of the complex, or that the Sm-Nd systematics were only slightly affected on a hand-sample scale by weathering processes. Rb-Sr systematics for the Steep Rock paleosol were clearly disturbed. Correlation of Rb and K indicate that K-metasomatism most likely occurred during the metamorphic event transforming 2:1 clays (smectite) to sericite and even paragonite. Sm-Nd data indicate that the REE were not mobilized to a significant degree after pedogenesis despite metamorphism, while Rb-Sr data indicate that elements such as Rb, Sr, Ca, and K were most likely mobilized during metamorphism. This study suggests that REE, as well as Rb-Sr and Sm-Nd studies of paleosols can help constrain the age of pedogenesis, evaluate the pedogenic and post-pedogenic mobility of elements, and help to constrain soil redox conditions.

4.0 PALEOENVIRONMENTAL INVESTIGATION OF THE STEEP ROCK PALEOSOL AND COMPARISON WITH THE HOKKALAMPI PALEOSOL

4.1 INTRODUCTION TO PALEOENVIRONMENTAL INVESTIGATION

Soils represent the interface between the atmosphere, lithosphere, hydrosphere, and biosphere. Paleosols, or fossil soils, document past life, climate and terrestrial landscapes. Ancient soils also preserve products of atmospheric-mineral interaction. This record is key to understanding the early composition and evolution of the Earth's atmosphere and the environments in which life developed and evolved.

Because Precambrian (>542 Ma ago) soil profiles lack significant effects from land plants, researchers (e.g., Holland and Zbinden, 1988; Pinto and Holland, 1988; Kirkham and Roscoe, 1993; Macfarlane *et al.*, 1994; Ohmoto, 1996) have applied a variety of geochemical methods, such as the mobility of the redox-sensitive elements Fe and Ce, to interpret atmosphere-mineral interaction in paleosol profiles that may have formed under different atmospheric conditions than exist today. Holland (1984; 1988) used geochemical data to calculate the ratio of oxygen demand to acid demand or "R-Value", where $R= (Do_2)/(Dco_2)= (\Delta M_{FeO})/8[\Delta M_{CaO}+\Delta M_{MgO}+\Delta M_{Na2O}+\Delta M_{K2O}+\Delta M_{MnO}]$. The R values for paleosols formed over Earth's history were divided into two categories: (1) paleosols >2.2 Ga in age, which show Fe loss, and (2) paleosols <2.2 Ga in age, which do not show significant Fe loss. In this model, the

loss of Fe in weathering profiles is attributed to a reducing atmosphere (Holland, 1984; Holland and Zbinden, 1988). The resulting Cloud-Walker-Kasting-Holland model theorizes that pO_2 increased from 10^{-13} of present atmospheric level (PAL) to greater than 15% of the PAL between 2.2 Ga and 1.9 Ga (Bekker *et al.*, 2004). However, reductive fluids, which are capable of forming even under an O_2-rich atmosphere, can also cause Fe transport (Ohmoto, 1996). To constrain the processes involved in Fe mobility, Ohmoto (1996) made a comparison of Fe^{3+} to Fe^{2+} in paleosols. In this model, the reductive loss of Fe is attributed to hydrothermal fluids and/or leaching by organic acids. The resulting Dimroth–Ohmoto model theorizes that pO_2 has remained essentially constant (within 50% of PAL) since at least 4 Ga ago.

Recent isotopic and microfossil evidence points to microbial life in Archean paleosols (Horodyski and Knauth, 1994; Rye and Holland, 2000; Watanabe *et al.*, 2000). This strengthens the argument that organic ligands, which are secreted by microbes to obtain nutrients, (Jones, 1998) may have increased redox element mobility in Archean paleosols. Experimental study of element mobility enhanced by ligands in basalt has also been documented (Neaman *et al.*, 2005). In recent studies of Precambrian paleosols where Al is relatively immobile (Holland and Rye, 1997; Ohmoto, 1997; Beukes *et al.*, 2002; Yang *et al.*, 2002), the mobility of Fe has been attributed to either an anoxic atmosphere or ligand-enhanced dissolution of Fe by microbes. Because microbes use ligands to release oxidized Fe in modern soils, the possibility exists that this process may have affected Fe and other redox element concentrations in Archean paleosols.

My research builds on earlier work, including Fe and Ce data, but includes additional redox-sensitive elements (U, V, and Cu) to further constrain Eh-pH conditions in the Steep Rock paleosol exposed at South Roberts Pit (SRP), one of the oldest weathering profiles preserved on

Earth. Comparisons are made with Steep Rock paleosol exposed at Caland Pit (CP) (see Schau and Henderson, 1983). This research considers the possibility of ligand-enhanced dissolution of redox elements based on experimental study (e.g., Neaman *et al.*, 2005). This will lead to a more accurate interpretation of the redox conditions in the fossil soil record, which has implications for understanding the Archean paleoenvironmental record.

4.2 BACKGROUND TO PALEOENVIRONMENTAL STUDY

4.2.1 Geologic Setting and Profile Description of the Steep Rock Paleosols

The Steep Rock paleosols formed on the Marmion Complex, an Archean granitoid unit located in the western Ontario, Canada (**see Figure 3.3**). The paleosol is directly overlain by a clastic unit comprising a basal metaconglomerate to sandstone (Wagita Formation), a carbonate platform succession of limestones and dolostones (Mosher Carbonate), a highly altered iron ore zone (Jolliffe Ore Zone), a series of volcanics (Dismal Ashrock) and metavolcanic/metasediments (Witch Bay). These units are collectively referred to as the Steep Rock Group (**see Figure 3.2**) (Jolliffe, 1966; Wilks and Nisbet, 1988; Kusky and Hudleston, 1999) and are thought to represent a portion of an Archean greenstone belt (Tomlinson *et al.*, 1999). The Marmion Complex at South Roberts pit has a generally tonalitic composition, although the weathering profile exposed at Caland Pit developed on granodiorite (Schau and Henderson, 1983). The Sm-Nd isotope data from samples taken at South Roberts Pit form an apparent isochron with an age of 3018 ± 90 Ma ago for pedogenesis *(see section 3.5.7.2)*. Only

the lowermost parts of the soil profiles are preserved. They consist of quartz grains and remnant plagioclase and biotite in a matrix of chlorite, clay (kaolinite and smectite, altered to sericite), with minor epidote, apatite, muscovite, titanite, and ilmenite.

4.2.2 Archean Rain Chemistry

The mobility of most redox element species is determined by the pH and Eh of the system. Therefore, constraints must be placed on the pH of rainfall interacting in the model of the Marmion Complex tonalite weathering to the Steep Rock soil. The pH of rainfall is a function of atmospheric CO_2 (pCO_2) and how efficiently CO_2 dissolves in water (Drever, 1997; Ohmoto, 1999; Watanabe *et al.*, 2004). Equations (4.1) and (4.2) show the relationship between pCO_2 and rainwater to form carbonic acid (H_2CO_3) and how the dissociation of H_2CO_3 affects pH (expressed as the $-\log[H^+]$):

$$CO_2(g)+H_20(l)=H_2CO_3(aq) \quad (4.1)$$

$$H_2CO_3(aq)=H^++HCO_3^- \quad (4.2)$$

The equilibrium constants for Equations (4.1; K_{CO2}) and (4.2; K_{H2CO3}) are expressed by the following reactions:

$$Logm_{CO2(aq),}\ initial=logK_{CO2}+log pCO_2 \quad (4.3)$$

$$pH=-0.5(logK_{CO2+}logK_{H2CO3}+log pCO_2) \quad (4.4)$$

The activity for pCO_2 for Equation (4.3) and (4.4) must be estimated. The estimate should be consistent with the relative immobility of Al in the Steep Rock paleosol and many other Precambrian paleosols (i.e. pH> 4 assuming an activity for Al of 10^{-4}, a temperature of 25°C, and 1 bar of atmospheric pressure) (Brookins, 1988). Estimates of pCO_2 vary depending on assumed methane (CH_4) levels in the models for the Archean atmosphere and range between 10 times present atmospheric level (PAL; $10^{-3.5}$) (Rye *et al.*, 1995; Pavlov *et al.*, 2001) if ~100 ppmv of CH_4 was present (Kasting, 2001) to 1000 PAL if no CH_4 is present (Kasting, 1987). For comparison to previous studies of redox mobility in paleosols, we will assume a modern pCO_2 of ~0.0003 atm (Neaman *et al.*, 2005), which is similar to today and results in a rainwater pH of 5.6. We also consider a pCO_2 100 PAL, which results in a rainwater pH of 4.66 (Ohmoto *et al.*, 2004; Watanabe *et al.*, 2004).

4.3 METHODS USED IN PALEOENVIRONMENTAL STUDY

Samples from the South Roberts pit paleosol, overlying sediments of the Steep Rock group, and parent tonalite were collected during a field excursion in 1999. **Figure 3.4** shows a schematic geologic column with the stratigraphic position of the samples collected from the weathering profile and the overlying Wagita formation conglomerate. Samples were ~0.5 kg in size; the samples were cut in the lab and oriented thin sections were prepared. Rock chips free of (modern) weathering rinds were segregated and ground to a fine powder in a tungsten-carbide ball mill. Splits of ~20 g were set aside for major and trace element analysis, and smaller splits of ~300 mg were set aside for isotopic analysis. Major and trace element data for whole rock samples were measured by Activation Laboratories Ltd., in Ontario, Canada. Whole rock

powders were dissolved by $LiBO_2$ fusion; major elements were analyzed by ICP-OES and trace elements were analyzed by ICP-MS. FeO was determined by dichromite titration. Geochemical data were normalized to a relatively immobile element, aluminum (Al), to account for concentration or dilution due to volume changes during pedogenesis (Nesbitt, 1979; Chadwick *et al.*, 1990; Kurtz *et al.*, 2001). Aluminum was chosen for normalization because of its abundance and relatively homogeneous distribution throughout the profile compared to other immobile elements *(see section 3.5.1)*. For comparison, the Caland Pit profile data (Schau and Henderson, 1983) were also normalized to Al.

4.4 REDOX ELEMENT MOBILITY

4.4.1 Iron Mobility

Variation of Al-normalized total Fe (Fe_T), Fe^{2+}, and Fe^{3+} from the parent tonalite with depth for the SRP paleosol is presented in **Table 4.1** and shown in **Figure 3.9**. Fe_T loss ranges from 43 to 58%. Fe^{3+} shows less depletion (up to 37%) than Fe^{2+} (up to 79%). Data for the Steep Rock paleosol that formed on granodiorite (CP profile) are presented in **Table 4.2** and shown in **Figure 3.9**. Like the SRP profile, the CP profile also exhibits Fe^{3+} values greater than Fe^{2+} (Schau and Henderson, 1983). However, Fe^{3+} shows relative enrichment compared to the parent and Fe_T increases (72%) in the middle of the profile. Only the bottom parts of the Steep Rock profiles are preserved *(see section 3.5.3)*; Fe_T loss may have been higher in the unpreserved upper horizons of the paleosols.

Table 4.1: Whole Rock Data for the South Roberts Pit Steep Rock Paleosol.

Sample Name	Depth (cm)	ppm[a]								
		Al	Fe^{3+}	Fe^{2+}	Fe_T	P	Cu	U	V	Ce/Ce*
Conglomerate										
99-SR-26	35	18890	5875	15080	20955	87	37	0.4	43	1.01
99-SR-27	10	17779	13359	10338	23697	87	101	0.4	62	1.00
Paleosol										
99-SR-28	0	94238	7974	3342	11316	87	<1	0.2	51	1.06
99-SR-29	-20	93656	7274	3498	10772	218	<1	0.2	231	1.01
99-SR-30	-90	99529	6784	5363	12148	306	<1	0.3	56	1.08
99-SR-31	-170	99106	6854	4819	11674	175	15	0.4	205	0.97
99-SR-32	-320	117679	10981	7618	18599	262	11	0.3	104	0.97
Parent Tonalite										
99-SR-42	-450	74819	8113	12592	20706	349	63	0.3	36	1.06

[a]Actavation Laboratories LTD; Method-LiBO2 Fusion, Analysis by ICP-ES. FeO by dichromate titration.

Table 4.2: Whole Rock Data for the Caland Pit Steep Rock Paleosol.

Sample Name	Depth Below Contact (cm)	ppm[a]						
		Al	Fe^{3+}	Fe^{2+}	Fe_T	P	Cu	V
Conglomerate								
3-11	35	23282	5595	777	6373	0	14	20
3-10	15	12170	4197	0	4197	0	7	20
3-9	2	25927	9093	2332	11425	0	54	31
Paleosol								
3-8	-3	121171	1399	2332	3731	0	5	63
3-7	-7	122758	2098	0	2098	0	5	53
3-6	-14	116938	5595	0	5595	0	5	67
3-5	-35	91010	18185	4664	22849	0	5	41
3-4	-70	85190	7694	777	8471	0	5	31
3-3	-70	89423	8393	0	8393	0	5	34
Granodiorite								
Avg (3-1 and 3.2)	-100	80692	2448	9328	11776	175	7	296

[a]from Schau and Henderson (1983)

Loss of Fe_T is prevalent at the top of pre-2.2 Ga paleosols and has been suggested as evidence for a reducing atmosphere (i.e. Holland, 1984; Kirkham and Roscoe, 1993; Holland, 1994). However, relative to average parent material, both weathering profiles show an increase in normalized Fe^{3+} down profile. The profiles also have a Fe^{3+}/Fe^{2+} ratio of >1. The evaluation of Fe^{3+} relative to Fe^{2+} has resulted in alternative interpretations for Fe loss in paleosols, such as oxidation followed by alteration due to reductive fluids (mixed-type paleosol; Ohmoto, 1996). The loss of Fe_T coupled with amounts of Fe^{3+} greater than Fe^{2+} in both Steep Rock paleosols could indicate that the soils interacted with oxidizing fluids to form Fe oxy-hydroxides, but were stripped of Fe during pedogenesis by organic acids (if microbes were present) or by post-pedogenic alteration (hydrothermal fluids), resulting in a Fe^{3+}/Fe^{2+} ratio of >1.

Driese (2004) has documented translocation of 10-50% of Fe within modern and Paleozoic paleo-vertisols profiles despite forming in oxygenated conditions. Experimental work by Neaman *et al*. (2005) shows that organic ligands can mobilize redox elements such as Fe in soil forming on basalt. Waterlogged conditions in modern soils are also capable of reducing and moving Fe despite an oxygen-rich atmosphere (Dia *et al.*, 2000).

To further explore Fe mobility in the Steep Rock paleosol profiles, the Eh values required to oxidize Fe were calculated for assumed pH values of 4.66 and 5.6. The Eh-pH diagram for the Fe-C -O-H system is shown in **Figure 4.1**. For **Figure 4.1**, activities assumed for dissolved species include $Fe=10^{-6}$ and $C=10^{-3}$. Temperature is assumed to be 25°C and pressure to be 1 bar. Fe^{3+} solid phases are assumed to be goethite and magnetite (Brookins, 1988). For modeling purposes, the phase boundary between the Fe^{2+} and Fe^{3+} can be calculated by the dissociation equation (4.5) and the equilibrium equation (4.6):

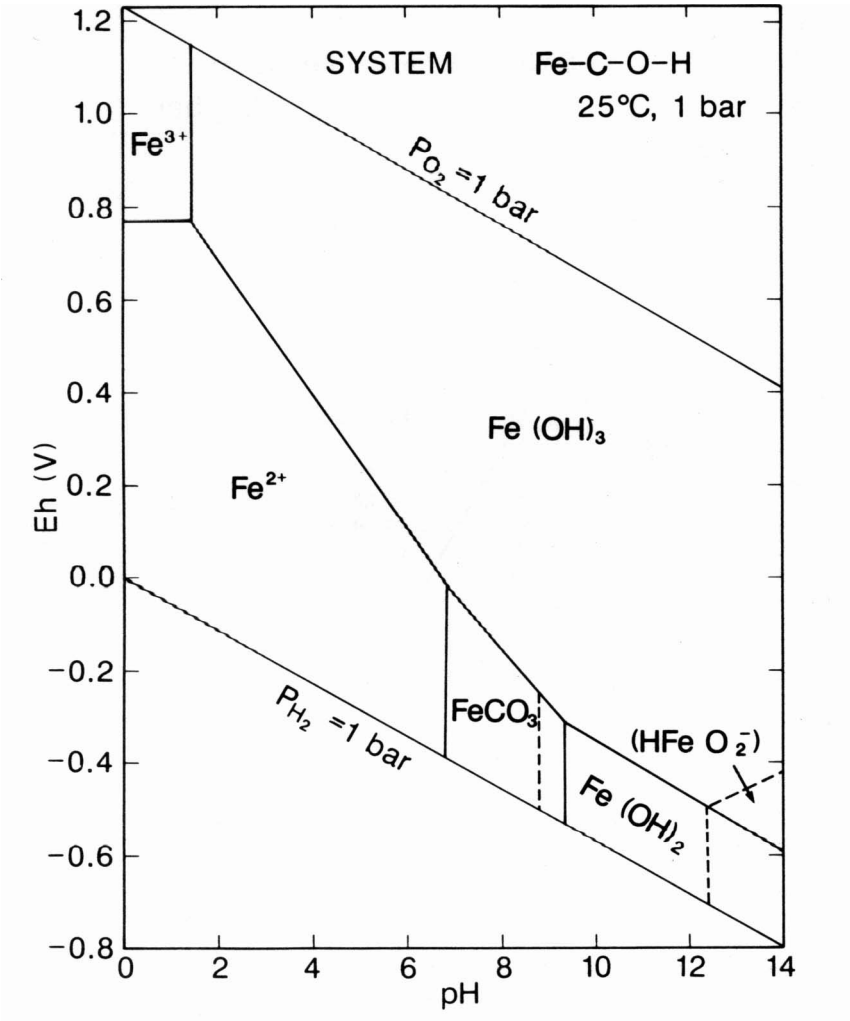

Figure 4.1: Eh-pH diagram for the Fe-C-O-H system. Activities assumed for dissolved species include $Fe=10^{-6}$ and $C=10^{-3}$. Temperature is assumed to be 25°C, and pressure is assumed to be 1 bar. Fe^{3+} solid phases are assumed to be goethite and magnetite (from Brookins, 1988)

$$Fe(OH)_3\ (c) + 3H^+ + e^- \rightarrow Fe^{2+}(aq) + 3\ H_20 \quad (4.5)$$

$$logK=log\ [Fe^{2+}] + 3pH + pe \quad (4.6)$$

The activity for Fe^{2+} is assumed to be 1.79 x 10^{-7} mol/L, which is the typical concentration of Fe in natural waters (Hem, 1985). The value for K=2.89 x 10^{-16} calculated using thermodynamic data from Wagman *et al.* (1982). If pH is assumed to be equal to 4.66, then the calculated phase change between Fe^{3+} and Fe^{2+} will take place at Eh= 0.545 based on equation (4.6). If pH is assumed to be 5.6, then the calculated phase change will take place at Eh=0.379.

The $Fe^{3+}/Fe^{2+} > 1$ and loss of Fe_T in both profiles points to a fluctuating Eh, which as stated above, could be caused by waterlogged conditions (at least seasonally) or organic material, as in modern soils. To further constrain redox conditions in the Steep Rock paleosols, other redox elements were considered.

4.4.2 Cerium Mobility

Anomalous concentrations of cerium in soil profiles are significant because these anomalies only develop under oxidizing conditions where Ce^{3+} can transform to highly immobile Ce^{4+} (Lipin and McKay, 1989). Positive Ce anomalies develop when REE other than Ce are partially removed by weathering, leaving behind a Ce-enriched residuum; negative Ce anomalies form in the regions of the profile where REE have accumulated from an overlying oxidized zone.

No significant Ce anomalies (calculated as $Ce/Ce^*=[Ce]_{N,C}/([La]_{N,C}[Pr]_{N,C})^{0.5}$, where the subscript "N,C" denotes normalization to chondrites) are apparent in the SRP profile (**see Table 4.1**). Slight negative anomalies (0.97) occur in the samples 170 and 320 cm below the

unconformity. Because the zones where these samples occur are not enriched in REE, the negative anomalies are probably not significant. The CP profile, developed on granodiorite, also lacks significant Ce anomalies (Schau and Henderson, 1983).

Positive Ce anomalies have been reported in modern soils on various types of parent rocks (e.g., Nesbitt, 1979; e.g., Braun *et al.*, 1990; Marsh, 1991). Braun *et al.* (1990) found positive Ce anomalies in chondrite-normalized samples in the heavily weathered interval of a saprolite derived from syenite. The Ce enriched layer was beneath a zone of iron oxide accumulation. The less-weathered parent rocks did not contain any Ce anomalies. Marsh (1991) reported positive Ce anomalies in a highly weathered section of an oxidized soil developed on dolerite in South Africa. Less weathered rocks in the profile were relatively depleted in Ce. Nesbitt (1979) described the weathering of the Torrongo granodiorite in southeastern Australia. This study proposed a model where aggressive CO_2-rich rainwater and organic acids weather REE into solution. As the acid-rich water flow downward through the weathering profile, the pH increases. The REE come out of solution, and are contained within the weathering profile.

However, not all modern profiles (formed under an oxygen-rich atmosphere) contain Ce anomalies. Dia *et al.* (2000) documented the lack of Ce anomalies in a waterlogged profile containing organic-rich waters, and the study showed that Ce may complex with organic colloids in groundwaters draining from wetland soils, masking the seasonal oxidation events of the wetland.

As stated above, the absence of a significant Ce anomaly does not require pedogenesis under an anoxic atmosphere, as modern soils, especially waterlogged profiles, forming under oxygenated atmospheric conditions frequently lack Ce anomalies (Braun *et al.*, 1990; Dia *et al.*,

2000). Lack of Ce anomalies in some modern soils suggests that there could have been sufficient oxygen to oxidize Fe in the Steep Rock profiles, but not Ce in the Steep Rock profiles.

To further explore Ce mobility in the Steep Rock paleosol profiles, the Eh values required to oxidize Ce were calculated for assumed pH values of 4.66 and 5.6. An Eh-pH diagram for the Ce-C-S-O-H system is shown in **Figure 4.2**. In **Figure 4.2**, activities assumed for dissolved species include $Ce=10^{-8,\ -6}$ and $C=10^{-3}$. Temperature is assumed to be 25°C and pressure to be 1 bar (Brookins, 1988). For modeling purposes, the phase boundary between the Ce^{3+} and Ce^{4+} can be calculated by equation (4.7) and the equilibrium equation (4.8):

$$Ce^{3+}(aq) + 2H_2O \rightarrow 4H^+ + CeO_2(c) + 3H_20 + e^- \quad (4.7)$$

$$\log K = -\log [Ce^{3+}] - 4pH - pe \quad (4.8)$$

The activity for Ce^{3+} is assumed to be 1.00×10^{-7} mol/L, which is the maximum concentration of Ce^{3+} in natural waters (McLennan, 1989). The value for $K=2.93 \times 10^{-22}$ calculated using thermodynamic data from Schumm *et al.* (1973) and Smith and Martell (1976). If pH is assumed to be equal to 4.66, then the phase change between Ce^{3+} and Ce^{4+} will take place at Eh= 0.585 based on equation (4.8). If pH is assumed to be 5.6, then the calculated phase change will take place at Eh=0.348. Note that for a pH of 5.6, the Eh value required to oxidize Ce is less than the value required to oxidize Fe *(Eh=0.379, see section 4.4.1)*. This contradicts the paleosol data. The data exhibit apparent enrichment of Fe, followed by mobility of Fe and mobility of Ce (i.e. no significant Ce anomalies). However, a pH of 5.6 is possible if Ce complexes with organics, causing it to be mobile despite oxidation and masking any possible Ce anomaly formation.

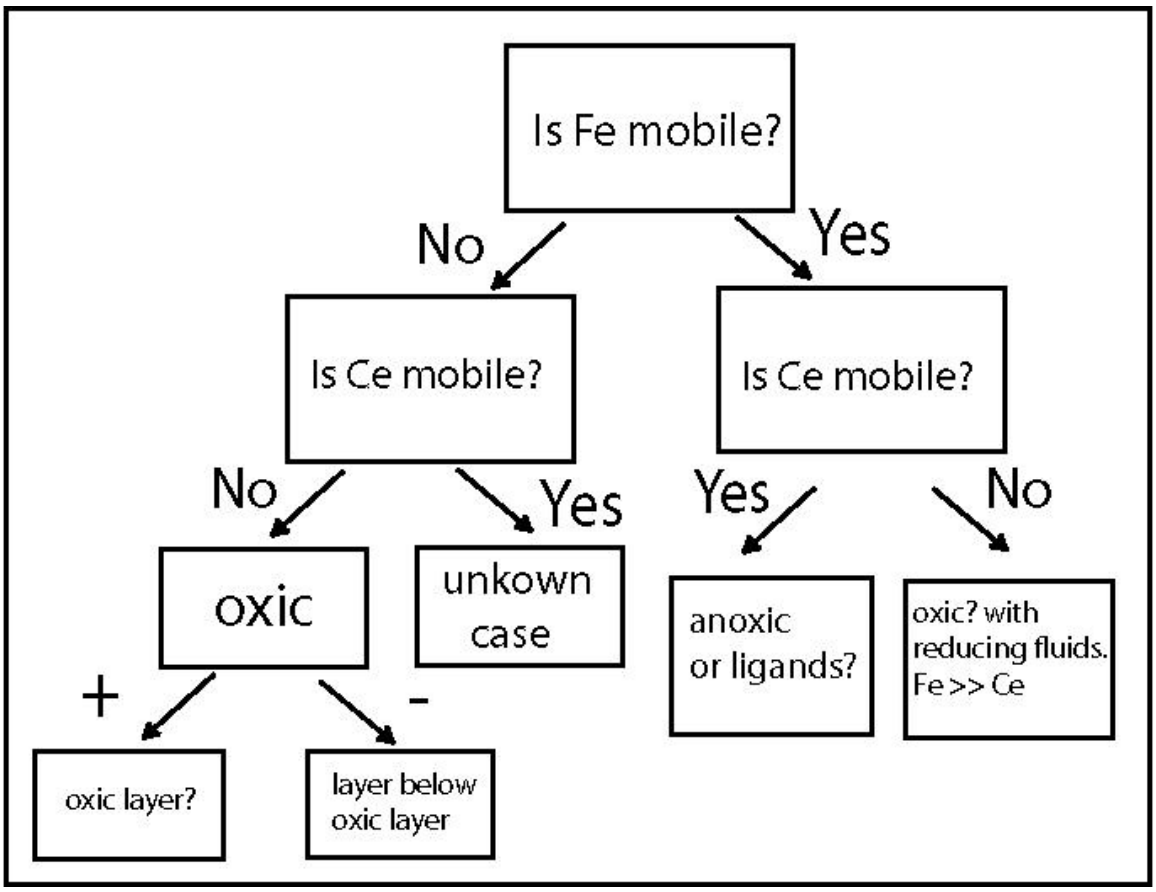

Figure 4.2: Flow chart summarizing possible cases of Fe and Ce mobility in soils and the possible interpretations.

Figure 4.3 summarizes possible Fe and Ce mobility cases and the possible interpretations. In modern laterite soils (e.g., Braun *et al.*, 1990), Ce anomalies are associated with the Fe-rich crust; when Fe is immobile, Ce is immobile. A positive Ce anomaly occurs in the REE depleted zone directly underneath the Fe layer; a negative Ce anomaly occurs in the REE enriched zone below the depleted zone with the positive Ce anomaly (Nesbitt, 1979; Braun *et al.*, 1990; Marsh, 1991). When Fe is mobile, Ce may or may not be mobile. If both Fe and Ce are mobile, it may be due to anoxic soil conditions *(i.e. waterlogged or organic ligands)* or to

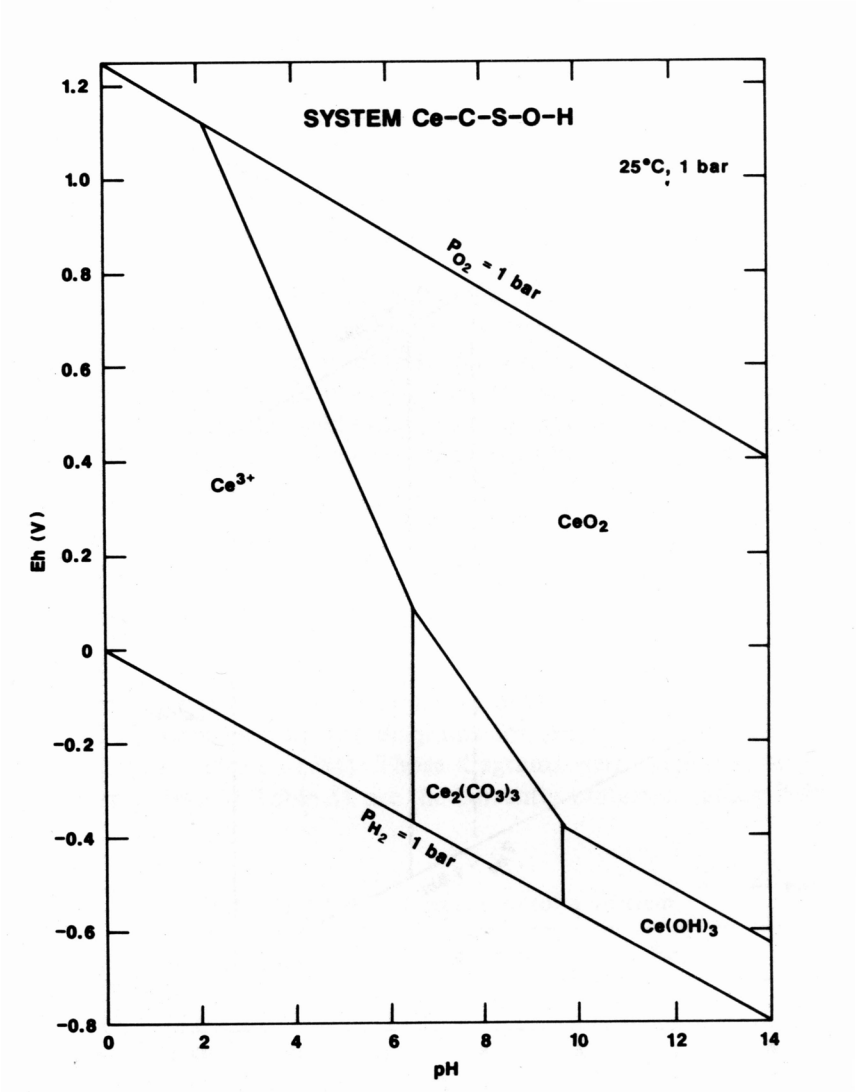

Figure 4.3: Eh-pH diagram for the Ce-C-S-O-H system. Activities assumed for dissolved species include Ce=10^{-8}, $^{-6}$ and C=10^{-3}. Temperature is assumed to be 25°C, and pressure is assumed to be 1 bar (from Brookins, 1988).

anoxic atmospheric conditions (Ohmoto, 1996; Holland and Rye, 1997; Ohmoto, 1997; Dia *et al.*, 2000; Beukes *et al.*, 2002; Yang *et al.*, 2002; Driese, 2004; Neaman *et al.*, 2005). If Fe is mobile, Fe^{3+}/Fe^{2+} >1, and Ce is not mobile, then soil development most likely took place in an oxic atmosphere and at least a seasonally oxic soil atmosphere. Soil formation was probably followed by post-pedogenic alteration with reduced hydrothermal (Ohmoto, 1996). To further constrain soil and atmospheric conditions during the formation of the Steep Rock paleosols profiles, P was used as a proxy for the presence of organic ligands (i.e., Neaman *et al.*, 2005).

4.4.3 Proxy for Organic Ligands in Paleosols

To determine if the Steep Rock paleosols may have contained organic ligands capable of enhancing redox element movement, a proxy for organic ligands was used. Neaman *et al.* (2005) carried out an experimental study on element mobility patterns in basalt with and without ligands and with and without oxygen. They proposed phosphorus (P) as a proxy for organic ligands, as P mobility was minor in organic ligand-free conditions with or without oxygen. Their study is based on the assumption that rainfall is less than the topsoil pore volume as indicated by the relative immobility of Al. This is important because controls in the study suggested that apatite can be weathered in high rainfall conditions, which would deplete P levels by rainfall rather than by ligand activity. Braun *et al.* (1990) documented apatite weathering during modern laterite development under high rainfall conditions.

Phosphorus data for the Steep Rock paleosols are shown in **Table 4.1 and 4.2**. The mobility of P for the SRP and CP profiles relative to parent material in both profiles is shown in **Figure 4.4**. Phosphorus is depleted by up to 80% at the top of the SRP profile and 100% throughout the CP profile. Phosphorus mobility in the Steep Rock paleosols suggests that

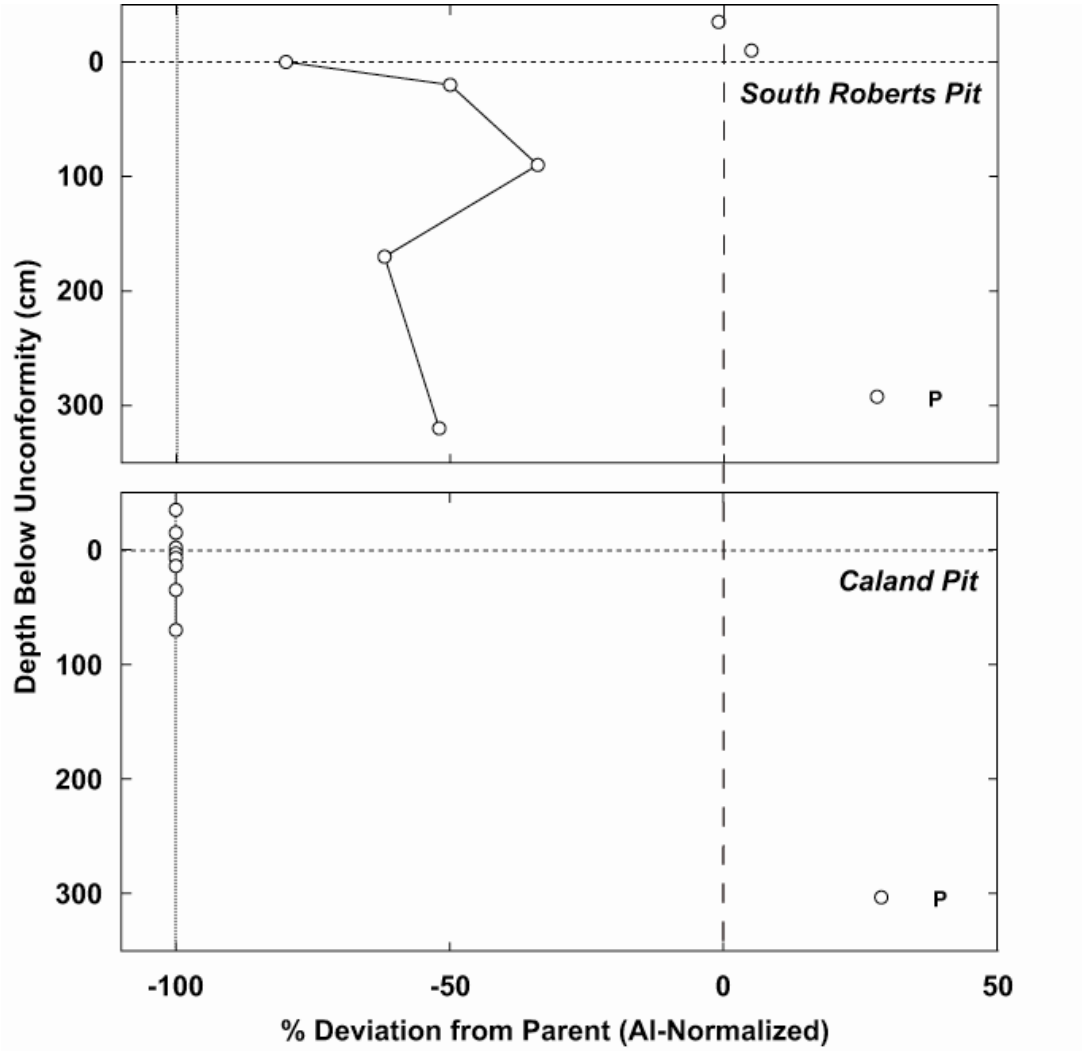

Figure 4.4: Percent variation of P (Al-normalized) from parent material in the SRP and CP profiles. Parent material =0.

organic ligands may have been present and that they could have affected redox mobility. If there was enough oxygen to oxidize Fe^{2+} to Fe^{3+}, which seems likely based on Fe^{3+}/Fe^{2+} ratios >1, the presence of organics could explain the loss of Fe_T from both profiles as well as the lack of Ce anomalies.

4.4.4 Copper Mobility

Phosphorus mobility itself is not an indicator of redox conditions, as P is mobile with ligands and with or without oxygen (Neaman *et al.*, 2005). Alternatively, Cu can be used. Neaman *et al.* (2005) documented the mobility of Cu solely as a function of oxygen and not ligands. Variation of Al-normalized Cu from the parent tonalite with depth for the SRP paleosol is presented in **Table 4.1** and shown in **Figure 4.5.** Cu loss ranges from 112% at the top of the profile to 89% at the bottom. Data for the CP profile is presented in **Table 4.2** and shown in **Figure 4.5.** Cu loss ranges from 52% at the top of the profile to 36% at the bottom of the profile. Because Cu mobility is most likely due to the oxygen content of the soil, and not the ligand content (Neaman *et al.*, 2005), Cu should be useful in estimating a minimum Eh for the atmosphere. Soils are generally more reduced than the atmosphere if they contain organic material, thus calculations would reflect a lower limit of atmospheric oxygen.

To further constrain the Eh conditions in the Steep Rock paleosol profiles, the Eh values required to oxidize Cu were calculated for assumed pH values of 4.66 and 5.6. The Eh-pH diagram for the Cu-C-S-O-H system is shown in **Figure 4.6**; no Cu^+ field is present because Cu^+ ions typically disproportionate yielding Cu^0 and Cu^{2+} (Hem, 1985). In **Figure 4.6**, activities assumed for dissolved species include $Cu=10^{-6}$ and $S=10^{-3}$, and $C=10^{-1,-3}$. Temperature is

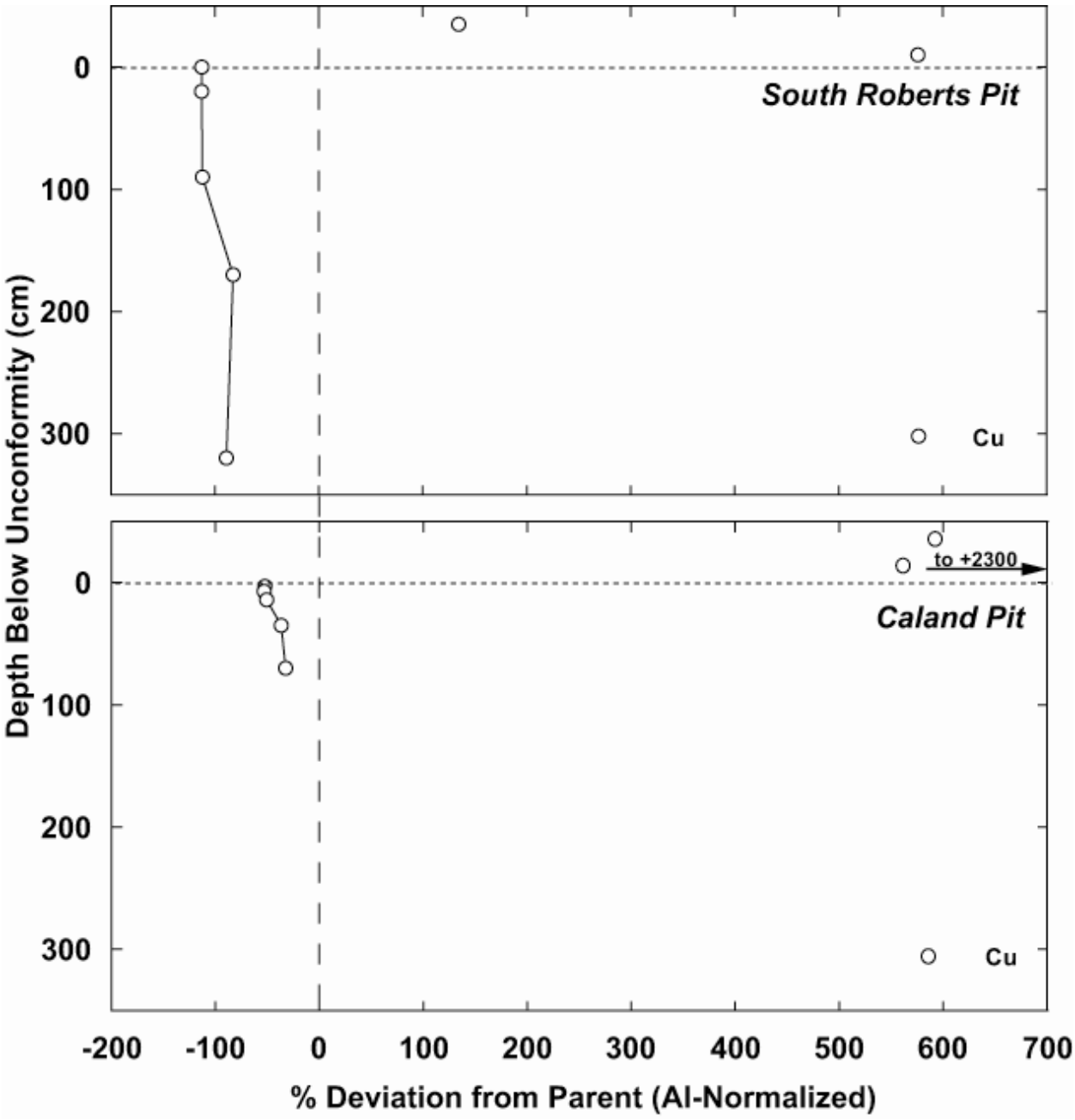

Figure 4.5: Percent variation of Cu (Al-normalized) from parent material in the SRP and CP profiles.

Parent material =0.

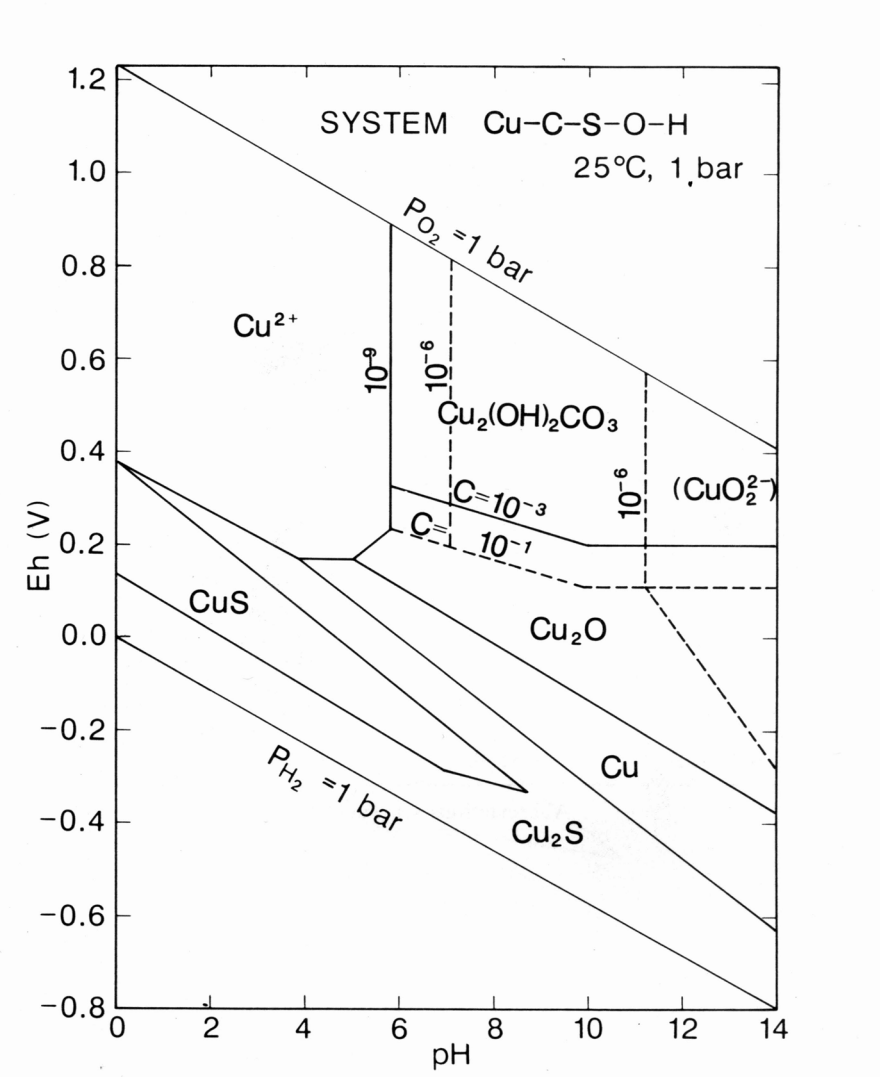

Figure 4.6: Eh-pH diagram for the Cu-C-S-O-H system. Activities assumed for dissolved species include Cu=10^{-6} and S=10^{-3}, and C=$10^{-1,-3}$. Temperature is assumed to be 25°C, and pressure is assumed to be 1 bar (from Brookins, 1988).

assumed to be 25°C and pressure to be 1 bar (Brookins, 1988). For an assumed pH of 4.66, the phase boundary between the Cu and Cu^{2+} can be calculated by equation (4.9) and the equilibrium equation (4.10):

$$Cu(s) \rightarrow Cu^{2+}(aq) + 2e^{-} \quad (4.9)$$

$$\log K = -\log [Cu^{2+}] - pe \quad (4.10)$$

The activity for Cu^{2+} is assumed to be 1.57×10^{-7} mol/L, which is the common concentration of Cu^{2+} in modern river waters (Turekian, 1969). The value for $K=3.39 \times 10^{-12}$ calculated using thermodynamic data from Wagman *et al.* (1982). At a pH of 4.66, the calculated phase change between Cu and Cu^{2+} will take place at Eh= 0.138 based on equation (4.10).

If pH is assumed to be 5.6, the phase boundary between the Cu and Cu^{2+} can be calculated by equation (4.11) and the equilibrium equation (4.12):

$$Cu_2O(s) + 2H^{+} \rightarrow 2Cu^{2+}(aq) + H_2O + 2e^{-} \quad (4.11)$$

$$\log K = 2\log [Cu^{2+}] - 2pe + 2pH \quad (4.12)$$

The activity for Cu^{2+} is assumed to be 1.57×10^{-7} mol/L, which is the common concentration of Cu^{2+} in modern river waters (Turekian, 1969). The value for $K=9.4 \times 10^{-8}$ calculated using thermodynamic data from Wagman *et al.* (1982). At a pH of 5.6, the calculated phase change between Cu and Cu^{2+} will take place at Eh= 0.136 based on equation (4.12). The

mobility of Cu suggests that the soil contained some oxygen. To further constrain the Eh and pH of the Steep Rock soil environment, we analyzed uranium (U), which has been used as a paleoenvironmental indicator in the Archean.

4.4.5 Uranium Mobility

Detrital uraninite has been used by many authors as evidence that the Earth's atmosphere was reducing prior to 2.2 Ga (Robinson and Spooner, 1984; Robb and Meyer, 1995; Buick and Rasmussen, 1998; Law *et al.*, 2003). It is considered a paleoenvironmental indicator because when it is oxidized from U^{4+} to U^{6+} it becomes mobile as uranyl complexes or uranyl carbonate complexes (Brookins, 1988). No data for the CP profile are available (Schau and Henderson, 1983). Whole rock U data for the SRP profile are shown in **Table 4.1**; Al-normalized U data compared to parent tonalite are shown in **Figure 4.7**. U is depleted (up to 45 %) in the soil profile compared to the parent tonalite, consistent with at least slightly oxidizing conditions. However, U movement has been attributed to diagenesis of uranium-bearing minerals in a study by Robinson and Spooner (1984). Uranium disturbance is suggested in the Steep Rock profile by discordant titanite U-Pb ages of 2809 Ma from the 3003 Ma Marmion complex (Davis and Jackson, 1988). Titanites yielding U-Pb ages of 2950 Ma have been reported as representing hydrothermal deposition concurrent with the formation of the Jolliffe Ore Zone (reported by Tomlinson *et al.*, 1999, as D. Davis, personal communication).

Assuming no disturbance of U during hydrothermal events, Eh constraints can be placed on the soil redox conditions. The Eh-pH diagram for the U-C-O-H system with the Fe-S-O-H system superimposed is shown in **Figure 4.8**. In **Figure 4.8**, activities assumed for dissolved species include $U=10^{-6, -8, -10}$ and $S=10^{-3}$, $Fe=10^{-6}$and $C=10^{-3}$. Temperature is assumed to be

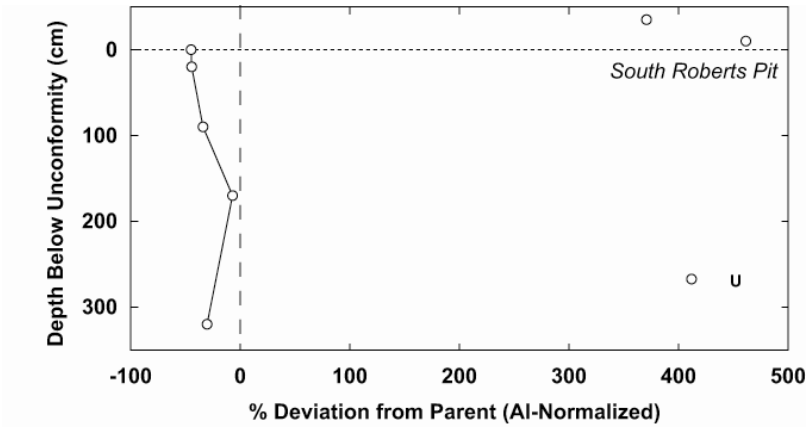

Figure 4.7: Percent variation of U (Al-normalized) from parent in the SRP profile. Parent material =0.

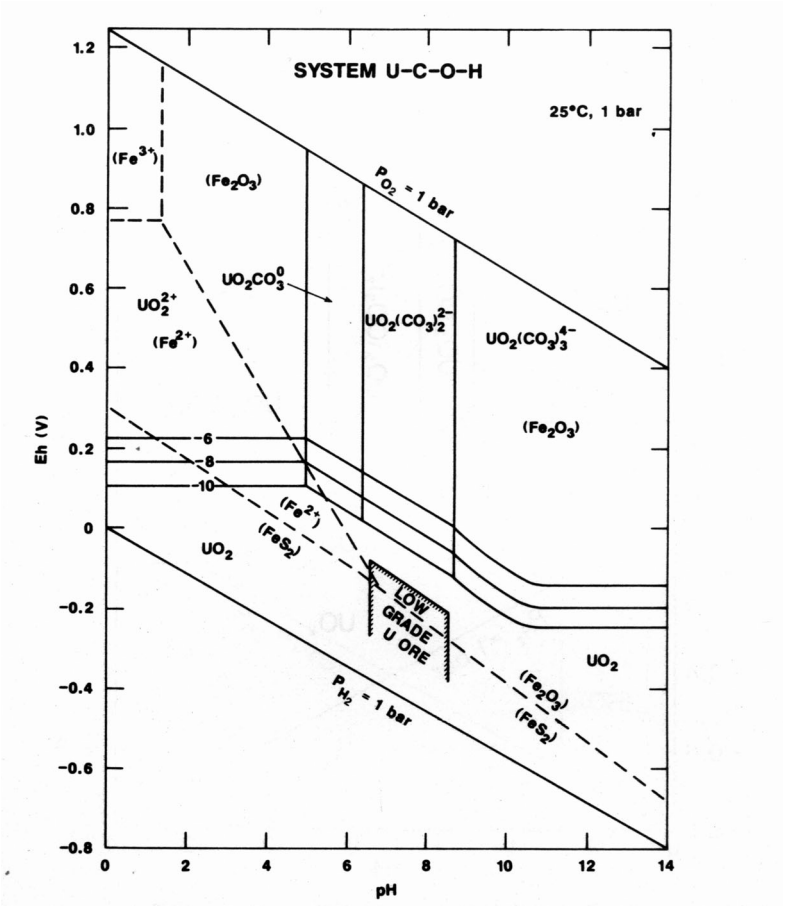

Figure 4.8: Eh-pH diagram for the U-C-O-H system with the Fe-S-O-H system superimposed. Activities assumed for dissolved species include U=10^{-6}, $^{-8}$, $^{-10}$ and S=10^{-3}, Fe=10^{-6} and C=10^{-3}. Temperature is assumed to be 25°C, and pressure is assumed to be 1 bar (from

25°C and pressure to be 1 bar (Brookins, 1988). For an assumed pH of 4.66, the phase boundary between the UO2 and UO22+ can be calculated by equation (4.13) and the equilibrium equation (4.14):

$$UO_2(s) \rightarrow UO_2^{2+}(aq) + 2e^- \quad (4.13)$$

$$\log K = \log [UO_2^{2+}] - 2pe \quad (4.14)$$

The activity for UO_2^{2+} is assumed to be 2.10×10^{-8} mol/L, which is the average concentration of U in modern natural waters (Hem, 1985). The value for $K=1.27 \times 10^{-14}$ calculated using thermodynamic data from OECD (1985). At a pH of 4.66, the calculated phase change between UO_2 and UO_2^{2+} will take place at Eh= 0.184 based on equation (4.14).

For an assumed pH of 5.6, the oxidized ion of U is $UO_2(CO_3)_2^{2-}$. The phase boundary between the UO_2 and $UO_2(CO_3)_2^{2-}$ can be calculated by equation (4.15) and the equilibrium equation (4.16):

$$UO_2(s) + 3HCO_3^- \rightarrow UO_2(CO_3)_2^{2-}(aq) + 2e^- + 2H^+ \quad (4.15)$$

$$\log K = \log [UO_2(CO_3)_2^{2-}] - 2pH - 2pe + 6 \quad (4.16)$$

The activity for $UO_2(CO_3)_2^{2-}$ is assumed to be 2.10×10^{-8} mol/L, which is the average concentration of U in natural waters (Hem, 1985). The value for $K=2.06 \times 10^{-18}$ calculated using thermodynamic data from OECD (1985). At a pH of 5.6, the calculated phase change between

UO_2 and $UO_2(CO_3)_2^{2-}$ will take place at Eh= 0.142 based on equation (4.16). If the mobility of U is only due to pedogenic processes and not diagenetic/hydrothermal processes, then calculated Eh data suggests a slightly oxidizing soil atmosphere.

4.4.6 Vanadium Mobility

Most vanadium (V) species are mobile. However, V_2O_4 and V_2O_3 are oxidized solid species that occur in the middle pH ranges. Most modern soils form between a pH of 4.5 and 9 (Brady and Weil, 1999). Whole rock V data for the SRP profile are shown in **Table 4.1**; Al-normalized V data for the SRP profile compared to parent tonalite are shown in **Figure 4.9**. V is enriched by a factor of 12 to 412%. Vanadium data for the CP profile are shown in **Table 4.2**; Al-normalized V data for the CP profile compared to parent granodiorite are shown in **Figure 4.9**. V in the CP profile is depleted 84-90% relative to its parent.

The Eh-pH diagram for the V-O-H system is shown in **Figure 4.10**. In **Figure 4.10**, activities assumed for dissolved species include $V=10^{-6}$. Temperature is assumed to be 25°C and pressure to be 1 bar (Brookins, 1988). For an assumed pH of 4.66, the phase boundary between the V_2O_3 and VO^{2+} can be calculated by equation (4.17) and equilibrium equation (4.18):

$$V_2O_3(s) + 2H^+ \rightarrow 2VO^{2+}(aq) + H_2O + 2e^- \quad (4.17)$$

$$\log K = 2\log [VO^{2+}] - 2pe + 2pH \quad (4.18)$$

The activity for VO^{2+} is assumed to be 9.8×10^{-8} mol/L, which is the average concentration of V in modern natural waters (Hem, 1985). The value for $K=2.32 \times 10^{-2}$. K was

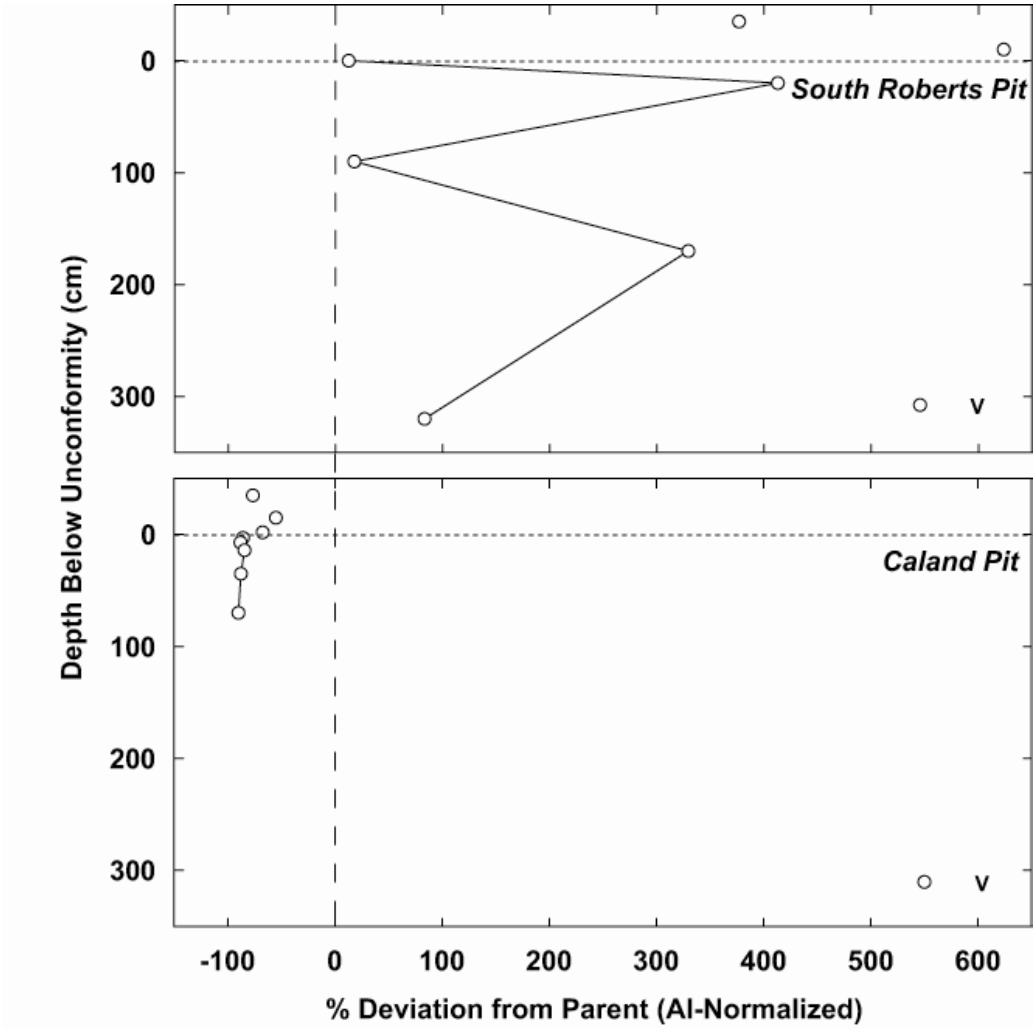

Figure 4.9: Percent variation of V (Al-normalized) from parent material in the SRP and CP profiles. Parent material =0.

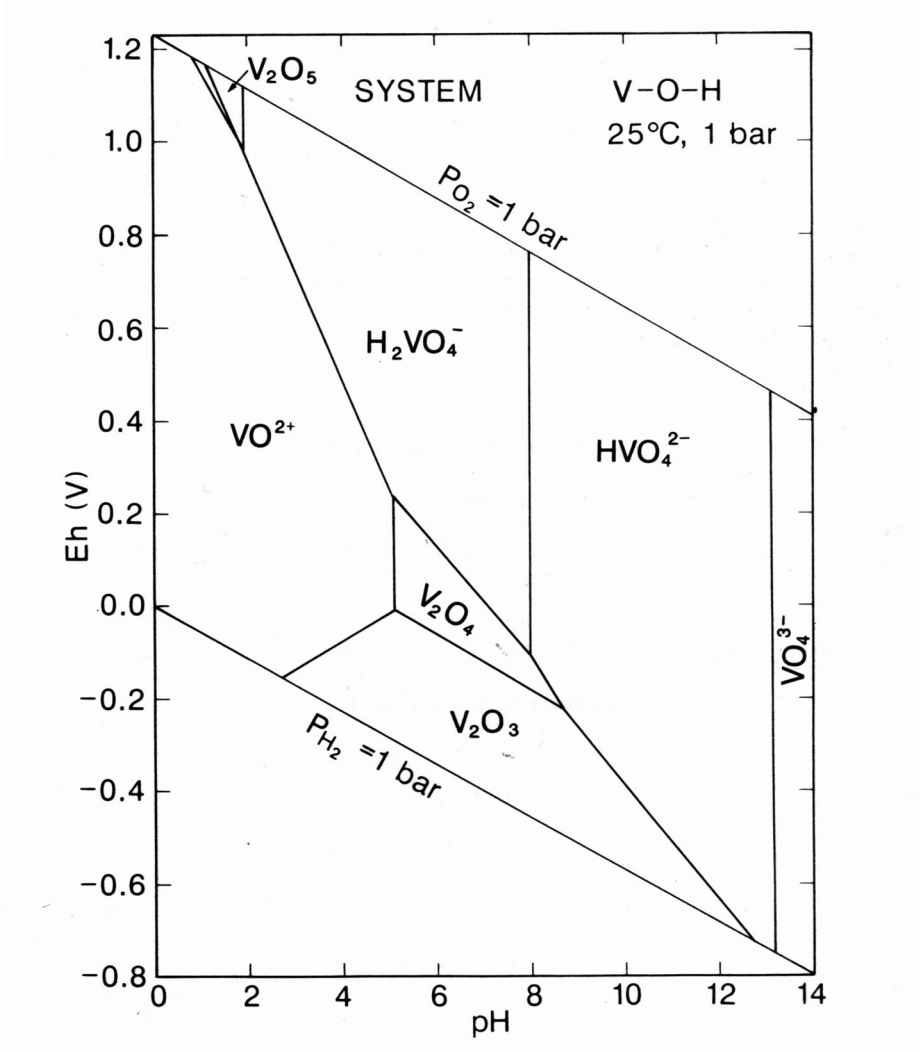

Figure 4.10: The Eh-pH diagram for the V-O-H system is shown. Activities assumed for dissolved species include V=10^{-6}. Temperature is assumed to be 25°C, and pressure is assumed to be 1 bar (from Brookins, 1988).

calculated using thermodynamic data from Wagman et al. (1982). At a pH of 4.66, the calculated phase change between V_2O_3 and VO^{2+} will take place at Eh= -0.091 based on equation (4.18). For an assumed pH of 5.6, the phase boundary between the V_2O_4 and $H_2VO_4^-$ can be calculated by equation (4.19) and the equilibrium equation (4.20):

$$V_2O_4(s) + 4H_2O \rightarrow 2H2VO_4^-(aq) + 2e^- + 4H^+ \quad (4.19)$$

$$\log K = 2 \log [H2VO_4^-] - 4pH - 2pe \quad (4.20)$$

The activity for $H_2VO_2^-$ is assumed to be 9.8×10^{-8} mol/L, which is the average concentration of V in modern natural waters (Hem, 1985). The value for $K=3.48 \times 10^{-40}$ calculated using thermodynamic data from Wagman *et al.* (1982). At a pH of 5.6, the calculated phase change between V_2O_4 and $H_2VO_4^-$ will take place at Eh= 0.090 based on equation (4.20).

The mobility of V in the CP profile suggests an oxidizing soil environment. This is consistent with the pronounced enrichment of Fe^{3+} of up to 1000% relative to parent in the middle of the profile. The retention of V in the SRP profile could indicate that the SRP profile was more affected by organic ligands, which reduced oxygen levels and created a slightly oxygenated to reducing environment, making V stable at moderate pH. However, this does not explain the $Fe^{3+}/Fe^{2+} > 1$ for this profile. An alternative explanation for V retention in the SRP is the incorporation of V into clay structures. Preliminary laser ablation data of the SRP samples indicates that V is associated with leucoxene, a Ti-oxide alteration product of titanite and ilmenite (Macpherson *et al.*, 2000). Vanadium may remain in the clay structure under slightly oxidizing conditions. Brookins (1976; 1977; 1979; 1984) studied the incorporation of U and V into clays in Grants Mineral Belt, New Mexico. Uranium and vanadium were incorporated into

clays at the same time; however, U became mobile with an increase in Eh, whereas V remained in the clay structures despite oxygen levels. The studies suggested that segregation of U from V can occur during weathering. Further study is needed to distinguish the difference between V-bearing phases in the SRP and CP profiles and how mineralogy may affect V mobility. A summary of possible Eh constraints constructed for the Steep Rock paleosols based on model assumptions is shown in **Table 4.3**.

Table 4.3: Summary of redox element Eh indicators for the Steep Rock Paleosol.

Species	Species Present SRP	CP	Species Eh (min or max) for model with pH = 4.66	Comment
Fe^{2+}(aq)	Yes	Yes	Eh < 0.545	] Varying Redox?
Fe^{3+}(s)	Yes	Yes	Eh > 0.545	
Ce^{4+}(s)	No	No	Eh > 0.585	Maximum Eh?
Cu^{2+}(aq)	Yes	Yes	Eh > 0.138	Minimum Eh?
UO_2^{2+}(aq)	Yes?*	Yes?*	Eh > 0.184	*Hydrothrmal?
VO^{2+}(aq)	No?**	Yes	Eh > -0.09	**Held in Clay?

Species	SRP	CP	Species Eh (min or max) for model with pH = 5.6	Comment
Fe^{2+}(aq)	Yes	Yes	Eh < 0.379	] Varying Redox?
Fe^{3+}(s)	Yes	Yes	Eh > 0.379	
Ce^{4+}(s)	No	No	Eh > 0.348	**Below Fe^{3+}?**
Cu^{2+}(aq)	Yes	Yes	Eh > 0.137	
$UO_2(CO3)_2^{2-}$(aq)	Yes?*	Yes?*	Eh > 0.142	*Hydrothrmal?
$H_2VO_4^-$(aq)	No?**	Yes	Eh > 0.090	**Held in Clay?

4.5 REDOX CONDITIONS DURING STEEP ROCK PEDOGENESIS

Based on estimates of pCO_2 in the Archean atmosphere and modern concentrations of redox metals in the hydrosphere, a preliminary model for Steep Rock soil Eh indicates at least enough oxygen to oxidize Fe and Cu but not enough to oxidize Ce. However, initial evidence of microbial activity based on the mobility of P suggests that Ce could have complexed with organic material, which could mask Ce anomalies. Organic ligands may have also caused variability in Fe redox states. Copper mobility is independent of organic ligands, based on experimental data by Neaman *et al.* (2005), making it a possible indicator of the minimum Eh of soil conditions. Uranium concentrations were only slightly depleted, indicating either slightly oxidizing soil conditions or the addition of U during hydrothermal alteration of the SRP profile. Different V behavior in the SRP and CP profiles may suggest that V was incorporated into clay structures in the SRP profile.

Paleosol data are consistent with modeled Eh values when a pH of 4.66 is assumed. Model results using pH=5.6 yield conditions with enough oxygen to oxidize Ce, but not Fe, which is inconsistent with the paleosol Fe and Ce data. Preliminary estimates for minimum and maximum soil Eh values of 0.137 and 0.585, respectively, were calculated using an assumed pH of 4.66. Although many assumptions go into redox modeling for paleosols, this study demonstrates the advantages for using several redox elements for constraining the soil environment in the Archean. To improve this model, mineral phases in the paleosol need to be better constrained, and additional tracers for soil microbes are needed.

4.6 COMPARISON BETWEEN THE STEEP ROCK AND HOKKALAMPI PALEOSOLS

Despite chemical overprinting by thermal events, both the ~3.0 Ga Steep Rock paleosol (northwest Ontario) and ~2.3 Ga Hokkalampi paleosol (eastern Finland) contain clear micromorphologic textures that are evidence of soil-forming processes and a general trend of increased weathering toward the paleo-surface (Stafford *et al.*, 1999; Stafford *et al.*, 2000). Whole rock Rb-Sr ages and secondary mineral assemblages (e.g., white mica and chlorite) are consistent with intense subaerial weathering followed by regional greenschist metamorphism (Stafford *et al.*, 1999; Stafford *et al.*, 2000). This likely resulted in post-pedogenic changes in the concentrations of alkali and alkaline earth element such as potassium, calcium and strontium. However, Sm-Nd isotope systematics for both paleosols suggest that REE concentrations were largely unaffected by regional metamorphism.

Terrestrial conditions recorded by the Hokkalampi paleosol during the proposed rise of atmospheric oxygen (e.g., Bekker *et al.*, 2004) ranged from oxidized to reduced. Hokkalampi soil formation was most likely affected by seasonal fluctuations as in modern lateritic soils: organic acid-rich and reducing during wet seasons, and oxic during dry season (i.e., O_2-diffusion through the unsaturated soil zone). Organic-rich water moving through the subsurface under saturated conditions was responsible for mobilization of rare earth elements and perhaps thorium. As suggested for the Hekpoort paleosol (Beukes *et al.*, 2002), iron was mobilized at the mid-levels of the paleosols deposited at depth as Fe^{2+}. During the dry seasons, a portion of this Fe was fixed as Fe^{3+} by oxic soil/ground waters ($Fe^{3+}/Fe^{2+}>1$). Some leaching of uranium at shallow to middle levels in the profile by these oxic waters may also have taken place, with

subsequent adsorption at depth by Fe hydroxides. This model would suggest that the reduced Hokkalampi profile at one time had an oxidized upper zone (analogous to the Hekpoort paleosol; Beukes *et al.*, 2002) that was subsequently eroded away.

The SRP/CP Steep Rock profiles and the reduced section of the Hokkalampi paleosol exhibit similar characteristics including: (1) Fe_T loss at the top of the profiles; (2) $Fe^{3+}/Fe^{2+}>1$; (3) minor to absent Ce anomalies; (4) mobility of U; and (5) evidence of organic material. (*i.e.,* mobility of P or Th). The shared characteristics of the Hokkalampi paleosol, which formed during the proposed rise of oxygen (e.g., Bekker *et al.*, 2004) and the much older Steep Rock paleosol (Sm-Nd isotope model age of 3018±90 Ma) are consistent with, but do not require, a model of significant atmospheric pO_2 levels as early as 3.0 Ga ago.

BIBLIOGRAPHY

Alibert C. and McCulloch M. T. (1993) Rare earth element and neodymium isotopic compositions of the banded iron-formations and associated shales from Hamersley, Western Australia. *Geochimica et Cosmochimica Acta* **57**(1), 187-204.

Aubert D., Stille P., and Probst A. (2001) REE fractionation during granite weathering and removal by waters and suspended loads; Sr and Nd isotopic evidence. *Geochimica et Cosmochimica Acta* **65**(3), 387-406.

Aurola E. (1959) The kyanite and pyrophyllite occurrences in north Karelia. *Geol. Tutkimusi Geoteknol* **63**, 36.

Balashov Y. A., Rovov A. B., Mogdisov A. A., and Turanskaya N. V. (1964) The effect of climate and facies environment on the fractionation of the rare earth elements during sedimentation. *Geochem. Int.* **10**, 995-1014.

Banfield J. F. and Eggleton R. A. (1989) Apatite replacement and rare earth mobilization, fractionation, and fixation during weathering. *Clays and Clay Mineralogy* **37**, 113-127.

Begle E. A. (1978) The Weathering of Granite, Llano Region, Central Texas, M.A. Thesis, The University of Texas at Austin.

Bekker A., Holland H. D., Wang P. L., Rumble III D., Stein H. J., Hannah J. L., Coetzee L. L., and Beukes N. J. (2004) Dating the rise of atmospheric oxygen. *Nature* **427**, 117-120.

Beukes N. J., Dorland H., Gutzmer J., Nedachi M., and Ohmoto H. (2002) Tropical laterites, life on land, and the history of atmospheric oxygen in the Paleoproterozoic. *Geology* **30**, 491-494.

Bouch J. E., Hole M. J., Trewin N. H., Chenery S., and Morton A. C. (2002) Authigenic apatite in a fluvial sandstone sequence: Evidence for rare-earth element mobility during diagenesis and a tool for diagenetic correlation. *J. Sed. Res.* **72**, 59-67.

Bouch J. E., Hole M. J., Trewin N. H., and Morton A. C. (1995) Low-temperature aqueous mobility of the rare-earth elements during sandstone diagenesis. *Journal of the Geological Society, London* **152**, 895-898.

Brady N. C. and Weil R. R. (1999) *Nature and Properties of Soils*. Prentice Hall, Inc., Upper Saddle River, N.J.

Braun J.-J., Pagel M., Muller J.-P., Bilong P., Michard A., and Guillet B. (1990) Cerium anomalies in lateritic profiles. *Geochimica et Cosmochimica Acta* **54**(3), 781-795.

Brewer R. (1964) *Fabric and Mineral Analysis of Soils*. Wiley.

Brewer R. (1976) *Fabric and Mineral Analysis of Soils*. Krieger Publishing Company.

Brookins D. G. (1976) The Grants mineral belt, New Mexico. *New Mexico Geol. Soc. Spec. Pub.* **6**, 255-269.

Brookins D. G. (1977) Uranium deposits of the Grants mineral belt. *Rocky Mt. Assoc. Geol. Gdbk.*, 337-352.

Brookins D. G. (1979) *Uranium deposits of the Grants, New Mexico mineral belt II*. U.S.D.O.E. Report BFEC-GJO-76-029E

Brookins D. G. (1984) *Geochemical aspects of radioactive water disposal*. Springer.

Brookins D. G. (1988) *Eh-PH Diagrams for Geochemistry*. Springer Verlag.

Buick R. and Rasmussen B. (1998) Archean oil; evidence for extensive hydrocarbon generation and migration 2.5-3.5 Ga. *AAPG Bulletin* **82**(1), 50-69.

Capo R. C. (1993) Micromorphology of a Cambrian paleosol developed on granite: Llano Uplift region, Central Texas, U.S.A. In *Soil Micromorphology: Studies in Management and Genesis. Developments in Soil Science 22* (ed. A. J. Ringrose-Voase and G. S. Humphreys), pp. 257-264. Elsevier.

Capo R. C. (1994) Micromorphology and geochemistry of a Cambrian paleosol developed on granite, Llano Uplift region, central Texas, USA. In *Soil Micromorphology:Studies in Management and Genesis* Vol. 22 (ed. A. Ringrose-Voase and G. Humphreys), pp. 257-264 Elsevier.

Chadwick O. A., Brimhall G. H., and Hendricks D. M. (1990) From a black box to a gray box - a mass balance interpretation of pedogenesis. *Geomorphology* **3**, 369-390.

Chadwick O. A., Gavenda R. T., Kelly E. F., Ziegler K., Olson C. G., Elliott W. C., and Hendricks D. M. (2003) The impact of climate on the biogeochemical functioning of volcanic soils. *Chemical Geology* **202**(3-4), 195-223.

Condie K. C. (1981) *Archean Greenstone Belts*. Elsevier Scientific Publishing Company.

Condie K. C., Dengate J., and Cullers R. L. (1995) Behavior of rare earth elements in a paleoweathering profile on granodiorite in the Front Range, Colorado, USA. *Geochimica et Cosmochimica Acta* **59**(2), 279-294.

Davis D. W. and Jackson M. C. (1988) Geochronology of the Lumby Lake greenstone belt: a 2 Ga complex within the Wabigoon subprovince, northwest Ontario. *Geological Society of America Bulletin* **100**, 818-824.

Deer W. A., Howie R. A., and Zussman J. (1966) *An Introduction to the Rock-Forming Minerals*. Wiley.

Delvigne. (1998) *Atlas of Micromorphology of Mineral Alteration and Weathering*. Mineralogical Association of Canada.

DePaolo D. J. (1981) Neodymium isotopes in the Colorado Front Range and crust-mantle evolution in the Proterozoic. *Nature* **291**, 193-196.

DePaolo D. J. and Wasserburg G. J. (1979) Sm-Nd age of the Stillwater complex and the mantle evolution curve for neodymium. *Geochimica et Cosmochimica Acta* **43**, 999-1008.

Dia A., Gruau G., Olivie-Lauquet G., Riou C., Molenat J., and Curmi P. (2000) The distribution of rare earth elements in groundwaters: assessing the role of source-rock composition, redox changes and colloidal particles. *Geochimica et Cosmochimica Acta* **64**(24), 4131-4151.

Drever J. I. (1997) *The Geochemistry of Natural Waters: Surface and Groundwater Environments (3rd ed.)*. Prentice Hall, Upper Saddle River, NJ

Driese S. G. (2004) Pedogenic translocation of Fe in modern and ancient vertisols and implications for interpretations of the Hekpoort paleosol (2.25 Ga). *Journal of Geology* **112**, 543-560.

Driese S. G., Mora C. I., Stiles C. A., Jocckel R. M., and Nordt L. C. (2000) Mass-balance reconstruction of a modern Vertisol: implications for interpretations of geochemistry and burial alteration of paleo-Vertisols. *Geoderma* **95**, 179-204.

Duddy I. R. (1980) Redistribution and fractionation of rare earth and other elements in a weathering profile. *Chemical Geology* **30**, 363-381.

Ehrenberg S. N. and Nadeau P. H. (2002) Postdepositional Sm/Nd fractionation in sandstones: Implications for neodymium-isotope stratigraphy. *J. Sed. Res.* **72**, 304-315.

Farmer G. L. and DePaolo D. J. (1987) Nd and Sr isotope study of hydrothermally altered granite at San Manuel, Arizona: Implications for element migration paths during formation of porphyry copper ore deposits. *Econ. Geol.* **82**, 1142-1151.

Feakes C. R., Holland H. D., and Zbinden E. A. (1989) Ordovician paleosols at Arisaig, Nova Scotia and the evolution of the atmosphere. In *Paleopedology: Nature, and Application of Paleosols*, Vol. 16 (ed. A. Bronder and J. A. Catt), pp. 207-232.

Folk R. L. and Patton E. B. (1982) Buttressed expansion of granite and development of grus in central Texas. *Zeitschrift fuer Geomorpholoie* **26**(1), 17-32.

Gall Q. (1992) Precambrian paleosols in Canada. *Canadian Journal of Earth Science* **29**, 2530-2536.

Gay A. L. and Grandstaff D. E. (1980) Chemistry and mineralogy of Precambrian paleosols at Elliot Lake, Ontario, Canada. *Precambrian Research* **12**, 349-373.

Girty G. H., Marsh J., Meltzner A., McConnell J. R., Nygren D., Nygren J., Prince G. M., Randall K., Johnson D., Heitman B., and Nielsen J. (2003) Assessing changes in elemental mass as a result of chemical weathering of granodiorite in a Mediterranean (hot summer) climate. *Journal of Sedimentary Research* **73**, 434-443.

Goldstein S. L., O'Nions R. K., and Hamilton P. J. (1984) A Sm-Nd isotopic study of atmospheric dusts and particulates from major river systems. *Earth and Planetary Science Letters* **70**, 221-236.

Gromet L. P. and Silver L. T. (1983) Rare earth element distributions among minerals in a granodiorite and their petrogenetic implications. *Geochimica et Cosmochimica Acta* **47**, 925-939.

Gruau G., Tourpin S., Fourcade S., and Blais S. (1992) Loss of isotopic (Nd, O) and chemical (REE) memory during metamorphism of komatiites: new evidence from eastern Finland. *Contributions to Mineralogy and Petrology* **112**, 66-82.

Gutzmer J. and Beukes N. J. (1998) Earliest laterites and possible evidence for terrestrial vegetation in the early Proterozoic. *Geology (Boulder)* **26**(3), 263-266.

Hamilton P. J., Evensen N. M., O'Nions R. K., and Tarney J. (1979) Sm-Nd dating of Onverwacht Group volcanics, southern Africa. *Nature* **279**, 298-300.

Harlavan Y. and Erel Y. (2002) The release of Pb and REE from granitoids by the dissolution of accessory phases. *Geochimica et Cosmochimica Acta* **66**, 837-848.

Hem J. D. (1985) Study and Interpretation of the Chemical Characteristics of Natural Water, 3rd ed. (ed. U. S. G. S. W.-S. P. 2252).

Hicks H. S. (1950) Geology of the iron deposits of Steep Rock Iron Mines Limited. *The Precambrian* **23**(5), 8-10.

Holland H. D. (1984) *The Chemical Evolution of the Atmosphere and Oceans*. Princeton University Press.

Holland H. D. (1994) Early Proterozoic atmospheric change. In *Early Life on Earth*, Vol. Nobel Symposium No. 84 (ed. S. Bengtson), pp. 237-389. Columbia University Press.

Holland H. D. and Beukes N. J. (1990) A paleoweathering profile from Griqualand West, South Africa: evidence for a dramatic rise in atmospheric oxygen between 2.2 and 1.9 BYBP. *American Journal of Science* **290-A**, 1-34.

Holland H. D., Feakes C. R., and Zbinden E. A. (1989) The Flin Flon paleosol and the composition of the atmosphere 1.8 BYBP. *American Journal of Science* **289**, 362-389.

Holland H. D. and Rye R. (1997) Evidence in pre-2.2 Ga paleosols for the early evolution of atmospheric oxygen and terrestrial biota: Comment. *Geology* **25**, 857-858.

Holland H. D. and Zbinden E. A. (1988) Paleosols and the evolution of the atomosphere: part I. In *Physical and Chemical Weathering in Geochemical Cycles* (ed. A. Lerman and M. Meybeck), pp. 61-82. Kluwer Academic Publishers.

Horodyski R. J. and Knauth L. P. (1994) Life on land in the Precambrian. *Science* **263**, 494-498.

Huhma H., Cliff R. A., Perttunen V., and Sakko M. (1990) Sm-Nd and Pb isotopic study of mafic rocks associated with early Proterozoic continental rifting: the Perapohja schist belt in northern Finland. *Contributions to Mineralogy and Petrology* **104**, 369-379.

Jackson M. L. and Sherman G. D. (1953) Chemical weathering of minerals in soils. *Adv. Agron.* **5**, 219-318.

Jahn B.-M., Gruau G., and Glickson A. Y. (1982) Komatiies of the Overwacht Group, S. Africa: REE geochemistry, Sm/Nd age, and mantle evolution. *Contributions to Mineralogy and Petrology* **80**, 25-40.

Jolliffe A. W. (1966) Stratigraphy of the Steeprock Group, Steep Rock Lake, Ontario. In *The Relationship of Mineralization to Precambrian Stratigraphy in Certain Mining Areas of Ontario and Quebec, The Geological Association of Canada Special Paper Number 3* (ed. A. M. Goodwin), pp. 75-98. Business and Economic Service Limited.

Jones D. L. (1998) Organic acids in the rhizosphere: a critical review. *Plant and Soil* **205**, 25-44.

Kasting J. F. (1987) Theoretical constraints on oxygen and carbon dioxide concentrations in the Precambrian atmosphere. *Precambrian Research* **34**, 205-228.

Kasting J. F. (2001) The rise of atmospheric oxygen. *Science* **293**(5531), 819-820.

Kimberley M. M. and Grandstaff D. E. (1986) Profiles of elemental concentrations in Precambrian paleosols on basaltic and granitic parent materials. *Precambrian Research* **32**, 133-154.

Kirkham R. V. and Roscoe S. M. (1993) Atmospheric evolution and ore deposit formation. *Resource Geology Special Issue* **15**, 1-17.

Kohonen J. and Marmo J. (1992) Proterozoic lithostratigraphy and sedimentation of Sariola and Jatuli-type rocks in the Nunnanlahti-Koli-Kaltimo area, eastern Finland: implications for regional basin evolution models. *Geologic Survey of Finland Bulletin* **364**, 67+ 2 app.

Kouvo O. and Tilton G. R. (1966) Mineral ages from the Finnish Precambrian. *Journal of Geology* **74**, 421-442.

Kuovo O., Huhma H., and Sakko M. (1983) Isotopic evidence for old crustal involvement in genesis of two granites from northern Finland. *Terra Cognita* **3**(2-3), 135.

Kurtz A. C., Derry L. A., and Chadwick O. A. (2001) Accretion of Asian dust to Hawaiian soils: isotopic, elemental, and mineral masses. *Geochimica et Cosmochimica Acta* **65**(12), 1971-1983.

Kurtz A. C., Derry L. A., Chadwick O. A., and Alfano M. J. (2000) Refractory element mobility in volcanic soils. *Geology* **28**, 683-686.

Kusky T. M. and Hudleston P. J. (1999) Growth and demise of an Archean carbonate platform, Steep Rock Lake, Ontario, Canada. *Can. J. Earth Sci.* **36**, 565-584.

Lambert D. D. (1994) Re-Os and Sm-Nd isotope geochemistry of the Stillwater Complex, Montana: implications for the petrogenesis of the J-M reef. *J. Petrology* **35**, 1717-1753.

Lång L.-O. (2000) Heavy mineral weathering under acidic soil conditions. *Applied Geochemistry* **15**, 415-423.

Langmuir D. (1997) *Aqueous Environmental Geochemistry*. Prentice Hall.

Law J. D., Phillips G. N., and Myers R. E. (2003) Relevance of the Archaean atmosphere to the genesis of banded iron formations. *Institution of Mining and Metallurgy, Transactions, Section B: Applied Earth Science* **112**(96), 96.

Lipin B. R. and McKay G. A. (1989) Geochemistry and Mineralogy of Rare Earth Elements. In *Reviews in Mineralogy*, Vol. 21 (ed. P. H. Ribbe), pp. 348. The Mineralogical Society of America.

Macfarlane A. W., Danielson A., Holland H. D., and Jacobsen S. B. (1994) REE chemistry and Sm-Nd systematics of late Archean weathering profiles in the Fortescue Group, Western Australia. *Geochimica et Cosmochimica Acta* **58**, 1777-1794.

Macfarlane A. W. and Holland H. D. (1991) The timing of alkali metasomatism in paleosols. *The Canadian Mineralogist* **29**, 1043-1050.

Macpherson G. L., Stafford S. L., Capo R. C., Stewart B. W., and Ohmoto H. (2000) Geochemistry of an Archean paleosol, Steep Rock, Ontario, Canada: whole rock and LAM-ICPMS analysis. *Geological Society of America Abstracts with Programs* **37,**(7), 485.

Marmo J. and Kohonen J. (1992) Early Proterozoic paleosols and origin of single-cycle quartzites of Fennoscandian Shield. *29th International Geological Congress* **2/3**, 290.

Marmo J. S. (1992) The Lower Proterozoic Hokkalampi paleosol in North Karelia, Eastern Finland. In *Early Organic Evolution: Implications for Mineral and Energy Resources* (ed. M. Schidlowsli, *et al.*). Springer-Verlag.

Marmo J. S., Kohonen J. J., Sarapää O., and Äikäs O. (1988) Sedimentology and stratigraphy of the lower Proterozoic Sariola and Jatuli Groups in the Koli-kaltimo area, eastern Finland. *GSF Special Paper* **5**, 11-28.

Marmo J. S. and Ojakangas R. W. (1984) Lower Proterozoic glaciogenic deposits, Eastern Finland. *Geological Society of America Bulletin* **95**, 1055-1062.

Marmo J. S. and Ojakangas R. W. (1998) Early Proterozoic glacial rocks, paleosols, and orthoquartzites in Finland. In *Paleoclimates and the evolution of paleogeographic environments in the Earth's geological history: international symposium* (ed. K. I. Heiskanen and V. V. Makarikhin). Russian Academy of Sciences.

Marsh J. S. (1991) REE fractionation and Ce anomalies in weathered Karoo dolerite. *Chemical Geology* **90**, 189-194.

Martin H. (1989) Archaean chronology in the eastern part of the Baltic Shield: a synthesis. *Precambrian Research* **43**, 63-77.

Maynard J. B. (1992) Chemistry of modern soils as a guide to interpreting Precambrian paleosols. *The Journal of Geology* **100**, 279-289.

McDaniel D. K., Hemming S. R., McLennan S. M., and Hanson G. N. (1994) Resetting of neodymium isotopes and redistribution of REEs during sedimentary processes: The early Proterozoic Chelmsford Formation, Sudbury Basin, Ontario, Canada. *Geochimica et Cosmochimica Acta* **58**, 931-941.

McLennan S. M. (1989) Rare earth elements in sedimentary rocks: influence of provenance and sedimentary processes. In *Geochemistry and Mineralogy of Rare Earth Elements*, Vol. 21 (ed. B. R. Lipin and G. A. McKay). Mineralogical Society of America.

Meriläinen K. (1980) On the stratigraphy of the Karelian formations. In *Jatulian geology in the eastern part of the Baltic Shield* (ed. A. Silvennoinen), pp. 97-112. Proceedings of a Finnish-Soviet Symposium.

Middelburg J. J., Van der Weijden C. H., and Woittiez J. R. W. (1988) Chemical processes affecting the mobility of major, minor and trace elements during weathering of granitic rocks. *Chemical Geology* **68**, 253-273.

Mongelli G. (1993) REE and other trace elements in a granitic weathering profile from "Serre", southern Italy. *Chemical Geology* **103**, 17-25.

Neaman A., Chorover J., and Brantley S. L. (2005) Element mobility patterns record organic ligands in soils on early Earth. *Geology* **33**(2), 117-120.

Nedachi Y., Nedachi M., Bennett G., and Ohmoto H. (2005) Geochemistry and mineralogy of the 2.45 Ga Pronto paleosols, Ontario, Canada. *Chemical Geology* **214**(1-2), 21-44.

Negrel P., Grosbois C., and Kloppmann E. (2000) The labile fraction of suspended matter in the Loire River (France): multi-element chemistry and isotopic (Rb-Sr and C-O) systematics. *Chemical Geology* **166**, 271-285.

Nesbitt H. W. (1979) Mobility and fractionation of rare earth elements during weathering of a granodiorite. *Nature* **279**, 206-210.

Nesbitt H. W., Markovcs G., and Price R. C. (1980) Chemical processes affecting alkalis and alkaline earths during continental weathering. *Geochemica et Cosmochimica Acta* **44**, 1659-1666.

Nesbitt H. W. and Markovics G. (1997) Weathering of granodioritic crust, long-term storage of elements in weathering profiles, and pedogensis of siliciclastic sediments. *Geochimica et Cosmochimica Acta* **61**(8), 1653-1670.

Nesbitt H. W. and Young G. M. (1984) Prediction of some weathering trends of plutonic and volcanic rocks based on thermodynamic and kinetic considerations. *Geochimica et Cosmochimica Acta* **48**, 1523-1534.

Nesbitt H. W. and Young G. M. (1989) Formation and diagenesis of weathering profiles. *Journal of Geology* **97**, 129-147.

Neuvonen K. J., Pesonen L. J., and Pietarinen H. (1997) Remanent magnetization in the Archaean basement and cutting diabase dykes in Finland, Fennoscandian Shield. In *Geophysica*, Vol. 33 (ed. L. J. Pesonen), pp. 111-146. Geological Survey of Finland.

OECD. (1985) Compilation of selected thermodynamic data (provided by Muller AB, Paris). *Organization for Economic Co-Operation and Development.*

.

Öhlander B., Land M., Ingri J., and Widerlund A. (1996) Mobility of rare earth elements during weathering of till in northern Sweden. *Applied Geochemistry* **11**, 93-99.

Ohmoto H. (1996) Evidence in pre-2.2 Ga paleosols for the early evolution of atmospheric oxygen and terrestrial biota. *Geology* **24**(12), 1135-1138.

Ohmoto H. (1997) Evidence in pre-2.2 Ga paleosols for the early evolution of atmospheric oxygen and terrestrial biota: Reply. *Geology* **25**, 858-859.

Ohmoto H. (1999) Redox state of the Archean atmosphere: Evidence from detrital heavy minerals in ca3250-2750 Ma sandstones from the Pilbara Craton, Australia: Comment and reply. *Geology* **27**, 1151-1152.

Ohmoto H. and Kerrick D. (1977) Devolatilization equilibria in graphitic systems. *Am. J. Sci.* **277**, 1013-1044.

Ohmoto H., Watanabe Y., Ikemi H., Poulson S. R., and Taylor B. E. (2006) Sulphur isotope evidence for an oxic Archean atmosphere. *Nature* **442**(7105), 908-911.

Ohmoto H., Watanabe Y., and Kazumasa K. (2004) Evidence from massive siderite beds for a CO2-rich atmosphere before ~1.8 billion years ago. *Nature* **429**(May 27), 395-399.

Ohr M., Halliday A. N., and Peacor D. R. (1994) Mobility and fractionation of rare earth elements in argillaceous sediments: Implications for dating diagenesis and low-grade metamorphism. *Geochimica et Cosmochimica Acta* **28**, 289-312.

Ojakangas R. W. (1965) Petrography and sedimentation of the Precambrian Jatulian quartzites of Finland. In *Bulletin de la Commission Ge'ologique de Finlande*, Vol. 214, pp. 74.

Ojakangas R. W., Richard W., Marmo J. S., and Heiskanen K. I. (2001) Basin evolution of the Paleoproterozoic Karelian Supergroup of the Fennoscandian (Baltic) Shield. *Sedimentary Geology* **141-142**, 255-285.

Panahi A., Young G. M., and Rainbird R. H. (2000) Behavior of major and trace elements (including REE) during Paleoproterozoic pedogenesis and diagenetic alteration of an Archean granite near Ville Marie, Quebec, Canada. *Geochimica et Cosmochimica Acta* **64**(13), 2199-2220.

Patchett J., Gorbatschev R., and Todt W. (1987) Origin of continental crust of 1.9-1.7 Ga age: Nd isotopes in the Svecofennian orogenic terrains of Sweden. *Precambrian Research* **35**, 145-160.

Pavlov A. A., Kasting J. F., Eigenbrode J. L., and Freeman K. H. (2001) Organic haze in Earth's early atmosphere: Source of low 13C Late Archean kerogens? *Geology* **29**(1003-1006).

Philpotts A. R. (1989) *Petrography of Igneous and Metamorphic Rocks*. Prentice Hall, Englewood Cliffs, New Jersey.

Pinto J. P. and Holland H. D. (1988) Paleosols and the evolution of the atmosphere; Part II. In *Paleosols and weathering through geologic time; principles and applications*, Vol. 216 (ed. J. Reinhardt and W. R. Sigleo), pp. 21-34. Geological Society of America.

Price R. C., Gray C. M., Wilson R. E., Frey F. A., and Taylor S. R. (1991) The effects of weathering on rare-earth elements, Y and Ba abundances in Tertiary basalts from southeastern Australia. *Chemical Geology* **93**, 245-265.

Rainbird R. H., Nesbitt H. W., and Donaldson J. A. (1990) Formation and diagenesis of a sub-Huronian saprolith: comparison with a modern weathering profile. *The Journal of Geology* **98**(6), 801-822.

Retallack G. J. (1988) Field Recognition of paleosols. *Geological Society of America Special paper 216*.

Retallack G. J. (1992) Paleozoic Paleosols. In *Developments in Earth Surface Processes (Vol. 2): Weathering, Soils and Paleosols*, Vol. 2 (ed. I. P. Martini and W. Chesworth), pp. 543-564.

Retallack G. J. (1997) *A Colour Guide to Paleosols*. John Wiley and Sons.

Robb L. J. and Meyer M. F. (1995) The Witwatersrand Basin, South Africa; geological framework and mineralization processes. *Ore Geology Reviews* **10**(2), 67-94.

Robinson A. G. and Spooner E. T. C. (1984) Postdepositional modification of uraninite-bearing quartz-pebble conglomerates from the Quirke ore zone, Elliot Lake, Ontario. *Economic Geology and the Bulletin of the Society of Economic Geologists* **79**(2), 297-321.

Rye R. (1998) Highly negative $d^{13}C$ values in organic carbon in Mt. Roe #2 paleosol; Terrestrial life at 2.765 Ga? *Mineralogical Magazine* **62A**, 1308-1309.

Rye R. and Holland H. D. (1998) Paleosols and the evolution of atmospheric oxygen: a critical review. *American Journal of Science* **298**, 621-672.

Rye R. and Holland H. D. (2000) Life associated with a 2.76 Ga ephermeral pond?: Evidence from Mount Roe #2 paleosol. *Geology* **28**, 483-486.

Rye R., Kuo P., and Holland H. D. (1995) Atmospheric carbon dioxide concentrations before 2.2 billion years ago. *Nature* **378**, 603-605.

Schaltegger U., Stille P., Rais N., Piquè A., and Clauer N. (1994) Neodymium and strontium isotopic dating of diagenesis and low-grade metamorphism of argillaceous sediments. *Geochimica et Cosmochimica Acta* **58**, 1471-1481.

Schau M. and Henderson J. B. (1983) Archean chemical weathering at three localities on the Canadian Shield. *Precambrian Research* **20**, 189-224.

Schmitt J.-M. (1999) Weathering, rainwater and atmosphere chemistry: example and modelling of granite weathering in present conditions in a CO_2-rich, and in an anoxic paleoatmosphere. In *Palaeoweathering, Palaeosurfaces and Related Continental Deposits*, Vol. 27 (ed. M. Thiry and R. Simon-Coincon), pp. 22-41. Blackwell Science.

Schumm R. H., Wagman D. D., Baily S., Evans W. H., and Parker V. B. (1973) Selected values of chemical thermodynamic properties. Tables for the lanthanide (rare earth) elements. National Bureau of Standards Tech Note. **270**(7:75).

Sharma A. and Rajamani V. (2000) Major element, REE, and other trace element behavior in amphibolite weathering under semiarid conditions in southern India. *The Journal of Geology* **108**, 487-496.

Shklanka R. (1972) Geology of the Steep Rock Lake Area District of Rainy River. In *Geological Report 93*, Vol. Geological Report 93, pp. 114 p. Ontario Department of Mines and Northern Mines.

Simonen A. (1980) *The Precambrian in Finland*. Geological Survey of Finland.

Singh P. and Rajamani V. (2001) REE geochemistry of recent clastic sediments from the Kaveri floodplains, southern India: Implications to source area weathering and sedimentary processes. *Geochimica et Cosmochimica Acta* **65**, 3093-3108.

Smith R. M. and Martell A. E. (1976) Critical stability constraints. In *Inorganic Complexes*, Vol. 4, pp. 176. Plenum Press.

Stafford S. L., Capo R. C., Stewart B. W., Macpherson G. L., and Ohmoto H. (1999) Micromorphology and geochemistry of an apparent Archean weathering profile, Ontario, Canada. *Eos, Trans. Am. Geophys. Union* **80**, F1167.

Stafford S. L., Stewart B. W., Capo R. C., and Ohmoto H. (2000) Neodymium isotope investigation of an Archean weathering profile: Steep Rock paleosol, Ontario, Canada. *Geological Society of America Abstracts with Programs* **37**(7), p. 485.

Stewart B. W. and DePaolo D. J. (1996) Isotopic studies of processes in mafic magma chambers: III. The Muskox intrusion, Northwest Territories, Canada. In *Earth Processes: Reading the Isotopic Code*, Vol. 95 (ed. A. R. Basu and S. R. Hart), pp. 277-292. American Geophysical Union.

Stone D., Kamineni D. C., and Jackson M. C. (1992) Precambrian Geology of the Atikokan Area, Northwestern Ontario, Vol. Bulletin 405, pp. 106. Geological Survey of Canada.

Stoops G. and Jongerius A. (1975) Proposal for a micromorphological classification of soil materials; I, A classification of the related distributions of fine and coarse particles. *Geoderma* **13**(3), 189-199.

Sturt B. A., Melezhik V. A., and Ramsay S. M. (1994) Early Proterozoic regolith at Pasvik, northeast Norway: palaeoenvironmental implications for the Baltic Shield. *Terra Nova* **6**, 618-633.

Tanton T. L. (1927) Mineral deposits of Steeprock Lake map-area, Ontario. In *Summary Report 1925, part C*, pp. 1-11. Geological Survey of Canada.

Tomlinson K. Y., Hughes D. J., Thurston P. C., and Hall R. P. (1999) Plume magmatism and crustal growth at 2.9 to 3.0 Ga in the Steep rock and Lumby Lake area, western Superior Province. *Lithos* **46**, 103-136.

Topp S. E., Salbu B., Roaldset E., and Jørgensen P. (1984) Vertical distribution of trace elements in laterite soil (Suriname). *Chemical Geology* **47**, 159-174.

Turekian K. K. (1969) The oceans, streams and atmosphere. In *Handbook of Geochemistry, v. 1* (ed. K. H. Wedepohl), pp. 297-323. Springer-Verlag.

Ulrich K., Rossberg A., Foerstendorf H., Zaenker H., and Scheinost A. C. (2006) Molecular characteriation of uranium(VI) sorption complexes on iron(III)-rich acid mine water colloids. *Geochimica et Cosmochimica Acta* **70**(22), 5469-5487.

Uysal I. T. and Golding S. D. (2003) Rare earth element fractionation in authigenic illite-smectite from Late Permian clastic rocks, Bowen Basin, Australia: Implications for physico-chemical environments of fluids during illitization. *Chemical Geology* **93**, 167-179.

Vidal P., Blais S., Jahn B.-M., Capdevila R., and Tilton G. R. (1980) U-Pb and Rb-Sr systematics of the Suomussalmi Archean greenstone belt (Eastern Finland). *Geochimica et Cosmochimica Acta* **44**, 2033-2044.

Vuollo J. (1991) Proterozoic mafic rock associations in North Karelia. In *Archean and Proterozoic geologic evolution and related ore-forming processes in North Karelia*, Vol. Report of investigation 3 (ed. T. Piirainen). University of Oulu.

Vuollo J., Piirainen T., and Huhma H. (1992) Two early Proterozoic tholeiitic diabase dyke swarms in the Koli-Kaltimo area, eastern Finland. *Geologic Survey of Finland Bulletin* **363**, 32 pp.

Wagman D. D., Evans W. H., Parker V. B., Schumm R. H., Halow I., Baily S. M., Churney K. L., and Buttall R. L. (1982) The NBS tables of chemical thermodynamic properties. Selected values for inorganic and C1 and C2 organic substances in SI units. *J. Phys Chem Ref Data* **11**(suppl. 2:392).

Watanabe Y., Martini J. E. J., and Ohmoto H. (2000) Geochemical evidence for terrestrial ecosystems 2.6 billion years ago. *Nature* **408**, 574-578.

Watanabe Y., Stewart B. W., and Ohmoto H. (2004) Organic-and carbonate-rich soil formation ~2.6 billion years ago at Schagen, East Transvall district, South Africa. *Geochimica et Cosmochimica Acta* **68**(9), 2129-2151.

Wilks M. E. and Nisbet E. G. (1988) Stratigraphy of the Steep Rock Group, northwest Ontario: a major Archean unconformity and Archean stromatolites. *Can. J. Earth Sci.* **25**, 370-391.

Wilson M. R., Hamilton P. J., Fallick A. E., Aftalion M., and Michard A. (1985) Granites and Early Proterozoic crustal evolution in Sweden: evidence from Sm-Nd, U-Pb, and O isotope systematics. *Earth and Planetary Science Letters* **72**, 376-388.

Yang W. B., Holland H. D., and Rye R. (2002) Evidence for low or no oxygen in the late Archean atmosphere from the ~2.76 Mount Roe #2 paleosol, Western Australia: Part 3. *Geochimica et Cosmochimica Acta* **66**, 3707-3718.

York D. (1969) Least squares fitting of a straight line with correlated errors. *Earth and Planetary Science Letters* **5**, 320-324.

Zbinden E. A., Holland H. D., Freakes C. R., and Dobos S. K. (1988) The Sturgeon Falls paleosol and the composition of the atmosphere 1.1 Ga BP. *Precambrian Research* **42**, 141-163.